The Composition of Arylstibonic Acids

THE UNIVERSITY OF
WAIKATO
Te Whare Wānanga o Waikato

A thesis submitted in partial fulfilment
of the requirements for the degree
of
Master of Science
in Chemistry
at
The University of Waikato
by

Cody Elvin Wright

The University of Waikato
2010

Abstract

This thesis describes a detailed ESI-MS investigation into the arylstibonic acids, organo-antimony-containing compounds that are currently of interest as anticancer reagents. Four arylstibonic acids, of nominal formula $RC_6H_4SbO_3H_2$ [R = *p*-chloro-, *p*-tolyl-, *p*-nitro- and *α*-naphthyl-] were synthesised, and a further eight archival samples from the National Cancer Institute Repository were obtained for use in the project.

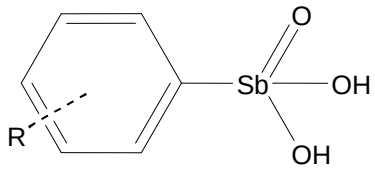

Arylstibonic acid

Results indicate clearly that the acids exist as polyoxometalate aggregates $[H_8(RSb)_{12}O_{28}]$, rather than monomeric species, in both the solid state and in acetonitrile solution, thus resolving a century-old debate concerning the nature of their molecular composition. Variations in solvent, time in solution and pH have also defined the stability of these aggregates under different conditions.

Synthesis of arylstibonic acids by traditional methods (pre-1940) has been shown to lead to products contaminated with cations present during their preparation. An improved method of synthesis has been devised, and the crystal structure of an intermediate in the synthesis of these acids, $[C_6NH_6][p\text{-}O_2NC_6H_4SbCl_5]$, is reported.

Salts of arylstibonic acids with a range of cations were investigated by ESI-MS and shown to form a diverse family of polyoxostibonates with nuclearities including Sb_{12}, Sb_{14} and Sb_{16}. Crystal structures containing some of these aggregates, verified through parallel studies with collaborators, are described. Preliminary study of mixed polyoxometalates (Sb/As) showed a strong tendency to form As_4Sb_2 species but these could not be fully characterised.

Acknowledgements

Firstly I would like to thank Professor Brian Nicholson for being a wonderful, encouraging and knowledgeable supervisor, cracking the whip when needed and sharing a laugh. All this considering he drives a Holden.

Chris Clark for ideas and contributions towards the research project, whilst simultaneously exhausting supplies of purified arylstibonic acids faster than I could prepare them.

Wendy Jackson, Amu Upreti, Jenny Stockdill and Annie Barker for their help in the lab.

Pat Gread for her expertise with the MicrOTOF and the training I received on it. Also her continued patience when my compounds blocked the instrument.

Nick Lloyd for supplying arylarsonic acids used in the mixed-metal polyoxometalates.

Dr Robert H Shoemaker and the Chemotherapeutic Agents Repository, Drug Synthesis and Chemistry Branch, National Cancer Institute, Rockville, MD, for supplying archival arylstibonic acid samples.

Cheryl Ward for her continued support and help with her extensive knowledge with all aspects regarding the preparation of this thesis.

Megan Grainger for help in problem solving minor annoyances with piecing this thesis together and sharing a laugh.

All of the students undertaking this degree during the last year and half for their help sidetracking me.

Everyone in C.3.04 for getting in my way and taking my glassware, particularly after I had cleaned it, while putting up with my research and the mess that it entailed.

My family for believing in me and their continued support, while keeping me down-to-earth.

Talia Heslop and the Science and Engineering administration for all their helping regarding enrolment.

And lastly I would like to thank all those involved with the Department of Chemistry at the University of Waikato for allowing me to gain my desired qualifications while making it thoroughly enjoyable in the process.

Table of Contents

List of Figures

List of Equations

List of Tables

1 Introduction

The late nineteenth and early twentieth century brought about a great increase in the research and synthesis of organoantimony compounds. The initial motivation was driven by research on organoarsenic compounds and their pharmaceutical effect on diseases such as syphilis, the incentive being the similarities between the closely-related elements of arsenic and antimony [1].

Research was mainly focused on the pharmacological properties of organic stibonic and stibinic acids, of nominal formula $RSbO_3H_2$ and R_2SbO_2H respectively (R = various aromatic substituents) [2]. This lead to several breakthroughs which included the treatment of schistosomiasis and leishmaniasis. Advancement in this field was sluggish due mainly to the lack of stability of organoantimony compounds compared to their organoarsenic analogues, but interest has since increased as the differing chemistry justifies further study [1].

Although arylstibonic acids have been recognized for over a century, their specific structure remains elusive. This is due to their intrinsic properties that make them difficult to characterise fully, i.e. amorphous powders with limited solubility. This is in contrast to the very well-defined arylarsonic acids [3]. What little evidence there was initially suggested that arylstibonic acids exist as oligomeric species [4], although other early studies showed results supporting monomeric species [5].

1.1 Preparation

As knowledge of the existence of naturally occurring organoantimony compounds was limited [6], much of the initial work went into synthesis. This began with the investigations of Michaelis *et al.* in 1882 [7]. Pioneers in this field included such chemists as Morgan, Löwig, Landolt, and Friedländer [1]. The synthesis of stibonic acids was initially depicted by a patent in 1911 [8]. This demonstrated that the Bart reaction, which was used for the preparation of arsonic acids, could also be applied to the preparation of the corresponding stibonic acids [1, 2]. The Bart reaction defines the process where an aromatic diazo compound reacts with an inorganic trivalent arsenic compound (such as sodium arsenite) under aqueous alkaline conditions to form arylarsonic acids with the evolution of nitrogen.

$$[Ar\text{-}N_2]^+ + [AsO_2]^- + H_2O \rightarrow ArAsO_3H_2 + N_2$$

Equation 1: Bart reaction (arylarsonic acids)

The yield of the Bart reaction is pH dependent and thus care is needed, a buffer is commonly used to increase yields [1]. Christiansen proposed a mechanism for this reaction [9].

This method was then reaffirmed when Schmidt proposed a variety of different procedures for the preparation of arylstibonic acids [10]. Although these adaptations were successful, they encountered a number of difficulties. These included the precipitation of unwanted by-products and the formation of a stiff foam [11]. Modifications by Dunning and Reid slightly improved yields, by the use of cooling and the slow addition of sodium hydroxide to halt the formation of the foam and aid the hydrolysis of the crude stibonic acid [12]. Although this increased yields, they were still quite poor and the purity of products was low due to their affinity for, and capacity to retain, impurities. Aryl antimony compounds are largely amorphous buff powders. Thus the ability to determine and improve the quality of these synthetic products was hampered by the fact that at that time, the easiest method of quality determination was the use of melting points [2].

Around the same time, Scheller [13] introduced major changes to the Bart reaction for preparing arylarsonic acids. An organic solvent was used to dissolve the amine, while concentrated aqueous sodium nitrite was used to diazotize the amine in the presence of arsenic trichloride. Heat and a cuprous salt catalyst were also used to assist the reaction. These alterations usually gave higher yields than the Bart reaction, but this was dependent on the electron donor/acceptor characteristics of the substituents. Electron-accepting substituents resulted in an increased yield, whereas electron-donating substituents decreased yield [13].

Doak and Steinman adapted the Scheller reaction for the preparation of arylstibonic acids [14]. Although the initial steps of the preparation only received minor modifications, the major advance was the use of quaternary ammonium salts as a purification step. Preparations of arylstibonic acids using a diazonium salt often contained inorganic antimony compounds as an impurity and because arylstibonic acids are generally insoluble in water and organic solvents, conventional recrystallization methods were not applicable. In this case, the crude arylstibonic acid was dissolved in a mixture of alcohol (ethanol or methanol)

and/or concentrated hydrochloric acid, a pyridinium reagent was added. This typically resulted in instantaneous precipitation of crystalline pyridinium arylchloroantimonate. The pyridinum salt could then be recrystallized and hydrolysed in aqueous sodium carbonate. Subsequent slow acidification resulted in the precipitation of analytically pure arylstibonic acids.

$$RSbO_3H_2 + \text{conc. HCl} \rightarrow [RSbCl_5]^-$$
$$[RSbCl_5]^- + [C_5H_5NH]^+ \rightarrow [C_5H_5NH]^+[RSbCl_5]^-$$
$$[C_5H_5NH]^+[RSbCl_5]^- + Na_2CO_3 \rightarrow [RSbO_3]^{2-}$$
$$[RSbO_3]^{2-} + HCl \rightarrow RSbO_3H_2$$

Equation 2: Doak purification scheme

This worked pleasingly with *para*- and *meta*- substituted anilines, but was less than satisfactory with anilines substituted in the *ortho*- position. This purification method lead to the reproducible characterisation of arylstibonic acids. Characterisation was by Sb analysis only [14].

As noted later in this thesis (Section 3.1) the acids may not have been completely pure, with entrainment of Na^+ ions likely.

In contrast to arylstibonic acids, aliphatic stibonic acids are virtually non-existent, with only methanestibonic acid being reported in the chemical literature presently [15].

1.2 Structure

While the synthesis of arylstibonic acids has been established for over a century and there is an ever-increasingly large number being described in the literature, their precise molecular structure has proved elusive. This has been due to: their lack of solubility in water and organic solvents; difficulty when trying to separate by filtration as when washed with water they peptize through the filter; and, decomposition on heating and thus a lack of a distinct melting point. These differing physical properties compared with the corresponding arsonic acids brought Schmidt [16] to the conclusion that they are polymeric in nature and that they exist in the solid state as a trimer. Schmidt proposed that the trimer exists as one of two structures that would dissociate to the monomeric form in alkali solution, Figure 1.1. The degree of associated water (*n* in Figure 1.1) is dependent

on the arylstibonic acid and the method of preparation. Macallum [5], through the use of molecular weight determinations, proposed that they have a monomeric structure. Schmidt's conclusion was generally preferred over that of Macallum.

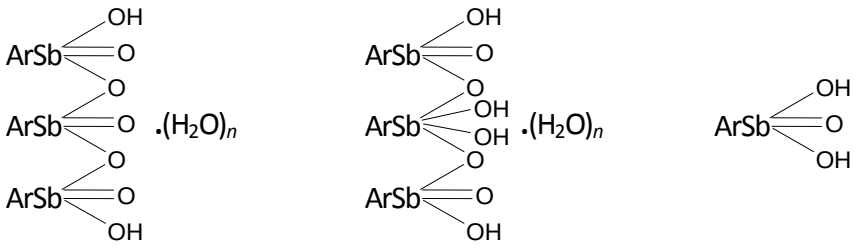

Figure 1.1: Proposed arylstibonic acid structures

Schmidt's structural conclusion was later supported by Gray *et al.* [17, 18] with their work on sodium salts of arylstibonic acids. Their findings showed that the Na:Sb ratio was significantly lower than the expected ratio for a monomeric species (1:1) and actually approached that of a trimeric species (1:3).

Further investigations by Doak [4] confirmed Schmidt's conclusions about the pseudo-acid behaviour of arylstibonic acids and molecular weight determinations on drying. Doak also questioned the results drawn from the molecular weight determinations. The lack of reproducibility and significant variations from calculated values, when using drying as the method for determination, lead Doak to the conclusion that the results were in fact a combination of drying and thermal decomposition, hence significant structural information could not be extracted from these results alone.

Cryoscopic molecular weight determinations of arylstibonic acids in benzene, acetic acid and formic acid disagreed with the results of Schmidt and Macallum. Instead, Doak suggested arylstibonic acids exist as high molecular weight polymeric species linked by hydrogen bonding. Hydrogen bonding also appeared to support the way in which arylstibonic acids behaved as pseudo-acids.

These analytical results, along with their colloidal properties, brought Doak to the conclusion that arylstibonic acids exist as polymeric species of the type $(ArSbO_3H_2)_x.(H_2O)_n$ as five- or six-coordinate Sb with μ-O linkages, but of unknown structure [1, 4].

Subsequent Mössbauer studies of amorphous arylstibonic acids showed that they have approximately trigonal-bipyramidal geometry, with bridging oxygen on

opposite sides of Sb, and OH or R groups in the equatorial plane [19]. This is in contrast to tetrahedral-coordinate arylarsonic acids [20].

A recent crystal structure determination of 2, 6-$Mes_2C_6H_3SbO_3H_2$ showed that it exists as a dimer with five-coordinate Sb and a Sb_2O_2 core [21]. Since this compound is sterically crowded it is unlikely to be indicative of arylstibonic acids with smaller, less bulky R groups.

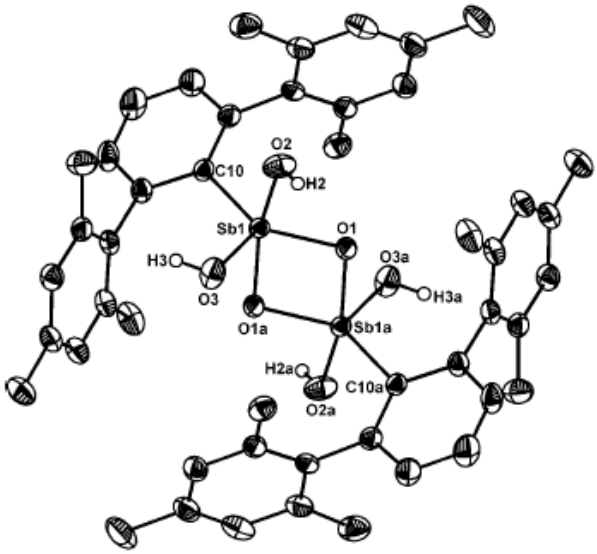

Figure 1.2: Molecular structure of 2,6-$Mes_2C_6H_3SbO_3H_2$ [21]

1.3 Thesis Outline

In an attempt to resolve the 100-year-old puzzle of the elusive structure of arylstibonic acid, this thesis reports the re-investigation of the preparations of some arylstibonic acids and has used ESI-MS to probe their solution structure (Section 3.3). Investigations into the nature and behaviour of arylstibonic acids have been carried out (Chapters 4 and 5). Some preliminary work on mixed-metal polyoxometalates (Sb/As acids) is also described (Chapter 6).

2 The Synthesis of Arylstibonic Acids

The following experimental procedures are based on the modification of the Scheller reaction as described by Doak and Steinman [14]. The *p*-chlorophenylstibonic, *p*-tolylstibonic and *p*-nitrophenylstibonic acids are known compounds. α-Naphthylstibonic acid has been reported briefly [2] but only included elemental analysis, so further characterisation details are reported here for the first time.

2.1 *para*-Chlorophenylstibonic Acid

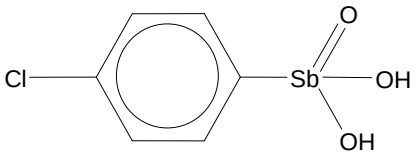

p-$ClC_6H_4SbO_3H_2$

The amine (4-chloroaniline 6.4 g, 0.05 moles) was dissolved in ethanol (125 mL) in a 250 mL wide-mouth conical flask with an efficient stirrer, surrounded by an ice-bath. Concentrated sulfuric acid (2.7 mL, 5 g) and antimony trichloride (11.4 g, 0.05 moles) were added. Once the latter had completely dissolved, a solution of sodium nitrite (3.5 g in 5 mL water) was added to initiate diazotization; at this point a pale brown precipitate formed. This thick mixture was stirred for 0.5 h. Cuprous bromide (1 g) was added and the ice-bath removed. As the mixture warmed, nitrogen evolved spontaneously. This was left stirring for 24 h to ensure complete nitrogen evolution, giving an off-white precipitate and a pale brown solution. Steam distillation was used to remove the alcohol, resulting in an off-white precipitate and pale light-blue solution. The crude stibonic acid was filtered on a Büchner flask, washed with water and left to dry. It was then dissolved in concentrated hydrochloric acid (*ca* 1000 mL) and a mixture of pyridine (5 mL) in concentrated hydrochloric acid (20 mL) was added. After cooling to room temperature the off-white pyridinium salt was collected on a sintered glass filter and washed several times with concentrated hydrochloric acid and left to dry. The salt was dissolved in dilute sodium carbonate solution (1-2%, *ca* 2000 mL). The free acid was obtained through acidification by the dropwise addition of dilute hydrochloric acid while stirring rapidly. The precipitate was filtered on a Büchner

flask, and washed thoroughly with water acidified with a few drops of dilute hydrochloric acid.

For further purification to remove entrained Na^+ ions, the free acid was suspended in water and concentrated ammonia added until just dissolved (*ca* 2:1 mixture, 2 g sample usually required a total volume of 300 mL). This was done in polypropylene beakers so as to minimise sodium contamination. Dissolution was aided by stirring rapidly for ~1 h. The pure acid was obtained by placing the open beakers in a large closed desiccator containing glacial acetic acid; this was left for several days to allow the acetic acid to diffuse and the pure stibonic acid to precipitate. Once complete diffusion had occurred the stibonic acid was recovered via gravity filtration and left to dry, giving an off-white amorphous powder.

2.1.1 Elemental Analysis

Found (%) C 26.93; H 2.46. Calculated for $C_6H_6ClO_3Sb$, C 25.44; H 2.13; Calculated for $C_{72}H_{56}Cl_{12}O_{28}Sb_{12}$, C 26.56; H 1.73.

2.1.2 IR Analysis

KBr disc, cm^{-1} (strength, s = strong, m = medium, w = weak, br = broad), 3400 (s, br), 3190 (s), 1634 (m), 1573 (m), 1477 (s), 1383 (s), 1181 (w), 1090 (s), 1067 (s), 1013 (s), 947 (w), 814 (s), 728 (s), 667 (s), 606 (w), 488 (s).

2.2 *para*-Tolylstibonic Acid

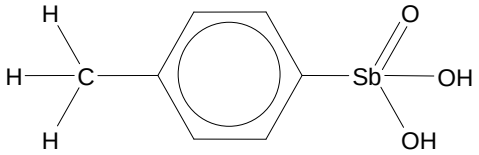

p-$MeC_6H_4SbO_3H_2$

Similarly the *p*-Me- analogue was prepared from 4-toluidine (5.4 g, 0.05 moles). A slight variation to the experimental procedure was a decrease in the volume of concentrated hydrochloric acid (*ca* 600 mL) required to disolve the crude stibonic acid. The product was an off-white amorphous powder.

2.2.1 Elemental Analysis

Found (%) C 33.35; H 3.49. Calculated for $C_7H_9O_3Sb$, C 31.98; H 3.45; Calculated for $C_{84}H_{92}O_{28}Sb_{12}$, C 33.51; H 3.08.

2.2.2 IR Analysis

KBr disc, cm^{-1}, 3401 (s, br), 3200 (s), 1635 (m), 1593 (m), 1493 (m), 1447 (w), 1395 (s), 1310 (w), 1280 (w), 1210 (w), 1187 (m), 1073 (m), 1018 (w), 802 (s), 743 (s), 667 (s), 600 (w), 486 (s), 460 (w).

2.3 *para*-Nitrophenylstibonic Acid

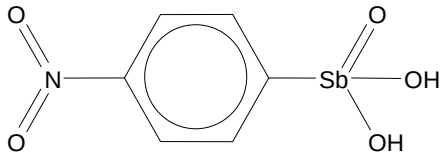

p-$O_2NC_6H_4SbO_3H_2$

The *p*-NO_2- analogue was prepared using 4-nitroaniline (6.9 g, 0.05 moles). Variations included: a mixture of concentrated hydrochloric acid and methanol (1:1, *ca* 1500 mL) was required to dissolve the crude acid and after adding the pyridine reagent, it was left for evaporation as the pyridinium salt did not initially precipitate out. Dilute ammonia (2 mol L^{-1}, *ca* 2000 mL) was used for the hydrolysis instead of sodium carbonate, giving a pale yellow amorphous powder.

2.3.1 Elemental Analysis

Found (%) C 26.11; H 2.76; N 4.76. Calculated for $C_6H_6NO_5Sb$, C 24.52; H 2.06; N 4.77; Calculated for $C_{72}H_{56}N_{12}O_{52}Sb_{12}$, C 25.57; H 1.67; N 4.97; Calculated for $C_{72}H_{55}N_{12}NaO_{52}Sb_{12}$, C 25.40; H 1.63; N 4.94.

2.3.2 IR Analysis

KBr disc, cm^{-1}, 3400 (s, br), 3190 (s, br), 1630 (m), 1597 (m), 1576 (m), 1516 (s), 1477 (w), 1390 (m), 1355 (s), 1315 (w) 1279 (w), 1105 (m), 1068 (m), 1014 (m), 937 (w), 854 (s), 738 (s), 710 (s), 684 (s), 600 (w), 533 (w), 466 (m).

2.4 *α*-Naphthylstibonic Acid

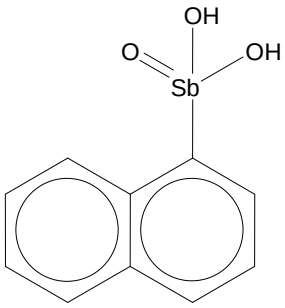

α-$C_{10}H_7SbO_3H_2$

The *α*-naphthylstibonic acid was prepared using *α*-naphthylamine (7.2 g, 0.05 moles). Similarly to the *p*-NO_2 analogue, a mixture of concentrated hydrochloric acid and methanol (1:1, *ca* 1500 mL) was required to dissolve the crude acid and after adding the pyridine reagent, it was left for evaporation as the pyridinium salt did not initially precipitate out. Dilute nitric acid was used to acidify the carbonate solution as dilute hydrochloric acid appeared to introduce some Cl^- into the product. The additional acetic acid diffusion step was deemed unnecessary as at this stage the free acid was relatively free of Na^+. This produced a pale brown amorphous powder.

2.4.1 Elemental Analysis

Found (%) C 38.80; H 2.55. Calculated for $C_{10}H_9O_3Sb$, C 40.18; H 3.03; Calculated for $C_{120}H_{92}O_{28}Sb_{12}$, C 41.86; H 2.69.

2.4.2 IR Analysis

KBr disc, cm^{-1}, 3401 (s, br), 3052 (s), 1656 (m), 1623 (w), 1590 (m), 1558 (w), 1504 (s), 1384 (s), 1335 (m), 1300 (w), 1263 (m), 1212 (w), 1166 (w), 1136 (w), 1058 (w), 1023 (m), 953 (w), 796 (s), 768 (s), 745 (m), 680 (m), 618 (w), 514 (w), 468 (m), 407 (w).

2.5 2,6-Dimethylphenylstibonic Acid

The standard methodology was unsuccessful in the preparation of 2,6-dimethylphenylstibonic acid from 2,6-dimethyl aniline. The addition of the pyridine reagent did not result in the precipitation of the pyridinium

arylchloroantimonate. Doak was also unsuccessful in producing the 2,6-dimethylphenylarsonic acid analogue via the Scheller reaction, this was not due to steric hindrance as the Bart reaction gave a 30% yield [13]. The method used by Beckman may prove to be useful in this case [21].

2.6 X-ray Crystal Structure Determination

During the preparation of *p*-nitrophenylstibonic acid, the addition of pyridine reagent to the solution of crude arylstibonic acid dissolved in concentrated hydrochloric acid formed a crystalline pyridinium salt, where crystallinity was maintained on exposure to air. Data was collected on a Bruker Apex II CCD diffractometer and processed routinely, including absorption corrections using a multi-scan method (SADABS) [22]. Structures were solved using the SHELXS97 program [23] and refinement on F_o^2 was with SHELXL97 [23] operating under the WinGx interface [24].

Crystal data and refinement details of pyridinium *p*-nitrophenylpentachloroantimonate are summarised in Table 1 & 2.

Table 1: Crystal data and refinement details for $[C_5NH_6][p\text{-}O_2NC_6H_4SbCl_5]$.

Empirical formula	$C_{11}\ H_{10}\ C_{l5}\ N_2\ O_2\ Sb$
Formula weight	501.21
Temperature	89(2) K
Wavelength	0.71073 Å
Crystal system, space group	Triclinic, P -1
Unit cell dimensions	a = 7.5153(1) Å α = 101.795(1) ° b = 8.2829(1) Å β = 90.702(1) ° c = 14.395(2) Å γ = 105.119(1) °
Volume	844.75(12) $Å^3$
Z, Calculated density	2, 1.970 Mg/m^3
Absorption coefficient	2.426 mm^{-1}
F(000)	484
Crystal size	0.42 x 0.21 x 0.12 mm
θ range for data collection	1.45 to 27.93 °
Limiting indices	-9<=h<=9, -10<=k<=10, -18<=l<=18
Reflections collected / unique	20328 / 4017 [R(int) = 0.0223]
Completeness to theta = 27.93	99.4 %
Absorption correction	Semi-empirical from equivalents
Max. and min. transmission	0.7595 and 0.4289
Refinement method	Full-matrix least-squares on F^2
Data / restraints / parameters	4017 / 0 / 230
Goodness-of-fit on F^2	1.076
Final R indices [I>2σ(I)]	R_1 = 0.0142, wR_2 = 0.0352
R indices (all data)	R_1 = 0.0151, wR_2 = 0.0356
Largest diff. peak and hole	0.399 and -0.250 $e.A^{-3}$

Table 2: Bond lengths and angles for $[C_5NH_6][p\text{-}O_2NC_6H_4SbCl_5]$.

Bond	Lenght (Å)
Sb(1)-C(1)	2.1485(13)
Sb(1)-Cl(1)	2.3801(3)
Sb(1)-Cl(5)	2.3895(3)
Sb(1)-Cl(4)	2.4030(3)
Sb(1)-Cl(3)	2.4101(3)
Sb(1)-Cl(2)	2.4204(3)
O(1)-N(1)	1.2319(17)
O(2)-N(1)	1.2211(17)
N(1)-C(4)	1.4731(17)
C(1)-C(2)	1.388(2)
C(1)-C(6)	1.388(2)
C(2)-C(3)	1.391(2)
C(3)-C(4)	1.383(2)
C(4)-C(5)	1.381(2)
C(5)-C(6)	1.391(2)
N(2)-C(11)	1.3319(19)
N(2)-C(15)	1.3452(19)
C(11)-C(12)	1.372(2)
C(12)-C(13)	1.385(2)
C(13)-C(14)	1.382(2)
C(14)-C(15)	1.374(2)

Bond	Angle (°)
C(1)-Sb(1)-Cl(1)	177.94(4)
C(1)-Sb(1)-Cl(5)	92.08(4)
Cl(1)-Sb(1)-Cl(5)	89.548(12)
C(1)-Sb(1)-Cl(4)	93.02(4)
Cl(1)-Sb(1)-Cl(4)	88.235(13)
Cl(5)-Sb(1)-Cl(4)	90.296(12)
C(1)-Sb(1)-Cl(3)	91.31(4)
Cl(1)-Sb(1)-Cl(3)	87.062(12)
Cl(5)-Sb(1)-Cl(3)	176.610(11)
Cl(4)-Sb(1)-Cl(3)	89.619(12)
C(1)-Sb(1)-Cl(2)	91.58(4)
Cl(1)-Sb(1)-Cl(2)	87.155(13)
Cl(5)-Sb(1)-Cl(2)	90.022(12)
Cl(4)-Sb(1)-Cl(2)	175.377(11)
Cl(3)-Sb(1)-Cl(2)	89.791(12)
O(2)-N(1)-O(1)	123.31(12)
O(2)-N(1)-C(4)	118.75(12)
O(1)-N(1)-C(4)	117.92(12)
C(2)-C(1)-C(6)	121.40(13)
C(2)-C(1)-Sb(1)	119.75(10)
C(6)-C(1)-Sb(1)	118.85(10)
C(1)-C(2)-C(3)	119.50(14)
C(4)-C(3)-C(2)	118.16(14)
C(5)-C(4)-C(3)	123.27(13)
C(5)-C(4)-N(1)	118.61(13)
C(3)-C(4)-N(1)	118.08(13)
C(4)-C(5)-C(6)	118.12(14)
C(1)-C(6)-C(5)	119.54(14)
C(11)-N(2)-C(15)	122.89(13)
N(2)-C(11)-C(12)	119.36(13)
C(11)-C(12)-C(13)	119.55(14)
C(14)-C(13)-C(12)	119.60(13)
C(15)-C(14)-C(13)	119.17(14)
N(2)-C(15)-C(14)	119.42(14)

2.7 Attempted Synthesis of Mixed Sb/As Polyoxometalates

2.7.1 *p*-$ClC_6H_4SbO_3H_2$ + *p*-$FC_6H_4AsO_3H_2$

p-Chlorophenylstibonic acid (0.051 g, 18 mmol) and *p*-fluorophenylarsonic acid (0.039 g, 18 mmol) were dissolved in the minimum amount of MeCN with the aid of mechanical stirring. Evaporation resulted in an off-white amorphous powder.

2.7.2 *p*-$ClC_6H_4SbO_3H_2$ + *p*-$O_2NC_6H_4AsO_3H_2$

Similarly this was prepared using *p*-nitrophenylarsonic acid (0.045 g, 18 mmol). Evaporation resulted in an off-white amorphous powder.

2.7.3 *p*-$ClC_6H_4SbO_3H_2$ + *m*-$O_2NC_6H_4AsO_3H_2$

Prepared using *m*-nitrophenylarsonic acid (0.046 g, 19 mmol). Evaporation resulted in an off-white amorphous powder.

2.7.4 *p*-$ClC_6H_4SbO_3H_2$ + *p*-$MeOC_6H_4AsO_3H_2$

Prepared using *p*-methoxyphenylarsonic acid (0.043 g, 18 mmol). Evaporation resulted in an off-white amorphous powder.

2.7.5 *p*-$ClC_6H_4SbO_3H_2$ + $C_6H_5AsO_3H_2$

Prepared using phenylarsonic acid (0.037 g, 18 mmol). Evaporation resulted in an off-white amorphous powder.

3 Results and Discussion

3.1 The Synthesis of Arylstibonic Acids

The *p*-chlorophenylstibonic, *p*-tolylstibonic and *p*-nitrophenylstibonic acids were prepared using the adapted Scheller reaction as depicted by Doak and Steinman [14]. A small number of minor adjustments were made, outlined in Chapter 2. These preparations gave relatively high yields, greater than those reported by Doak (Table 3).

Table 3: Summary of the yields of arylstibonic acids

Arylstibonic acid	Yield (%)	Doak's yield (%) [14]
p-chloro-	87	78
p-tolyl-	79	47
p-nitro-	92	53
α-naphthyl-	20	-

While *α*-naphthylstibonic acid has been reported in the literature, it was prepared via a different procedure, for which the yield was not reported [2]. *α*-Naphthylstibonic acid has been prepared using a modified Doak procedure (Section 2.4) and reported here for the first time. This was done to provide an arylstibonic acid with a more bulky substituent while determining the efficacy of the methodology for previously untried substituents. Only a relatively low yield was obtained with limited attempts made at optimising the procedure. The other arylstibonic acids were all prepared several times, with consistent and reproducible yields.

It appears that the use of steam distillation as a means of removing the ethanol may in fact aid the reaction process in some way. A batch of *p*-tolylstibonic acid was prepared using a rotary evaporator to remove the solvent as a substitute for the steam distillation procedure. The resultant compound was of particularly low yield and purity with the majority of the compound still containing $Sb^{(III)}$. Presumably steam distillation (*i.e.* heat and the addition of water) is involved in oxidising antimony from III in the starting material to V in the product.

Preliminary investigations showed that the acids contained Na^+ ions that were believed to have been introduced from the hydrolysis step involving aqueous sodium carbonate. As a means of removing this and other contaminants and thus increasing the purity of the compounds even further, a new procedure was

introduced. This additional purification involved an ammonia/acetic acid diffusion procedure [25]. The arylstibonic acid sample was dissolved in the minimum amount of water and concentrated aqueous ammonia in an open flask. Arylstibonic acids showed the ability to leach Na^+ out of glassware while in solution, so polypropylene flasks were used. The flask was placed in a closed desiccator and glacial acetic acid was allowed to diffuse slowly into the sample solution. This procedure typically resulted in the precipitation of amorphous arylstibonic acids that were free of contaminants and had a high degree of purity as judged by ESI-MS. This addition proved to be very effective for *p*-chlorophenylstibonic acid and *p*-tolylstibonic acid.

In other cases this has been less than satisfactory. Sodium has shown a tenacious affinity for *p*-nitrophenylstibonic acid, proving difficult to completely eliminate. It was believed that the source of the Na^+ was the sodium carbonate used to hydrolyse the pyridinium arylchloroantimonate. Hence a batch of *p*-nitrophenylstibonic acid was prepared using dilute ammonia in place of sodium carbonate, while the rest of the procedure was followed as before. This resulted in a sample that did not appear to have formed any adducts with sodium but the overall purity was greatly compromised. After a final subsequent ammonia/acetic acid diffusion step, analysis showed that although the purity of the compound had increased, the dominant species present in solution was still that of sodium adducts thought with greatly reduced Na^+ content. The additional purification step typically resulted in a high recovery of pure arylstibonic acids, typically 85-95%.

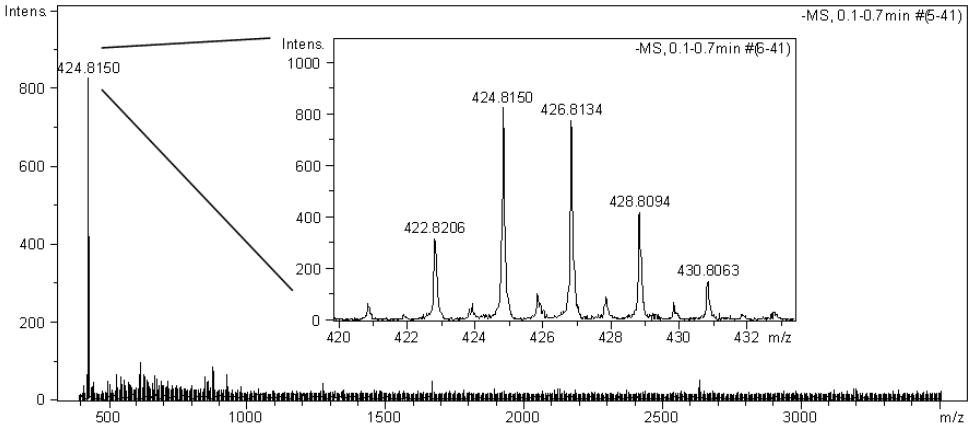

Figure 3.1: ESI-MS of α-naphthylpentachloroantimonate

The preparation of *α*-naphthylstibonic acid also encountered difficulty as samples prepared via the Doak route halted proceedings because of incomplete hydrolysis of the pyridinium arylchloroantimonate. An ESI-MS spectrum (Figure 3.1) of a sample after the pyridinium salt had been dissolved in sodium carbonate

and acidified with dilute hydrochloric acid showed that the compound was still in the arylchloroantimonate form ($[C_{10}H_7SbCl_5]^-$).

Dilute nitric acid was therefore used instead of dilute hydrochloric acid as the first step in trying to eliminate Cl^-. This proved to be successful in forming an arylstibonic acid relatively free of Na^+ ions.

3.2 X-ray Crystal Structure Determination

Crystals of pyridinium *p*-nitrophenylpentachloroantimonate suitable for X-ray analysis were obtained during the preparation of *p*-nitrophenylstibonic acid (outlined in section 2.6). These crystals appeared to be stable in air and gave particularly good data, with refinement resulting in $R_1 = 0.0142$ ($I>2\sigma(I)$), $wR_2 = 0.0356$ (all data).

The X-ray structural analysis showed the lattice to consist of a pyridinium cation and a *p*-nitrophenylpentachloroantimonate anion (Figure 3.2). The anion structure is that of octahedral antimony bonded to five chlorine atoms with average bond length 2.4006(3) Å, ranging from 2.3801(3) Å to 2.4204(3) Å. The antimony is then bonded to a phenyl ring, Sb(1)-C(1) 2.1485(13) Å. The phenyl ring plane is orientated at 38.6° to the C(1)-Cl(3)-Cl(1)-Cl(5) plane. The aromatic ring has C-C bonds of average length 1.387(2) Å. Bound in the *para* position on the phenyl ring is a nitro functional group where C(4)-N(1) is 1.4731(17) Å and the average N(1)-O bond length is 1.2265(17) Å. The bond angles centring around N(1) are *ca* 120°, orientated in plane to the phenyl ring. The pyridinium cation is of normal structure.

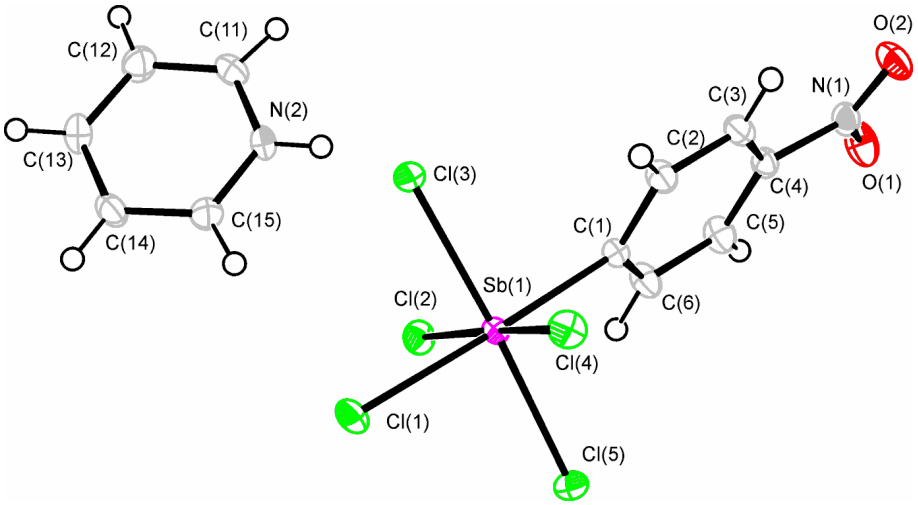

Figure 3.2: Molecular structure of $[C_5NH_6][p\text{-}O_2NC_6H_4SbCl_5]$

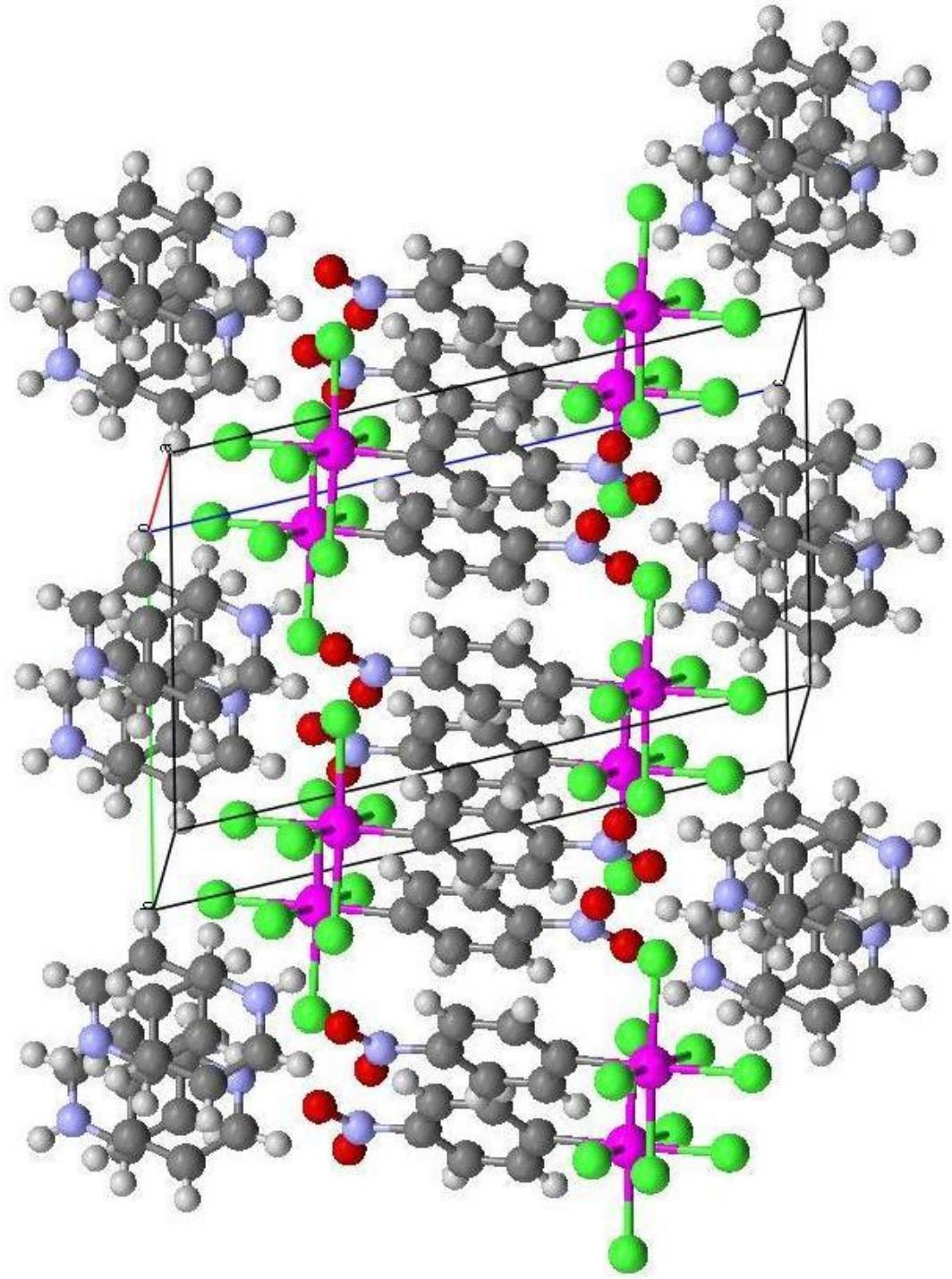

Figure 3.3: Unit cell packing of $[C_5NH_6][p\text{-}O_2NC_6H_4SbCl_5]$

Purple = antimony, green = chlorine, red = oxygen, blue = nitrogen, grey = carbon, white = hydrogen.

The unit cell packing arrangement consists of alternating layers of arylchloroantimonate and the pyridinium cation, Figure 3.3. The *p*-nitrophenylpentachloroantimonate anions are arranged in a zigzag configuration alternating through 90^{o}. In this configuration the aromatic ring systems between anions and between the anion and the cation are displaced so that π- π stacking interactions does not exist.

The *p*-nitro- group appears to have had little effect on the overall structure of the molecule as the bond lengths and angles are within agreement of previously published non-substituted arylchloroantimonates [26-28]. For some of the crystal structures published by Zaitseva *et al.* the phenyl ring system deviates from linearity and their unit cell packing configuration varies.

3.3 ESI-MS Analysis of Arylstibonic Acids

Electrospray ionisation (ESI) coupled with a high resolution time-of-flight (TOF) mass spectrometer was chosen as a practical technique for probing the solution behaviour of arylstibonic acids.

The sample introduction technique of electrospray ionisation is ideal as it is a relatively soft ionisation process resulting in very little sample fragmentation. This is in comparison to other ionisations processes such as inductively coupled plasma ionisation (ICP) where all molecular information is lost due to complete sample degradation. Electron ionisation (EI) is precluded by lack of volatility. ESI is particularly useful when analysing macromolecules as they have a tendency to fragment when ionised by other techniques.

The use of a high resolution time-of-flight mass spectrometer in conjunction with arylstibonic acids is exceptionally useful as antimony has a very distinctive isotope envelope pattern arising from its two stable isotopes, ^{121}Sb (57%) and ^{123}Sb (47%), Figure 3.4.

This characteristic pattern is immensely helpful with the assignment of peak envelopes, *i.e.* calculated isotope envelope *vs* experimental peak envelope. This pattern along with the mass difference of adjacent peaks within the envelope also allows for the protonation state of the species to be easily determined. This is one of the downfalls of other techniques such as X-ray crystallographic structural determinations where the protonation state and thus the associated charge of a species is not always intrinsically obvious [29].

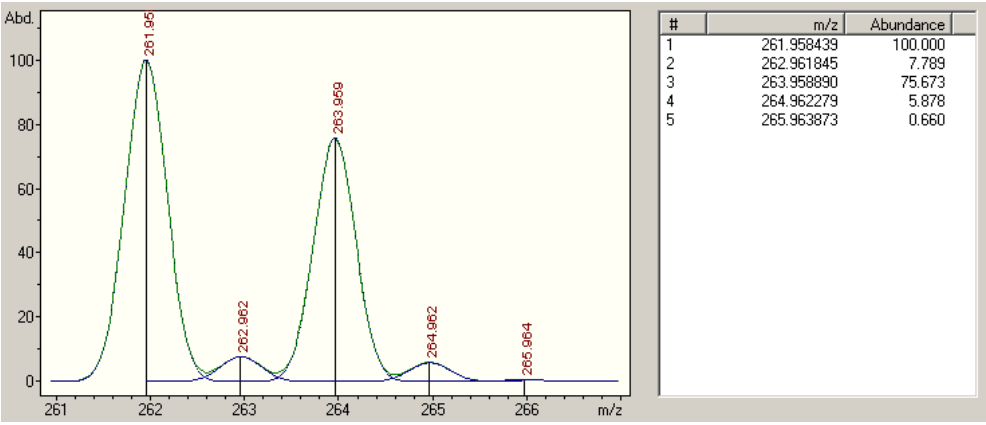

Figure 3.4: Calculated isotopic envelope for p-$MeC_6H_4SbO_3H_2$

ESI-MS data were collected using a Bruker MicrOTOF under standard operation conditions (Table 4), in negative ion mode. A small sample of each arylstibonic acid was dissolved in acetonitrile, centrifuged and injected into the spectrometer (180 µL/h), with the sample processed and spectra collected within 15 minutes of sample preparation. Although arylstibonic acids appear to be indefinitely stable in acetonitrile (see Section 3.3.5).

The instrument was calibrated prior to each use with Tune Mix (1:50, H_2O:90% MeCN). This offered quite a large range over which the instrument could be calibrated. Furthermore, as this was used instead of sodium formate, it also significantly reduced the amount of adventitious Na^+ contaminant within the instrument.

The accuracy of comparison between that of experimentally found values and calculated values was acceptable if it was ±0.020 m/z.

A summary appears in Table 5 of experimentally obtained values and their assignments, along with calculated values and relative intensities.

Table 4: Operating conditions of the Bruker MicrOTOF in negative ion mode

Acquisition parameter	*Low range*	*Wide range*	*High range*
Scan start	50 m/z	50 m/z	500 m/z
Scan end	1000 m/z	3000 m/z	3500 m/z
End plate offset	500 V	500 V	500 V
Nebuliser pressure	0.3 Bar	0.3 Bar	0.3 Bar
Dry gas flow rate	4.0 L/min	4.0 L/min	4.0 L/min
Dry temperature	200 ^{o}C	200 ^{o}C	200 ^{o}C
Capillary	4500 V	4500 V	4500 V
Capillary exit	-100 V	-150 V	-150 V
Skimmer 1	-33.3 V	-50 V	-50 V
Skimmer 2	-25.5 V	-25.5 V	-25.5 V
Hexapole 1	-25.5 V	-25.5 V	-25.5 V
Hexapole RF	80 Vpp	400 Vpp	800 Vpp
Lens 1 transfer	52.0 µs	88.0 µs	92.0 µs
Lens 1 pre pulse	1.0 µs	14.0 µs	14.0 µs
Corrector fill	53 V	53 V	53 V
Pulsar pull	395 V	395 V	395 V
Pulsar push	395 V	395 V	395 V
Reflector	1311 V	1311 V	1311 V
Flight tube	9000 V	9000 V	9000 V
Detector	1976 V	1976 V	1976 V

3.3.1 *para*-Chlorophenylstibonic Acid

Preliminary ESI-MS investigations into samples prepared using the Doak methodology show that *p*-chlorophenylstibonic acid was not present in solution as the previously described monomeric or trimeric species. There was an absence of significant peaks below m/z 1500. The monomeric $[(ClC_6H_4SbO_2)OH]^-$ and trimeric $[(ClC_6H_4SbO_2)_3OH]^-$ species would be evident as peaks at *ca* m/z 283 and *ca* m/z 813, respectively, but were absent.

A typical spectrum is shown in Figure 3.5 which suggested that arylstibonic acids exist in solution as high molecular weight species. Through the use of isotope patterns and peak spacing it was determined that the majority of species present were Sb_{12} clusters, with 1^- and 2^- charges. The highest intensity peak at m/z 1648.364 was assigned to $[Na_2H_4(RSb)_{12}O_{28}]^{2-}$ (calc. m/z 1648.356) and the peak at m/z 3275.755 equating to $[NaH_6(RSb)_{12}O_{28}]^-$ (calc. m/z 3275.738).

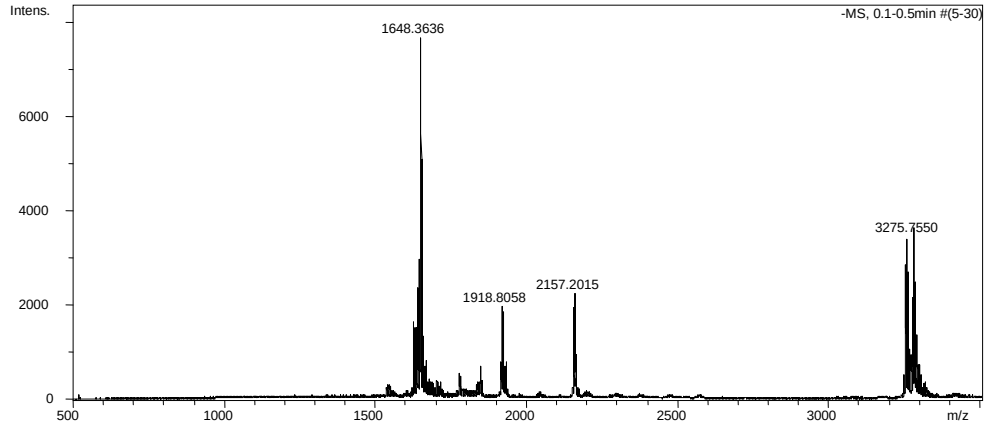

Figure 3.5: ESI-MS of p-$ClC_6H_4SbO_3H_2$ pre purification

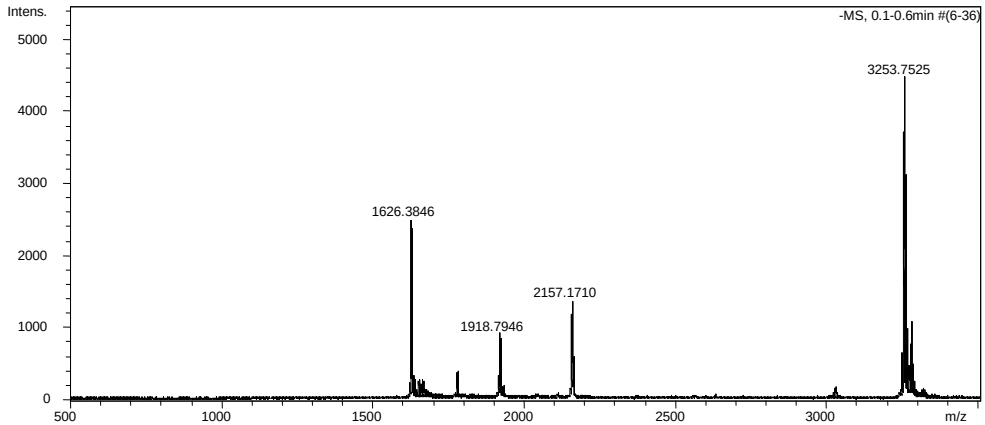

Figure 3.6: ESI-MS of p-$ClC_6H_4SbO_3H_2$ post purification

From the ESI-MS investigations it became apparent that the majority of species present in solution where those that had entrained sodium. It was not clear whether the sodium was only present as an associated species or if the arylstibonic acid was complexing with and using sodium as a nucleating agent. The latter would mean that the arylstibonic acid would not be in its true free acid form. Therefore the additional purification process as outlined in section 2.1 and discussed in section 3.1 was carried out in an attempt to remove as much Na^+ as possible.

Subsequent ESI-MS spectra of a sample of *p*-chlorophenylstibonic acid that had been further purified through the use of the ammonia/acetic acid diffusion showed that the resultant compound was particularly clean and free from impurities (Figure 3.6). More importantly, it showed that the procedure was successful in removing the majority of sodium.

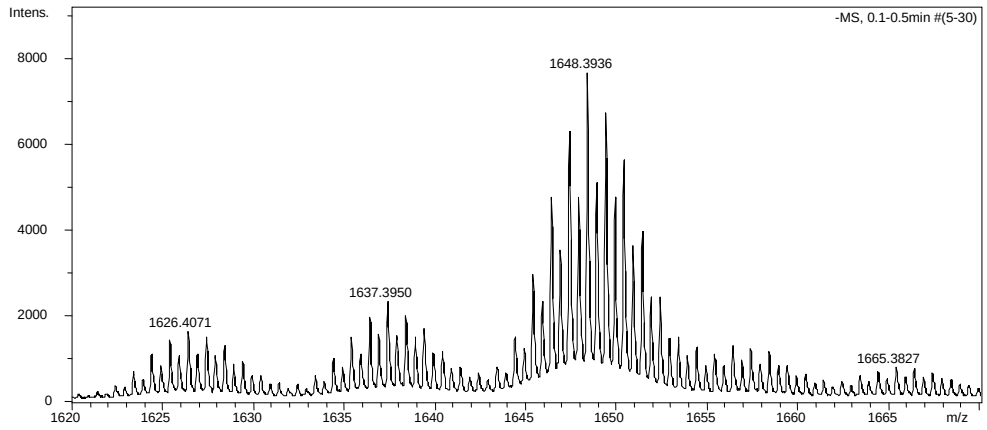

Figure 3.7: ESI-MS of p-$ClC_6H_4SbO_3H_2$ sodium adducts pre purification

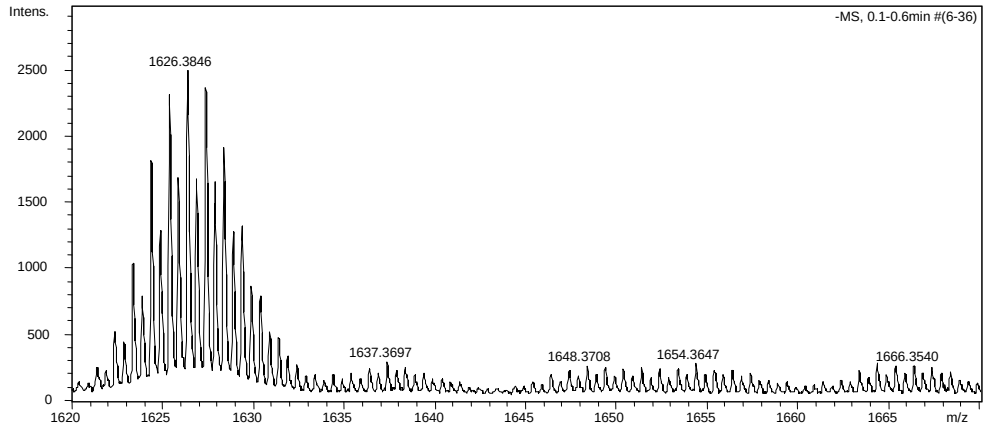

Figure 3.8: ESI-MS of p-$ClC_6H_4SbO_3H_2$ sodium adducts post purification

Figure 3.7 and 3.8 show the change in intensities of the sodium adducts and sodium-free species before and after the diffusion purification step. The peaks at

m/z 1626.385, m/z 1637.370 and m/z 1648.371 can be attributed to the following species, $[H_6(RSb)_{12}O_{28}]^{2-}$ (calc. m/z 1626.375), $[NaH_5(RSb)_{12}O_{28}]^{2-}$ (calc. m/z 1637.366) and $[Na_2H_4(RSb)_{12}O_{28}]^{2-}$ (calc. m/z 1648.356) respectively. The increase in intensity of the sodium-free species and the heavily reduced intensities of the sodium adducts can be attributed to the purification steps employed, justifying their inclusion.

The peak at m/z 3253.753 (Figure 3.9) is now the dominant one and can be assigned to $[H_7(ClC_6H_4Sb)_{12}O_{28}]^-$ (calc. m/z 3253.756), which is the singly charged $[H_6(RSb)_{12}O_{28}]^{2-}$ equivalent. This species also had only a small amount of the sodium adduct associated with it, evident by a weak peak at m/z 3275.747 ($[NaH_6(ClC_6H_4Sb)_{12}O_{28}]^-$ calc. m/z 3275.738).

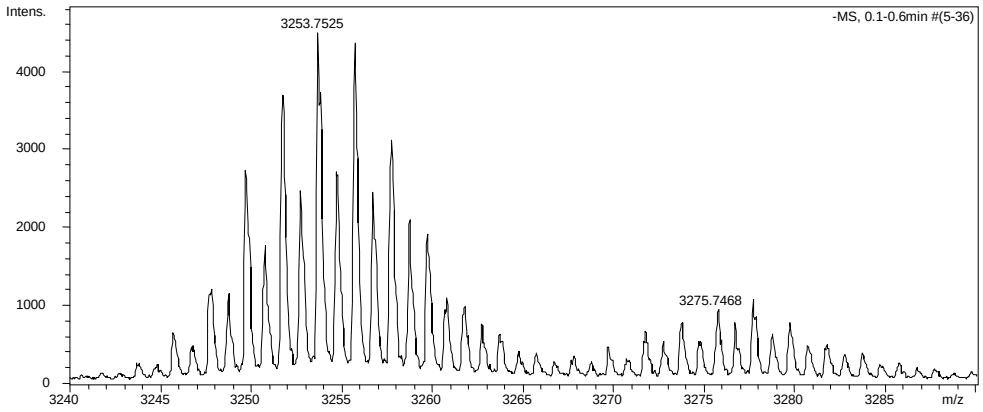

Figure 3.9: ESI-MS of $[H_7(ClC_6H_4Sb)_{12}O_{28}]^-$ post purification

There is supporting evidence of species that have various different nucleations. However, they were always minor components. Peaks at m/z 1777.345, 1918.795 and 2157.171 can be attributed to the following various species $[H_{10}(RSb)_{13}O_{32}]^{2-}$ (calc. m/z 1777.332), $[H_{10}(RSb)_{14}O_{34}.NH_3]^{2-}$ (calc. m/z 1918.792) and $[H_6(RSb)_{16}O_{36}]^{2-}$ (calc. m/z 2157.162) respectively. The entrainment of NH_3 in the Sb_{14} species can be attributed to the use of ammonia in the final purification procedure. These other species appear only as 2^- ions with no corresponding 1^- species. This is in contrast to the Sb_{12} species where the singly charged species dominate.

Thus it can be concluded that *p*-chlorophenylstibonic acid exists in acetonitrile solution as a high molecular weight cluster of formula $[H_8(ClC_6H_4Sb)_{12}O_{28}]$.

A full summary of the species present, their associated peaks, calculated values and relative intensities for this arylstibonic acid is in Table 5.

3.3.2 *para*-Tolylstibonic Acid

A sample of purified *p*-tolylstibonic acid was prepared for ESI-MS and processed to give the following characteristic spectrum (Figure 3.10).

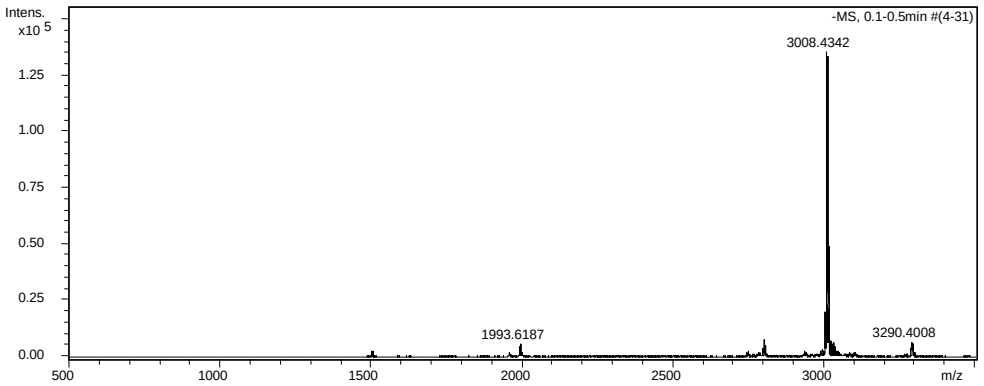

Figure 3.10: ESI-MS of p-$MeC_6H_4SbO_3H_2$

As for *p*-chlorophenylstibonic acid, any monomeric and trimeric species were absent. The only significant peak was m/z 3008.434 and thus could be assigned to $[H_7(MeC_6H_4Sb)_{12}O_{28}]^-$ (calc. m/z 3008.420). The corresponding 2^- ion $[H_6(MeC_6H_4Sb)_{12}O_{28}]^{2-}$ at 1503.719 (calc. m/z 1503.706) was extremely weak in comparison. Unlike the *p*-chloro- derivative, this arylstibonic acid appears to be completely free of sodium adducts (Figure 3.11).

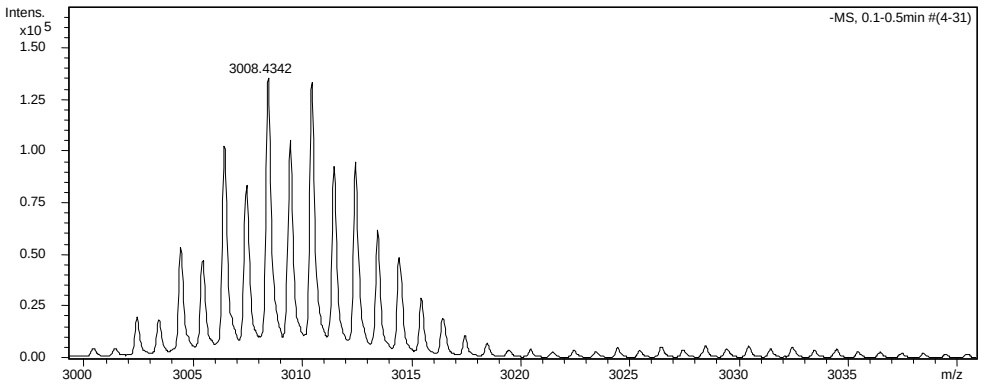

Figure 3.11: ESI-MS of $[H_7(MeC_6H_4Sb)_{12}O_{28}]^-$

As a very minor component, *p*-tolylstibonic acid also exhibits alternative nucleations but they vary in charge and aggregation. These include; $[H_6(RSb)_{16}O_{36}]^{2-}$ at m/z 1993.619 (calc. m/z 1993.604), $[H_{11}(RSb)_{11}O_{28}]^-$ at m/z 2800.503 (calc. m/z 2800.493) and $[H_{11}(RSb)_{13}O_{32}]^-$ at m/z 3290.401 (calc. m/z 3290.391).

As before, ESI-MS investigations of *p*-tolylstibonic acid lead to the conclusion that it exists as an aggregate of high molecular weight with the formula $[H_8(MeC_6H_4Sb)_{12}O_{28}]$.

See Table 5 for a full summary of the species present, their associated peaks, calculated values and relative intensities for *p*-tolylstibonic acid.

3.3.3 *para*-Nitrophenylstibonic Acid

Initial samples of *p*-nitrophenylstibonic acid produced the following representative spectrum (Figure 3.12). Again monomeric or trimeric species are nonexistent. The peaks that are present can be assigned to Sb_{12} cluster species, with the peaks at m/z 1133.353 and m/z 1711.517 arising from $[NaH_4(O_2NC_6H_4Sb)_{12}O_{28}]^{3-}$ (calc. m/z 1133.340) and $[Na_2H_4(O_2NC_6H_4Sb)_{12}O_{28}]^{2-}$ (calc. m/z 1711.505), respectively. As with the previously examined arylstibonic acids, the major species present are those that contain sodium ions.

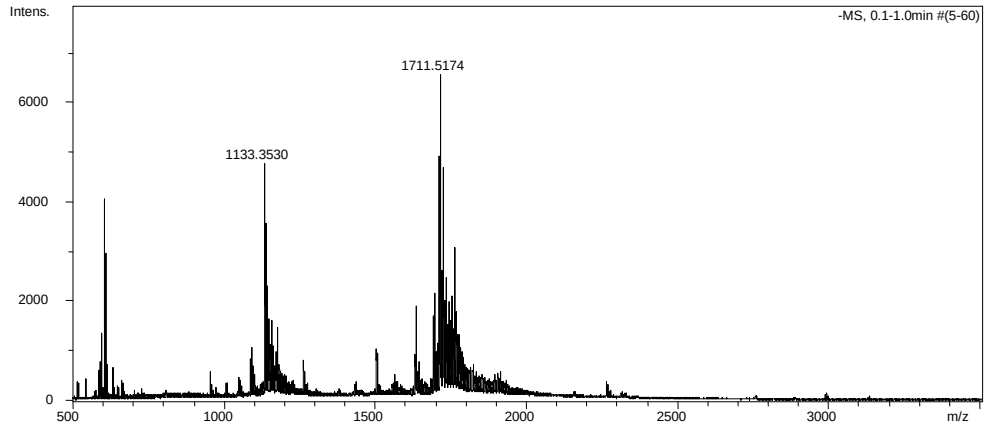

Figure 3.12: ESI-MS of p-$O_2NC_6H_4SbO_3H_2$ pre purification

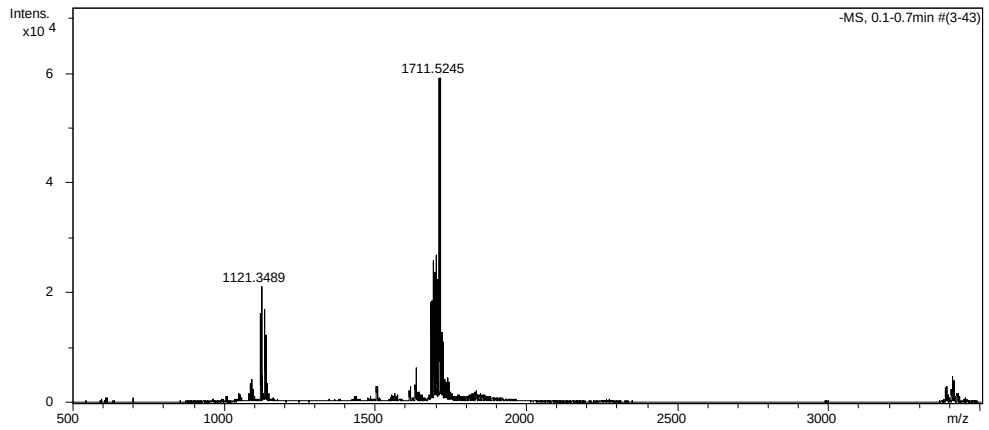

Figure 3.13: ESI-MS of p-$O_2NC_6H_4SbO_3H_2$ post purification

Since the additional ammonia/acetic acid diffusion step proved effective in removing sodium from other arylstibonic acids, it was also applied here. This resulted in a *p*-nitrophenylstibonic acid sample practically clean of the major impurities (Figure 3.13). However upon closer inspection, the main species present are still those of sodium adducts where the major peak remains $[Na_2H_4(O_2NC_6H_4Sb)_{12}O_{28}]^{2-}$ at m/z 1711.525. The peak at m/z 1121.349 is assigned as $[Na(O_2NC_6H_4Sb)_{12}O_{26}]^{3-}$ (calc. m/z 1121.333) which can be linked to the species present at m/z 1133.383 $[NaH_4(O_2NC_6H_4Sb)_{12}O_{28}]^{3-}$ in Figure 3.12 through loss of two water molecules. Even thought the peak at *ca* m/z 600 is in the correct mass range for a trimeric species, it is attributed to an impurity.

In an effort to remedy the inclusion of sodium and the formation of sodium adducts as the major species present in solution, additional steps were taken to halt their development. The sodium contaminant was undoubtedly being introduced during the hydrolysis step (see Equation 2) from sodium carbonate. So in its place, dilute ammonia was used. This alteration has been outlined in section 2.3 and discussed in section 3.1.

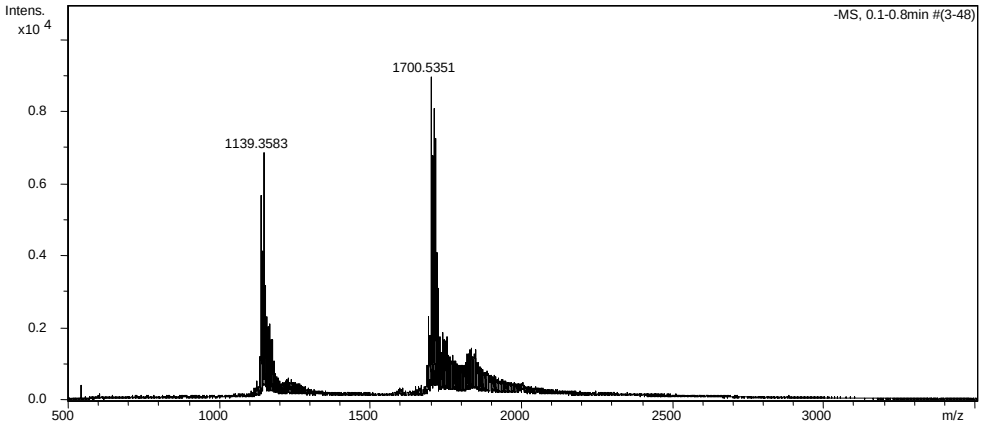

Figure 3.14: ESI-MS of p-$O_2NC_6H_4SbO_3H_2$ prepared using NH_3

This amendment resulted in the spectrum as shown in Figure 3.14. The principle species present are still those of sodium adducts, m/z 1700.535 = $[NaH_5(O_2NC_6H_4Sb)_{12}O_{28}]^{2-}$ (calc. m/z 1700.514) and m/z 1139.358 $[NaH_6(O_2NC_6H_4Sb)_{12}O_{29}]^{3-}$ (calc. m/z 1139.344) ($[NaH_4(O_2NC_6H_4Sb)_{12}O_{28}]^{3-}$ with the addition of a water molecule).). Nevertheless, the comparison of Figure 3.16 with Figure 3.15 showed that the sodium content had indeed been significantly reduced with the increased relative intensity of the mono sodium complex $[NaH_5(O_2NC_6H_4Sb)_{12}O_{28}]^{2-}$ at m/z 1700.535.

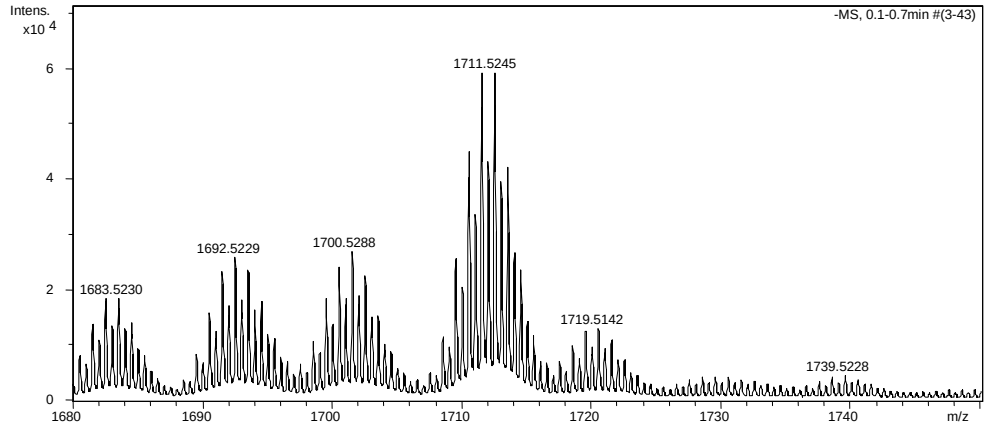

Figure 3.15: ESI-MS of p-$O_2NC_6H_4SbO_3H_2$ sodium adducts prepared using Na_2CO_3

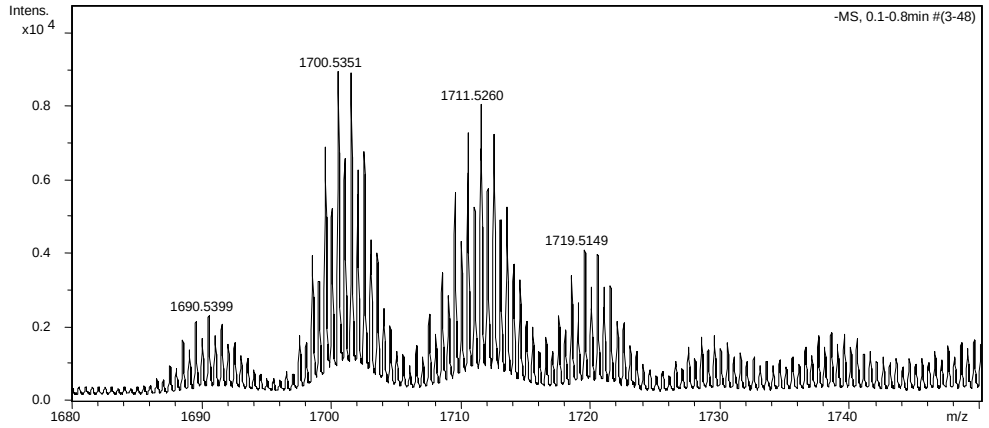

Figure 3.16: ESI-MS of p-$O_2NC_6H_4SbO_3H_2$ sodium adducts prepared using NH_3

Although the peak at m/z 1711.526 is in agreement with the calculated value of m/z 1711.505 for $[Na_2H_4(O_2NC_6H_4Sb)_{12}O_{28}]^{2-}$, the isotope pattern of the peak does not match the expected arrangement (*c.f.* isotope pattern of the peak at m/z 1700.535). This change in the isotope pattern could have arisen due to an overlapping of isotope patterns of different species present in solution, *e.g.* $[NaH_7(O_2NC_6H_4Sb)_{12}O_{29}]^{2-}$ at a calculated value of m/z 1709.519. Due to the slight ambiguity of this peak, it has been omitted from the summary of this arylstibonic acid in Table 5.

This ESI-MS investigation into the behaviour of *p*-nitrophenylstibonic acid showed that in acetonitrile it exists as $[H_8(O_2NC_6H_4Sb)_{12}O_{28}]$ or the corresponding Na^+ salts.

3.3.4 *α*-Naphthylstibonic Acid

As discussed in section 3.1, difficulties were encountered during the early stages of preparation for *α*-naphthylstibonic acid (outlined in section 2.4). Dilute nitric acid was used instead of dilute hydrochloric acid to acidify the sodium

carbonate solution. This alteration resulted in a compound with the following typical spectrum, Figure 3.17.

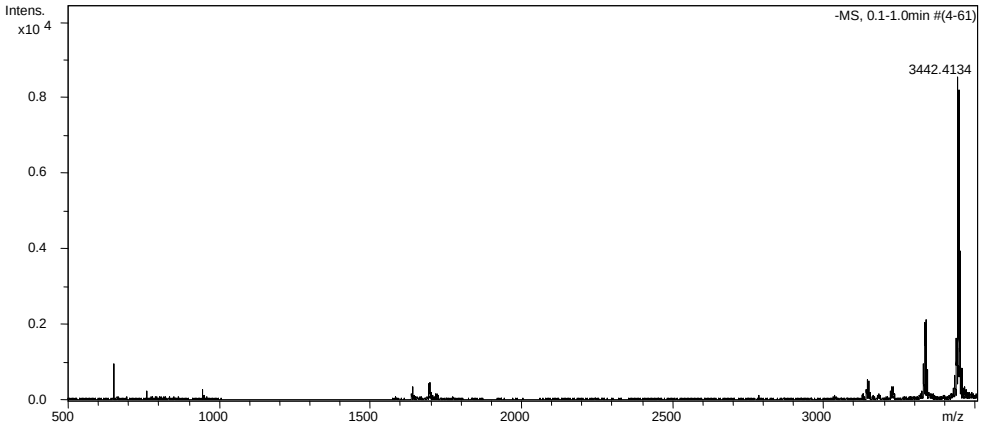

Figure 3.17: ESI-MS of α-$C_{10}H_7SbO_3H_2$

There is, once again, a complete absence of peaks containing Sb at lower mass. Instead the peak at m/z 3442.413 can be attributed to $[H_7(C_{10}H_7Sb)_{12}O_{28}]^-$ (calc. m/z 3442.422) which is again an Sb_{12} species. This arylstibonic acid, as with the *p*-methyl- derivative, appears to favour the loss of only one proton. For this example peaks associated with Sb_{11}, Sb_{13}, Sb_{14} and Sb_{16} species are completely absent. As the preparation of this arylstibonic acid gave a particularly low yield, this could be indicative of higher purity and account for the lack of species with differing nucleations.

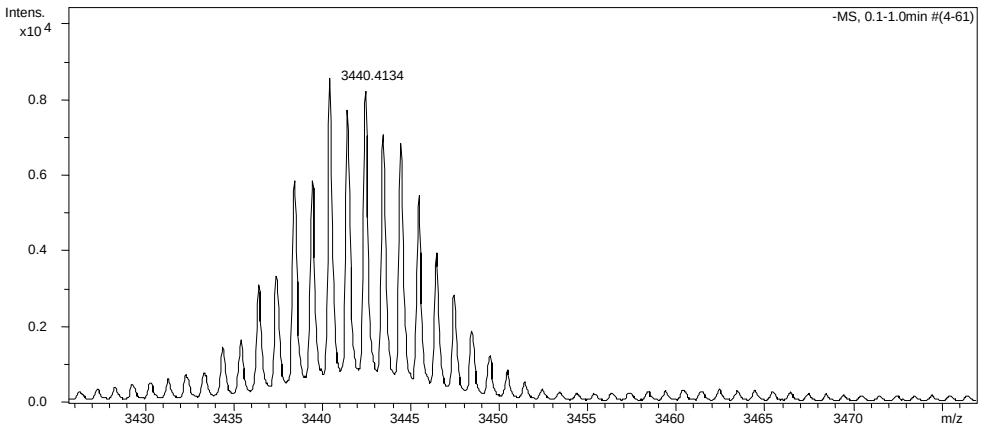

Figure 3.18: ESI-MS of $[H_7(C_{10}H_7Sb)_{12}O_{28}]^-$ pre purification

As previously discussed in section 3.1, Figure 3.18 shows that prior to purification the species present were relatively free of sodium with no unambiguously assignable peaks associated with sodium adducts. This in

conjunction with the relatively high purity suggested use of the additional purification procedure was unnecessary.

3.3.5 ESI-MS Injection Solvent

For the ESI-MS studies a suitable solvent was needed. The ideal solvent dissolves the substrate, encourages ionisation of neutral species but does not otherwise react with it, resulting in the unaltered transmission of molecular information present within the sample. Initially a range of solvents was taken to determine their viability for analysing arylstibonic acids. These tests were run mainly using *p*-chlorophenylstibonic acid (R = *p*-ClC_6H_4-).

Investigations into arylstibonic acids using ESI-MS in positive ion mode showed that significant ions were present but negative ion spectra were more intense and allowed the majority of information to be harvested. This could be attributed to the fact that all species present were acids so readily underwent proton loss.

3.3.5.1 Solvent Effect

- MeCN

Samples prepared using acetonitrile produced spectra with $[H_7(RSb)_{12}O_{28}]^-$ (m/z 3253.762, calc m/z 3253.756) and $[H_6(RSb)_{12}O_{28}]^{2-}$ (m/z 1626.384, calc m/z 1626.375) as the major species, together with adduct ions such as $[NaH_5(RSb)_{12}O_{28}]^{2-}$. In comparison to other solvents, acetonitrile resulted in very clean spectra of relatively high intensities with very little noise.

- MeOH

Similarly to acetonitrile, methanol resulted in spectra with $[H_7(RSb)_{12}O_{28}]^-$ (m/z 3253.748, calc m/z 3253.756) and $[H_6(RSb)_{12}O_{28}]^{2-}$ (m/z 1626.384, calc m/z 1626.375) as the dominant species present, with the inclusion of similar adduct ions and overall intensities.

- MeOH/H_2O (1:1)

Spectra show the presence of $[H_7(RSb)_{12}O_{28}]^-$ (m/z 3253.774, calc. m/z 3253.756) and $[H_6(RSb)_{12}O_{28}]^{2-}$ (m/z 1626.395, calc. m/z 1626.375) but water

appears to have resulted in a decreased signal to noise ratio, possibly as a result of lower solubility.

- THF

Tetrahydrofuran brought about sample degradation with a broad range of peaks between m/z 500 and m/z 1000 and with no significant peaks above m/z 1000. Peaks that were present showed an isotope pattern associated with a single antimony being present within the species. Overall tetrahydrofuran produced spectra with relatively weak intensities.

- 1,2-dichloroethane

This non-basic solvent resulted in a particularly clean spectrum that only showed $[H_7(RSb)_{12}O_{28}]^-$ (m/z 3253.769, calc. m/z 3253.756), but with comparatively weak intensities. Again this could possibly be because of lower solubility.

3.3.5.2 Time Effect

Next, samples were left in solution (t = 48 h) before further spectra were collected. This was done to determine how stable arylstibonic acids were in the solvents over a period of time.

- MeCN

Very little change in spectra *vs* time, the only significant difference being a change in relative intensities of the dominant peaks, $[H_7(RSb)_{12}O_{28}]^-$ (m/z 3253.769, calc. m/z 3253.756) and $[H_6(RSb)_{12}O_{28}]^{2-}$ (m/z 1626.391, calc. m/z 1626.375), from 2:3 to 1:1, respectively.

- MeOH

The original $[H_7(RSb)_{12}O_{28}]^-$ and $[H_6(RSb)_{12}O_{28}]^{2-}$ species were no longer present. In their place methanol had formed esters with the sample, $[H_6(RSb)_{12}O_{28}(OMe)]^-$ (m/z 3267.789, calc. m/z 3267.772) and $[H_5(RSb)_{12}O_{28}(OMe)]^{2-}$ (m/z 1633.400, calc. m/z 1633.382), of similar intensities to the original peaks.

- 1,2-dichloroethane

The spectrum was still particularly clean consisting of only $[H_7(RSb)_{12}O_{28}]^-$ (m/z 3253.772, calc. m/z 3253.756) with weak intensity.

3.3.5.3 Discussion

When analysing arylstibonic acids by ESI-MS, the use of acetonitrile and methanol as a matrix injection solvent both produced clean spectra with high relative intensities. However, the slow formation of esters with methanol over time by replacement of Sb-O-OH with Sb-O-Me added complexity. Since molecular species in acetonitrile appear to be stable over an extended period, this has subsequently been used as the solvent of choice.

3.3.6 ESI-MS Summary and Discussion

Table 5: Negative ion ESI-MS data for arylstibonic acids in MeCN

(m/z; found, (calculated), relative intensity (s = strong, m= medium, w = weak))

	Molecular formula	R = *p*-ClC_6H_4-	R = *p*-$H_3CC_6H_4$-	R = *p*-$O_2NC_6H_4$-	R = α-$C_{10}H_7$-
1^- ions	$[H_{11}(RSb)_{11}O_{28}]^-$		2800.503 (2800.493) w		
	$[H_7(RSb)_{12}O_{28}]^-$	**3253.753 (3253.756) s**	**3008.434 (3008.420) s**		**3442.413 (3442.422) s**
	$[NaH_6(RSb)_{12}O_{28}]^-$	3275.747 (3275.738) w			
	$[H_{11}(RSb)_{13}O_{32}]^-$		3290.401 (3290.391) w		
2^- ions	$[H_6(RSb)_{12}O_{28}]^{2-}$	1626.385 (1626.375) m	1503.719 (1503.706) w		
	$[NaH_5(RSb)_{12}O_{28}]^{2-}$	1637.370 (1637.366) w		**1700.535 (1700.514) s**	
	$[Na_2H_4(RSb)_{12}O_{28}]^{2-}$	1648.371 (1648.356) w			
	$[H_{10}(RSb)_{13}O_{32}]^{2-}$	1777.345 (1777.332) w			
	$[NH_{13}(RSb)_{14}O_{34}]^{2-}$	1918.795 (1918.792) w			
	$[H_6(RSb)_{16}O_{36}]^{2-}$	2157.171 (2157.162) w	1993.619 (1993.604) w		
3^- ions	$[H_5(RSb)_{12}O_{28}]^{3-}$				
	$[NaH_4(RSb)_{12}O_{28}]^{3-}$			1133.354 (1133.340) w	
	$[H_7(RSb)_{12}O_{29}]^{3-}$				
	$[NaH_6(RSb)_{12}O_{29}]^{3-}$			1139.359 (1139.344) m	
	$[Na_2H_5(RSb)_{12}O_{29}]^{3-}$			1146.688 (1146.671) s	
	$[Na_2H_7(RSb)_{12}O_{30}]^{3-}$			1152.681 (1152.674) w	
	$[Na_2H_9(RSb)_{12}O_{31}]^{3-}$			1158.676 (1158.678) w	

Table 5 shows how the seemingly minor alteration of the substituent on the phenyl ring has a significant effect on the behaviour of arylstibonic acids. The *p*-chloro-, *p*-tolyl- and *α*-naphthylstibonic acids share a similarity in that they all favour the same dominant species ($[H_7(RSb)_{12}O_{28}]^-$, the peaks in bold for each arylstibonic acid represent the dominant species present) but the similarities end there. The Sb_{12} species of *p*-chloro- and *p*-tolylstibonic acid also appear to be stable with a higher degree of deprotonation resulting in two associated negative charges, but with the *p*-tolylstibonic derivative having significantly less sodium entrained. These two arylstibonic acid derivatives also form stable clusters of alternative nucleations *i.e.* the Sb_{16} species $[H_6(RSb)_{16}O_{36}]^{2-}$, but differ in which nucleations they form and the degree of deprotonation. All of these alternative nucleations are a minor component and are relatively weak in comparison to the dominant Sb_{12} species. In contrast the *p*-nitro- and *α*-naphthylstibonic acid derivatives only favour the formation of Sb_{12} clusters.

The *p*-nitrophenylstibonic acid has shown a persistent affinity for complexing in the presence of sodium, proof of which is that only sodium adduct species are present when analysed with ESI-MS. The inclusion of the unobserved species $[H_5(RSb)_{12}O_{28}]^{3-}$ and $[H_7(RSb)_{12}O_{29}]^{3-}$ (which are related through the loss/gain of a water molecule) in Table 5 is done so as to indicated this. *p*-Nitrophenylstibonic acid also favours higher degrees of deprotonation compared to the other arylstibonic acids investigated. It is not known whether the inclusion of sodium is responsible for the higher degree of ionisation.

The tendency of these arylstibonic acids towards their favoured degree of deprotonation shows that their relative acidity appears to be in the order of *p*-NO_2- > *p*-Cl- > *p*-Me- = *α*-$C_{10}H_7$-. This trend makes sense as it parallels the electronic trend of the substituents, although this is somewhat qualitative as the exact pH in solution is unknown since the samples were run in acetonitrile because of their limited solubility in water.

This investigation into arylstibonic acids through the use of ESI-MS has shown that even with differing substituents on the phenyl ring, they all exist as high molecular weight clusters with the nominal formula $H_8(RSb)_{12}O_{28}$, where R = *p*-ClC_6H_4-, *p*-$H_3CC_6H_4$-, *p*-$O_2NC_6H_4$- and *α*-$C_{10}H_7$-.

3.3.7 ESI-MS of other Arylstibonic Acids

Recent developments by Rishi *et al.* illustrated the ability of twelve arylstibonic acids to bind to B-ZIP dimers and, as a result, disrupt DNA binding [30]. The arylstibonic acids used in this investigation along with those used by Simmons and McCloud [31] were procured from the National Cancer Institute repository. The majority of these were synthesised in the 1940's with varying degrees of purity (R. H. Shoemaker, personal communication, 2010). In an effort to broaden the ESI-MS investigation of arylstibonic acid in this thesis, samples were requested and obtained from the Chemotherapeutic Agents Repository (Drug Synthesis and Chemistry Branch, National Cancer Institute, Rockville, MD).

Some of the arylstibonic acids were chosen to allow further investigation into the effect of steric hindrance on the formation of polyoxometalates, *i.e. p*-nitro- *vs* *m*-nitro and *o*-nitro-phenylstibonic acid. Some of the samples were acquired in an effort to alleviate the problem of the arylstibonic acids investigated thus far having very limited water solubility. This would allow for investigations into the effect of pH on aggregate formation to be carried out.

Initially, ESI-MS analyses were carried out under the same conditions used previously (Section 3.3). The results are compiled in Table 6.

Table 6: Negative ion ESI-MS data for arylstibonic acids obtained from NCI

Arylstibonic acid[I]	*NCI #*	*Solvent*	*Molecular formula, m/z*[II]	
R = *p*-Cl-*m*-$O_2NC_6H_4$-	13735	MeCN	$[H_6(RSb)_{12}O_{28}]^{2-}$	**1896.280 (1896.285) s**
			$[NaH_5(RSb)_{12}O_{28}]^{2-}$	1907.271 (1907.276) w
			$[H_6(RSb)_{13}O_{30}]^{2-}$	2051.723 (2051.725) m
		H_2O	-	-
R = *o*-$O_2NC_6H_4$-	13742	MeCN	$[H_7(RSb)_{12}O_{28}]^{-}$	**3402.074 (3402.034) s**
		H_2O	-	-
R = *m*-$O_2NC_6H_4$-	13743	MeCN	$[H_7(RSb)_{12}O_{28}]^{-}$	**3380.069 (3380.053) s**
			$[NaH_6(RSb)_{12}O_{28}]^{-}$	3402.042 (3402.034) w
			$[H_6(RSb)_{12}O_{28}]^{2-}$	1689.525 (1689.523) w
			$[H_4(RSb)_{13}O_{29}]^{2-}$	1818.981 (1818.977) w
			$[H_6(RSb)_{13}O_{30}]^{2-}$	1327.988 (1827.982) w
		H_2O	-	-
R = *p*-$HO_3SC_6H_4$-	13746	MeCN	-	-
		H_2O	$[H(RSb)O_3]^{-}$	**326.886 (326.893) s**
R = *p*-$(H_2N)O_2SC_6H_4$-	13748	MeCN	$[H_6(RSb)_{12}O_{28}]^{2-}$	1894.458 (1894.448) w
			$[NaH_5(RSb)_{12}O_{28}]^{2-}$	1905.457 (1905.439) w
			$[Na_2H_4(RSb)_{12}O_{28}]^{2-}$	1916.444 (1916.430) w
			$[NaH_4(RSb)_{12}O_{28}]^{3-}$	1269.966 (1269.957) w
			$[Na_2H_3(RSb)_{12}O_{28}]^{3-}$	1277.299 (1277.284) w
			$[Na_2H_5(RSb)_{12}O_{29}]^{3-}$	1283.306 (1283.288) w
			$[H_5(RSb)_{16}O_{36}]^{3-}$	1675.851 (1675.838) m
			$[NaH_4(RSb)_{16}O_{36}]^{3-}$	**1683.182 (1683.165) s**
			$[Na_2H_3(RSb)_{16}O_{36}]^{3-}$	1690.510 (1690.492) m
			$[Na_2H_7(RSb)_{16}O_{38}]^{3-}$	1702.504 (1702.499) w
		H_2O	$[H(RSb)O_3]^{-}$	**325.901 (325.909) s**
			$[H_3(RSb)O_4]^{-}$	343.910 (343.919) w
			$[H_5(RSb)O_5]^{-}$	361.923 (361.930) m
			$[H(RSb)_2O_5]^{-}$	636.815 (636.815) m
			$[H_3(RSb)_2O_6]^{-}$	654.825 (654.825) m
			$[H_5(RSb)_{16}O_{36}]^{3-}$	1675.873 (1675.838) w
			$[H_4(RSb)_{16}O_{36}]^{4-}$	1256.660 (1656.626) w

Arylstibonic acid[I]	*NCI #*	*Solvent*	*Molecular formula, m/z*[II]	
R = *p*-[(HOC_2H_4)NH]$O_2SC_6H_4$-	13776	MeCN	-	-
		H_2O	$[H(RSb)O_3]^-$	369.925 (369.935) w
			$[H_3(RSb)O_4]^-$	387.935 (387.945) w
			$[H_5(RSb)O_5]^-$	**405.946 (405.956) s**
R = *o*-(HO_2CCHCH)C_6H_4-	13778	MeCN	-	-
		H_2O	-	-
R = *p*-(HOC_2H_4NH)C(O)C_6H_4-	13782	MeCN	-	-
		H_2O	-	-

[I] Of nominal formula $RSbO_3H_2$.

[II] m/z; found, (calculated), relative intensity (s = strong, m = medium, w = weak).

3.3.7.1 Discussion

These results lead to similar conclusions to the investigations previously carried out with the other arylstibonic acids synthesised for this thesis project (see section 3.3.6). In acetonitrile, the *o*-nitro-, *m*-nitro- and *p*-chloro-*m*-nitro-derivatives appear to similarly aggregate favouring the formation of Sb_{12} clusters, while the last of the three examples has a slightly elevated propensity to form Sb_{13} clusters. This may in part be due to electronic considerations brought about by the inclusion of multiple substituents. If this attribute was because of steric considerations then similar results should be observed for the *meta* substituted nitro derivative, but this is not the case. The *p*-chloro- substituent would have a negligible effect on steric considerations due in part to its relative position and size.

The *p*-HO_3S- and *p*-[(HOC_2H_4)NH]O_2S- arylstibonic acids gave no equivalent Sb_{12} aggregates in acetonitrile which may possibly be due to their limited solubility. Conversely, their relatively high solubility in water facilitated their further investigation. This gave rise to peaks associated with their respective monomers $[H(RSb)O_3]^-$.

p-Sulfamoylphenylstibonic acid (*p*-(H_2N)O_2S-) appears to behave differently to other arylstibonic acids examined previously. In both acetonitrile and water it gives rise to peaks associated with Sb_{16} clusters as the dominant species. In this case the bulky substituent may result in greater steric interactions thus destabilising the lower Sb_{12} aggregations and now favouring the higher Sb_{16}

aggregation. The monomeric equivalent of this derivative also starts to appear, increasing in relative intensity with time, when analysed in conjunction with water. This anomalous behaviour of arylstibonic acids in water subsequently lead onto the investigations carried out in the following section, 3.3.8.

3.3.8 Stability of Polyoxostibonates

The results from sections 3.3.6 and 3.3.7 along with the conclusion that arylstibonic acids exist as high molecular weight clusters of the formula $[H_8(RSb)_{12}O_{28}]$, appears initially to disagree with the results published by Simmons and McCloud [31]. They used HPLC/ESI-MS to analyse a range of arylstibonic acids and concluded that they exist as monomers. However, the analyses they carried out were done by dissolving the arylstibonic acids in 0.05 M NaOH with stirring for 30 min at 45^{o}C. This solution was then run using a mobile phase of NH_4OAc buffered with NH_4OH to pH 9.

Under these conditions it appeared that the high molecular weight aggregates were hydrolysing to the monomeric form. In an effort to confirm this hypothesis a sample of *p*-chlorophenylstibonic acid was exposed to the same conditions (0.05 M NaOH, 30 min at 45^{o}C). ESI-MS analysis of the solution gave the following spectra (Figure 3.19 and 3.20).

These resultant spectrum showed the decrease in intensities of peaks related to arylstibonic acid aggregates, *i.e.* the complete absence of Sb_{12}^{-} species and the reduction of Sb_{12}^{2-} species (m/z 1659.363 = $[Na_3H_3(RSb)_{12}O_{28}]^{2-}$ calc. m/z 1659.347). Also the unexpected formation of previously unseen 3^{-} species for this arylstibonic acid, the peak at m/z 1123.924 can be assigned to $[Na_3H_8(RSb)_{12}O_{31}]^{3-}$ (calc. m/z 1123.906). More importantly, the formation of monomeric species is observed. The peaks at m/z 282.899, 298.910 and 318.923 can be attributed to monomeric species with varying degrees of hydration, $[H(RSbO_2)O]^{-}$ (calc. m/z 282.897), $[H_3(RSbO_2)O_2]^{-}$ (calc. m/z 298.908) and $[H_5(RSbO_2)O_3]^{-}$ (calc. m/z 318.918) respectively. Over a period of time the monomeric species increase further in intensity and the aggregate species decrease proportionally to this.

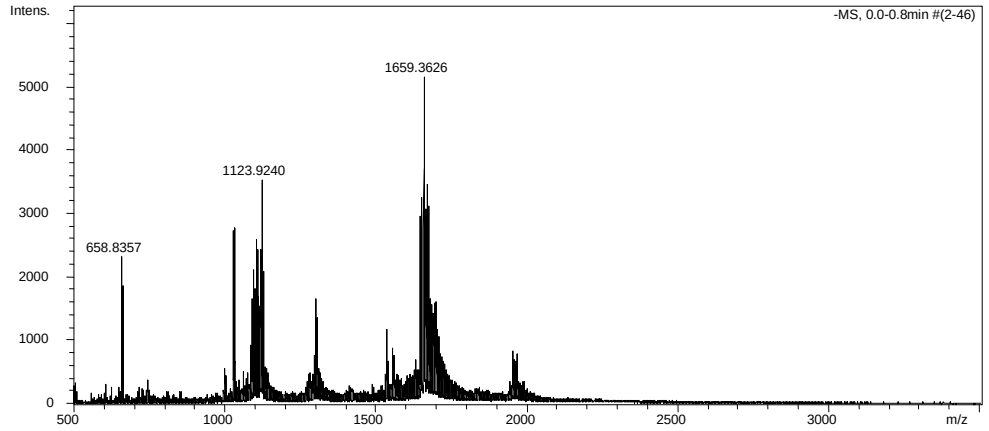

Figure 3.19: ESI-MS of p-$ClC_6H_4SbO_3H_2$ in 0.05 M NaOH

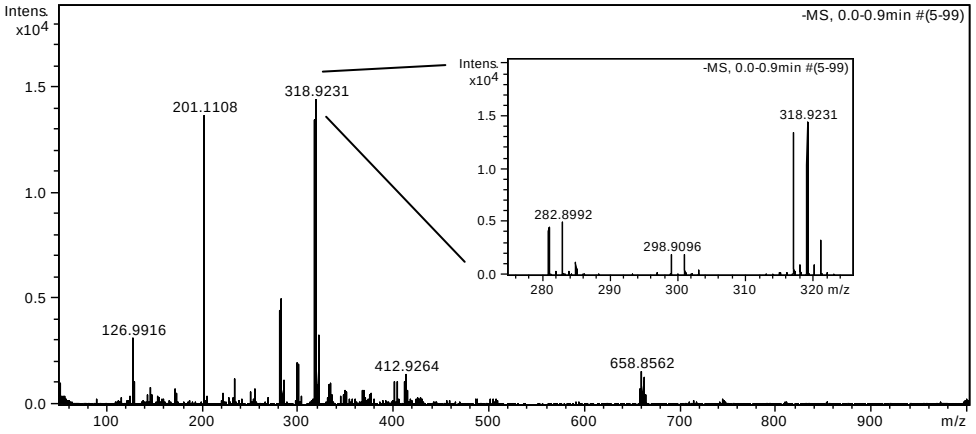

Figure 3.20: ESI-MS of p-$ClC_6H_4SbO_3H_2$ in 0.05 M NaOH, low mass

As a comparative exercise to further confirm the relatively high stability of arylstibonic acids aggregates in acetonitrile, a 1:1 mole ratio mixture of *p*-chlorophenyl- and *p*-tolyl-stibonic acid were dissolved in acetonitrile and observed over a period of one week. ESI-MS was used to examine the solution for any mixing of the two arylstibonic acids (Figure 3.21 and 3.22).

Initially no mixing of the two arylstibonic acids was observed, where all major peaks could be assigned to individual arylstibonic species, m/z 1599.367 ($[(ClC_6H_4Sb)_{12}O_{25}]^{2-}$ calc. m/z 1599.357), m/z 1874.269 ($[H_2(ClC_6H_4Sb)_{14}O_{26}]^{2-}$ calc. m/z 1874.257), m/z 2157.177 ($[H_6(ClC_6H_4Sb)_{16}O_{28}]^{2-}$ calc. m/z 2157.162), m/z 3253.760 ($[H_7(ClC_6H_4Sb)_{12}O_{28}]^{-}$ calc. m/z 3253.756) and m/z 3008.435 ($[H_7(MeC_6H_4Sb)_{12}O_{28}]^{-}$ calc. m/z 3008.420).

Upon allowing the solution to stand at room temperature for a week there was very little noticeable difference compared to when the mixture was first made. There was a slight change in the relative intensities of the species present, but no peaks indicating the formation of mixed species aggregates.

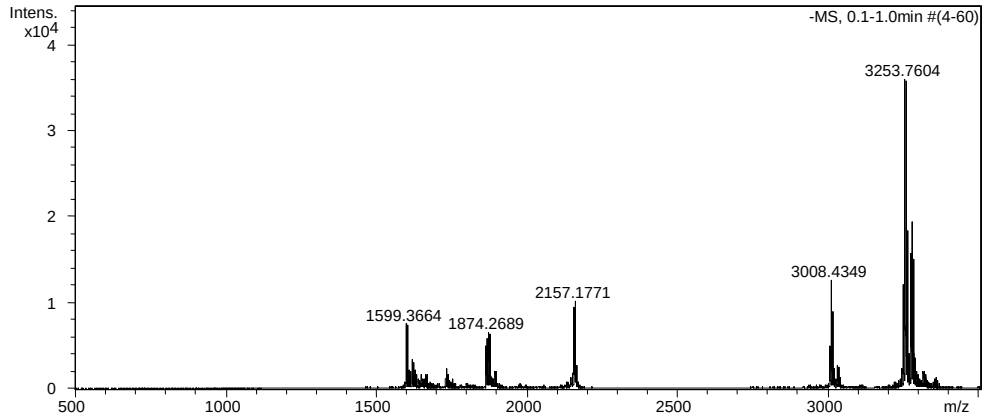

Figure 3.21: ESI-MS of arylstibonic acid mixture, t = 30 min

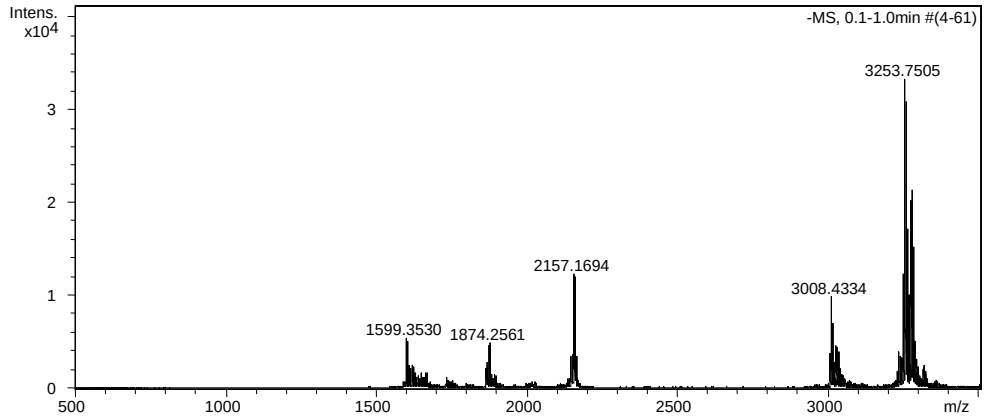

Figure 3.22: ESI-MS of arylstibonic acid mixture, t = 1 week

These results confirmed that in water arylstibonic acids hydrolyse to their monomeric form, aided by an increase in pH, while arylstibonic acids are indefinitely stable in acetonitrile. This also accounts for the results observed by Simmons and McCloud.

3.4 Elemental Analysis

Microanalytical data for each compound are included in Chapter 2 of this thesis under their respective experimental procedure sections. The samples were prepared for analysis by leaving them to dry for 24 h in an evacuated desiccator.

Data was obtained for carbon, hydrogen and in some cases, nitrogen. Along with their experimentally acquired values, the expected values for their respective monomeric and cluster forms have been calculated. The cluster form is that of the dodeca-nuclear aggregation $[H_8(RSb)_{12}O_{28}]$ as indicated by the ESI-MS investigations.

Values for the sodium adduct of *p*-nitrophenylstibonic acid ($[NaH_5(O_2NC_6H_4Sb)_{12}O_{28}]$) have also been calculated (C 25.40, H 1.63, N 4.94) but excluded from the table as the experimental values are in better agreement with the non-sodium adduct cluster despite ESI-MS investigations indicating otherwise. The naphthylstibonic acid is not quite within agreement of the calculated values but this could possibly be due to entrainment of water molecules in the sample.

Table 7: Elemental analysis data for arylstibonic acids

Arylstibonic Acid[III]	R = *p*-chloro-	R = *p*-tolyl-	R = *p*-nitro-	R = *α*-naphthyl-
C (found, %)	**26.93**	**33.35**	**26.11**	**38.80**
C (calc., mono., %)	25.44	31.98	24.52	40.18
C (calc., cluster, %)	26.56	33.51	25.57	41.86
H (found, %)	**2.46**	**3.49**	**2.76**	**2.55**
H (calc., mono., %)	2.13	3.46	2.06	3.03
H (calc., cluster, %)	1.73	3.08	1.67	2.69
N (found, %)			**4.76**	
N (found, %)[IV]			4.62	
N (calc., mono., %)			4.77	
N (calc., cluster, %)			4.97	
Sb (found %)[IV]	**40.2**	**46.3**	**38.7**	
Sb (calc., mono., %)	42.98	46.31	41.43	40.73
Sb (calc., cluster, %)	44.88	48.53	43.20	42.44

[III] Of nominal formula $RSbO_3H_2$.

[IV] Results obtained by Doak [14].

These values show that the C, H (and N) elemental analysis of the arylstibonic acids investigated in this thesis are in better agreement with the aggregated Sb_{12} clusters than the monomeric form. This is in further agreement with the results obtained through ESI-MS analysis. However, uncertainty in the degree of hydration precludes definite conclusions.

Also given in the Table are the Sb values reported for these acids by Doak. These tend to be generally lower than expected for either formula, which may reflect difficulties with accurate analysis with the methods of the time.

3.5 IR Analysis

Infrared spectroscopy was used to analyse the arylstibonic acids investigated within this thesis. IR data for each of the arylstibonic acids is included in Chapter 2 under their respective sections. The IR analysis of *p*-chlorophenylstibonic acid resulted in the following spectrum and assignment [32], Figure 3.23

The broad peak at *ca* 3400-3000 cm^{-1} is attributed to an O-H stretch and the peak at *ca* 1630 cm^{-1} is an H-O-H bending frequency. There is a noticeable difference in %T of these two peaks, with the O-H stretch being the dominant peak. This implies that the dominant hydroxide functional group present is that of terminal –O-H and not water. If water were present in a higher abundance then the bending frequency would be much stronger. The aromatic portion of the compound gave rise to peaks in the region around *ca* 1440 cm^{-1}. This varies slightly between compounds due to the different substituents. The peak at *ca* 730 cm^{-1} is attributed to the presence of Sb-O bonds while the peak at *ca* 490 cm^{-1} is due to a Sb-C bond.

Similar assignments can be made for the spectra of the other arylstibonic acids, which are included in the appendix, Figure 9.1-9.3.

Very little additional information was gained from IR analysis as the compounds are comparatively similar, only varying in their phenyl ring substituents.

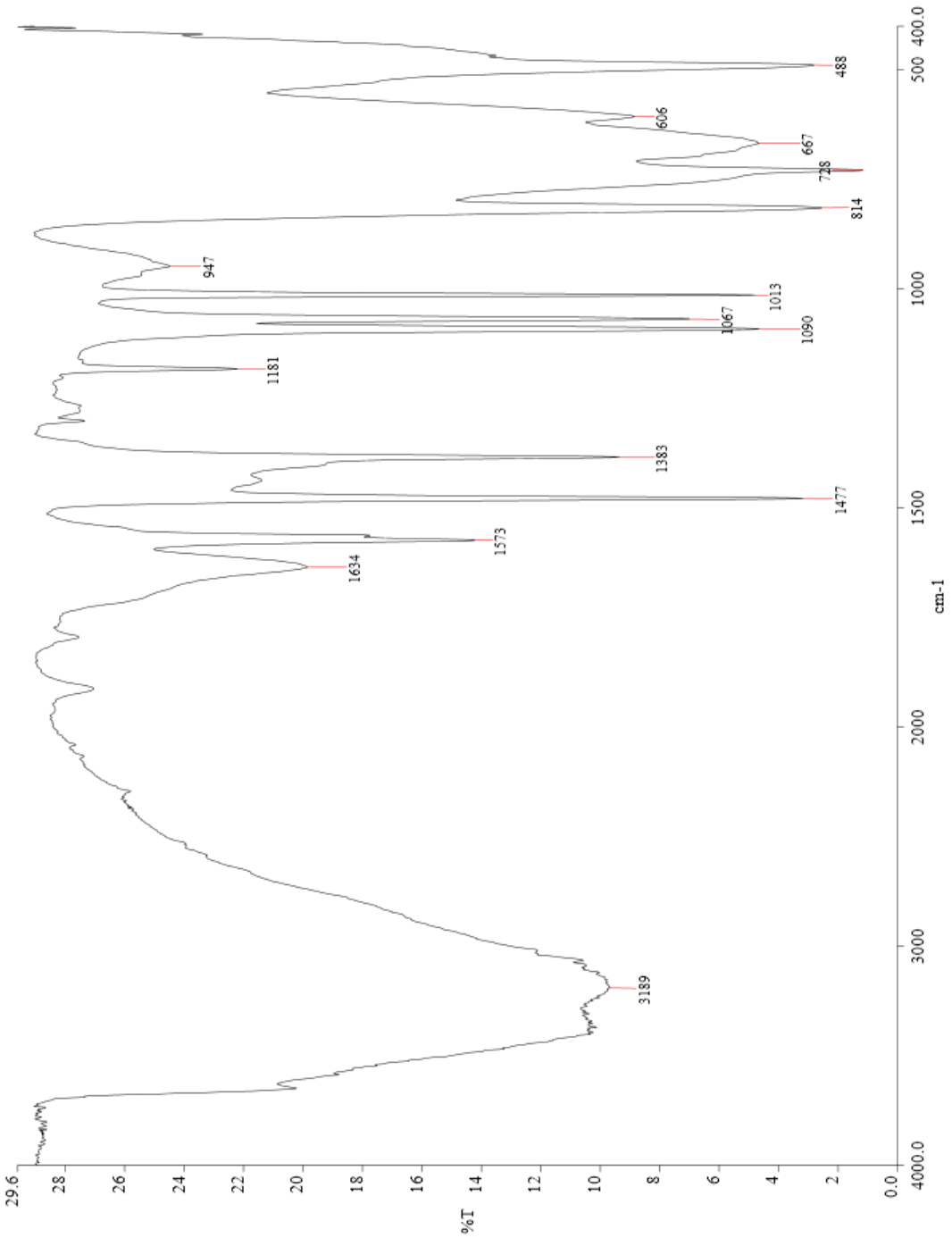

Figure 3.23: IR spectrum of p-chlorophenylstibonic acid

4 Derivatives of Arylstibonic Acids with Metal Ions

From the ESI-MS investigations into arylstibonic acids it became apparent that they displayed a strong affinity for cations, Na^+ in particular. To gauge the extent of the tendency and as a guide to parallel studies aimed at crystallising salts for X-ray studies. An ESI-MS survey of arylstibonic acids in the presence of other cations was performed.

The arylstibonic acid (usually *p*-chlorophenylstibonic acid) was prepared in a solution of acetonitrile for ESI-MS as previously described, section 3.3. The cations were then added to this solution as either oxide or hydroxide unless otherwise stated. A wide variety of cations were selected, ranging from M^+ to M^{4+}.

4.1.1 M^+ Ions

- Caesium

Addition of caesium hydroxide to a solution of *p*-chlorophenylstibonic acid resulted in the formation of $[CsNaH_9(RSb)_{12}O_{31}]^{3-}$ (m/z 1153.211, calc. m/z 1153.218), $[Cs_2NaH_6(RSb)_{12}O_{30}]^{3-}$ (m/z 1191.195, calc. m/z 1191.180), $[CsNaH_4(RSb)_{12}O_{28}]^{2-}$ (m/z 1703.318, calc. m/z 1703.314) and $[Cs_2H_4(RSb)_{12}O_{28}]^{2-}$ (m/z 1758.277, calc. m/z 1758.272).

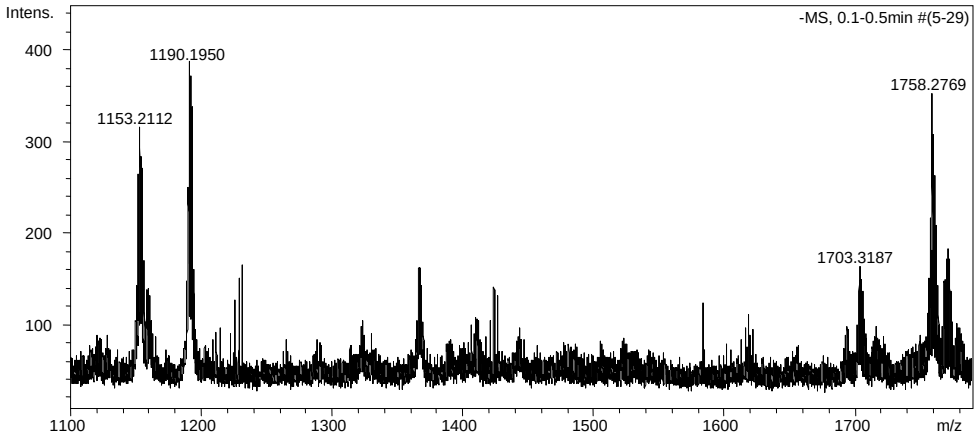

Figure 4.1: ESI-MS of Cs^+ + p-$ClC_6H_4SbO_3H_2$

- Thallium

This was added as thallium$^{(III)}$ oxide but the only significant new peaks could be assigned to $[TlH_9(RSb)_{14}O_{34}]^{2-}$ (m/z 2011.278, calc. m/z 2011.262) which contains Tl^+. Reduction of thallium has occurred, but the affinity for either Tl^{3+} or Tl^+ is low. Upon leaving the solution to stand for a week at room temperature,

very little change was observed and the peaks associated with the 'free' acid were still the dominant species present.

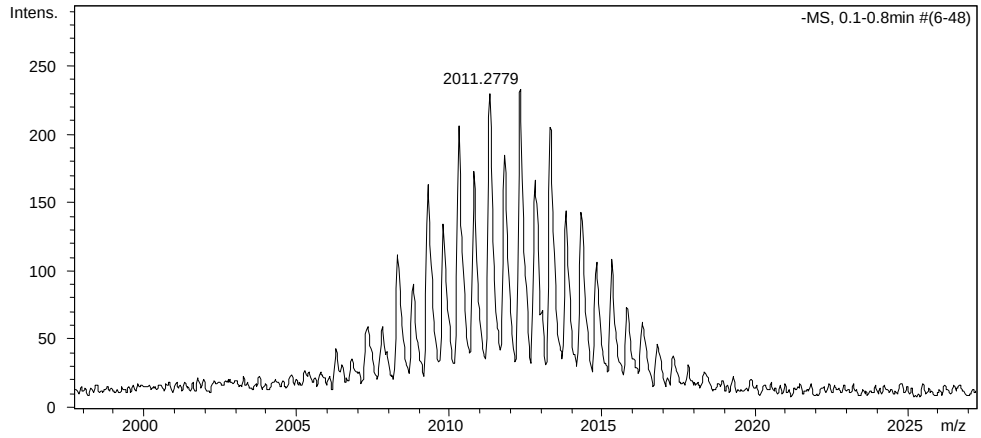

Figure 4.2: ESI-MS of Tl^+ + p-$ClC_6H_4SbO_3H_2$

- Uranium

This was added as uranyl acetate, giving UO_2^+. This resulted in complete sample degradation with only peaks associated with organic compounds remaining.

4.1.2 M^{2+} Ions

- Manganese

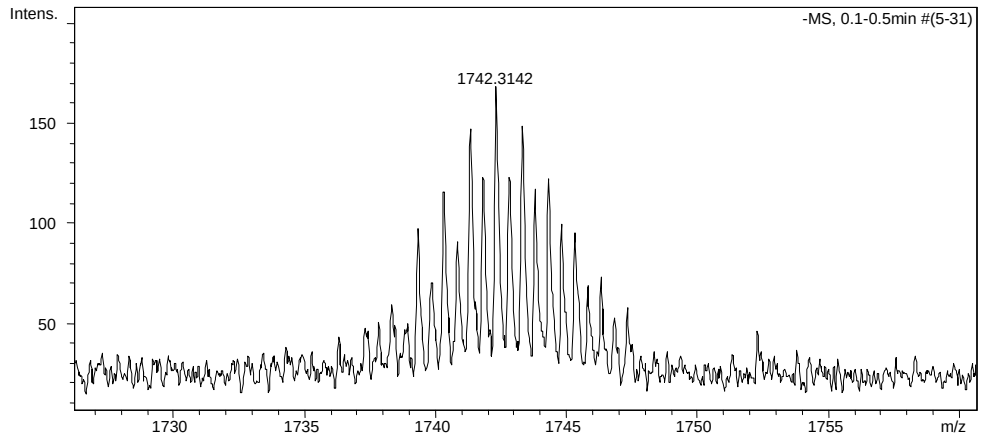

Figure 4.3: ESI-MS of Mn^{2+} + p-$ClC_6H_4SbO_3H_2$

The addition of MnO resulted in a spectrum showing peaks that could be tentatively assigned to $[Mn_2H_{16}(RSb)_{12}O_{35}]^{2-}$ (m/z 1742.314, calc. m/z 1742.334). Although this assignment is in agreement with the experimental value, it required the species to have a large number of water molecules associated with it.

- Copper

At first the addition of CuO produced a very weak spectrum with few to no assignable peaks. Upon leaving the solution to sit at room temperature for a week the following species could be assigned to new peaks in the positive ion mode, $[CuH_{12}(RSb)_{11}O_{28}]^{2+}$ (m/z 1544.928, calc. m/z 1544.909) and $[CuH_{11}(RSb)_{11}O_{28}]^{+}$ (m/z 3088.827, calc. m/z 3088.812). The dominant peak at m/z 1601.366 is attributed to the presence of $[H_4(RSb)_{12}O_{25}]^{2+}$ (calc. m/z 1601.373).

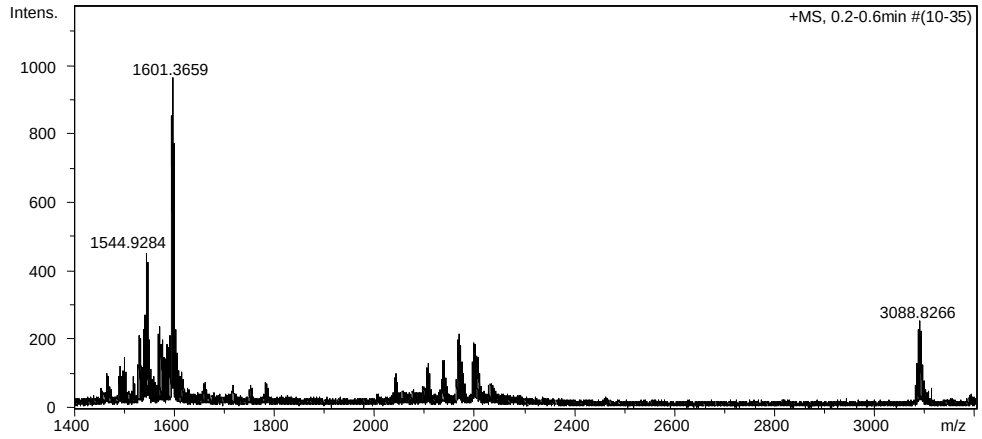

Figure 4.4: ESI-MS of Cu^{2+} + p-$ClC_6H_4SbO_3H_2$

- Zinc

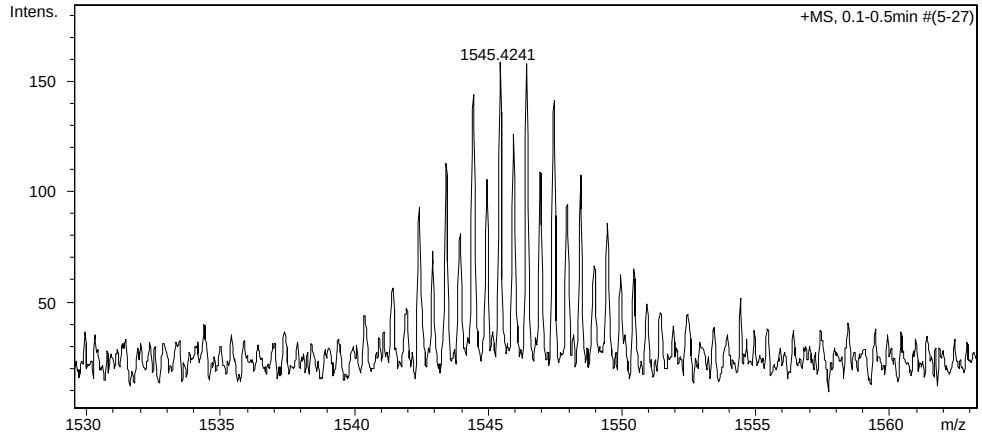

Figure 4.5: ESI-MS of Zn^{2+} + p-$ClC_6H_4SbO_3H_2$

Very similar behaviour to copper with nothing of initial interest being produced in either positive or negative ion mode, but after a week at room temperature, $[ZnH_{12}(RSb)_{11}O_{28}]^{2+}$ (m/z 1545.424, calc. m/z 1545.410) had formed.

- Barium

The addition of Ba^{2+} as BaO appeared to quite readily form $[BaH_8(RSb)_{14}O_{34}]^{2-}$ (m/z 1977.233, calc. m/z 1977.224) with the formation of a precipitate. Leaving the solution for a week at room temperature saw the reduction in all peaks associated with the 'free' acid form and a doubling of the relative intensity of the peak associated with $[BaH_8(RSb)_{14}O_{34}]^{2-}$. Associated positive ions, $[BaH_{12}(RSb)_{14}O_{34}]^{2+}$ (m/z 1979.246, calc. m/z 1979.238), $[BaH_{11}(RSb)_{14}O_{34}]^{+}$ (m/z 3959.527, calc. m/z 3959.485) also increased, and there was some evidence for the possible formation of even higher nucleations such as Sb_{21}. A peak at m/z 3002.848 could be associated with $[Ba_2H_{16}(RSb)_{21}O_{51}]^{2+}$ (calc. m/z 3002.826) but was relatively weak so couldn't be assigned unambiguously.

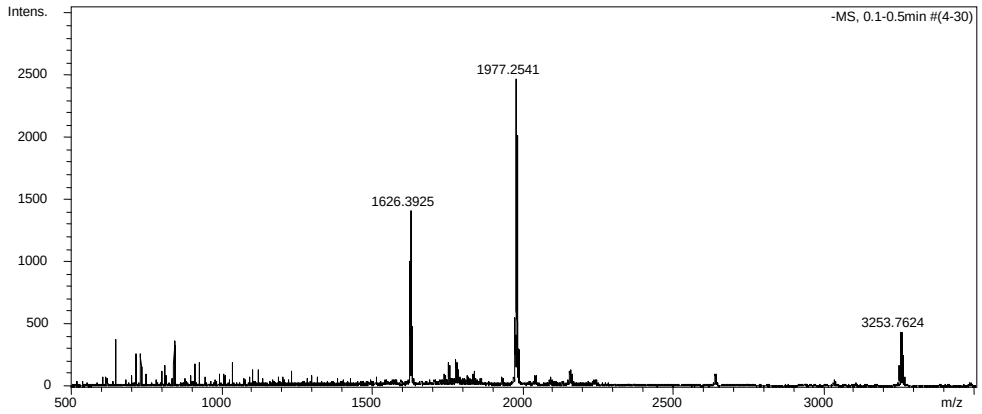

Figure 4.6: ESI-MS of Ba^{2+} + p-$ClC_6H_4SbO_3H_2$, t = 1 week

- Calcium

The addition of Ca^{2+} to a solution of *p*-chlorophenylstibonic acid resulted in a spectrum devoid of any significant peaks of interest.

- Lead

The introduction of Pb^{2+} to a solution of *p*-chlorophenylstibonic acid resulted in the instantaneous formation of an off-white precipitate and a spectrum void of any discernible peaks of interest.

- Mercury

This was added in the form of mercury acetate. The resultant spectrum gave no peaks of interest.

4.1.3 M^{3+} Ions

- Gadolinium

Initially the addition of Ga_2O_3 resulted in the formation of peaks that were consistent with the presence of $[Gd_2H_{18}(RSb)_{12}O_{37}]^{2-}$ (m/z 1862.341, calc. m/z 1862.323) and $[GdH_{23}(RSb)_{14}O_{42}]^{2-}$ (m/z 2058.790, calc. m/z 2058.772). The latter was initially the dominant species but after standing for a week at room temperature this species disappeared completely, leaving only $[Gd_2H_{18}(RSb)_{12}O_{37}]^{2-}$. Both of these assignments are slightly dubious as they involve an unusually high O:Sb ratio.

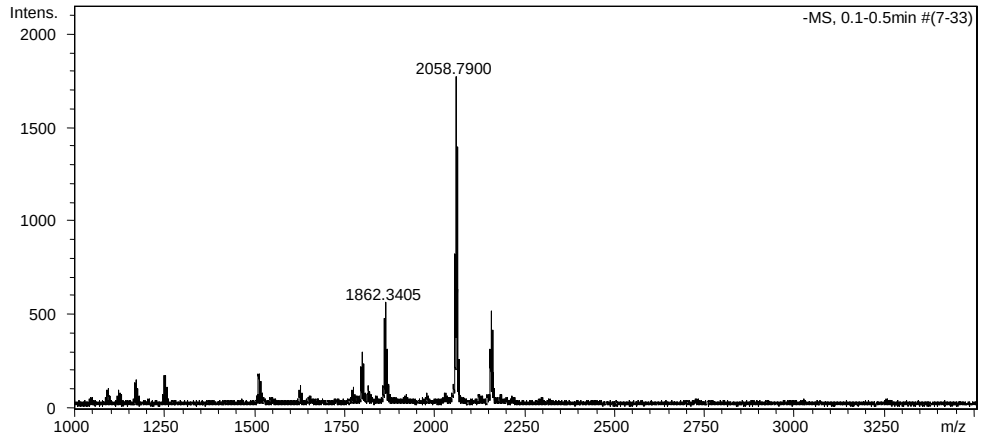

Figure 4.7: ESI-MS of Gd^{3+} + p-$ClC_6H_4SbO_3H_2$

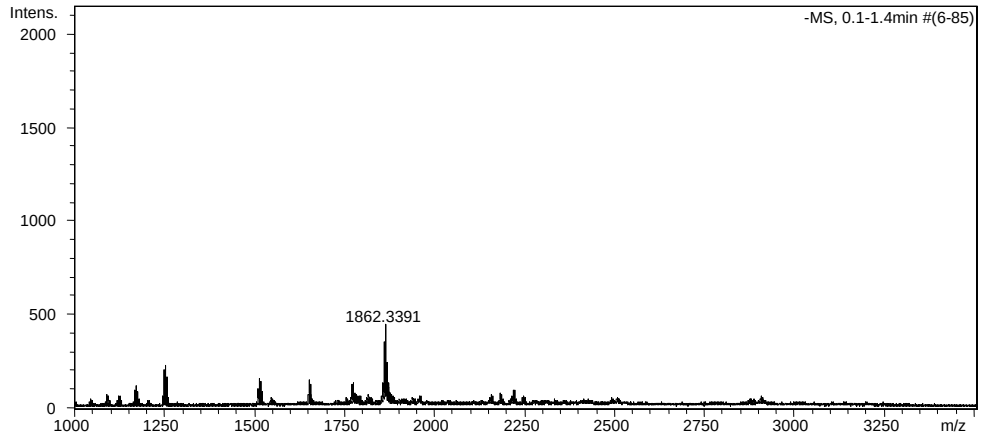

Figure 4.8: ESI-MS of Gd^{3+} + p-$ClC_6H_4SbO_3H_2$, t = 1 week

- Lanthanum

Similarly to gadolinium, the addition of lanthanum oxide saw the degradation of peaks associated with the 'free' acid and the formation of species such as $[La_2H_{18}(RSb)_{12}O_{37}]^{2-}$ (m/z 1843.325, calc. m/z 1843.305) but of relatively weak

intensities. The high degree of associated water molecules adds to the uncertainty of this assignment.

- Erbium

Produced no discernible peaks that could be associated with an erbium complex but the peaks associate with the 'free' acid were still present.

- Indium

The addition of indium oxide produced no significantly new peaks associated with a species that had complexed with indium.

4.1.4 M^{4+} Ions

- Terbium

Initially only the peaks attributed with the 'free' acid were present. Time (a week at room temperature) gave rise to a peak that could possibly be attributed to a species where both Tb^{3+} and Tb^{4+} are present, $[Tb_2NaH_{12}(RSb)_{12}O_{35}]^{2-}$ (m/z 1855.839, calc. m/z 1855.800). This species is not quite within normal agreement of the calculated value, thus it cannot be considered to be unambiguously assigned. There is also a species present that contains only a single Tb^{4+}, $[TbNaH_7(RSb)_{12}O_{31}]^{2-}$ (m/z 1741.836, calc. m/z 1741.828).

4.1.5 Discussion

Of the M^+ cations considered in this investigation, caesium has shown some promise with its ability to form Sb_{12} species. They appear to favour a particularly high degree of deprotonation resulting in a high number of associated charges, 2^- and 3^-. This appears to parallel the Na^+ adducts with *p*-nitrophenylstibonic acid.

The addition of manganese showed the formation of Sb_{12} salts associated with multiple Mn^{2+}, favouring a lower degree of deprotonation. The species formed also appear to have a very high number of associated water molecules.

Copper and zinc behave very similarly since it is only after a period of time that any species of interest start to appear, favouring only one associated ion with an Sb_{11} type aggregation.

The introduction of gadolinium and lanthanum to a solution containing *p*-chlorophenylstibonic acid formed Sb_{12} clusters.

Barium initially showed similarities to thallium in its ability to form Sb_{14} species with two associated charges, even though thallium has a different oxidation state. This alone may justify further study.

5 Arylstibonic Acid Salt Derivatives

Unfortunately single crystals of the arylstibonic acids investigated in this thesis have been elusive. Procuring such crystals would allow for the full structural characterisation of arylstibonic acids via X-ray crystallographic techniques. In an effort to gain insight into the structure of arylstibonic acids, investigations have been carried out by Dr Chris Clark into parallel work with salt derivatives of the arylstibonic acids prepared [25, 33].

This has lead to the structural elucidation of several derivatives with varying antimony cores. Although their structural work was not directly part of this thesis, a brief summary of key examples and their structural analyses is presented, as it provides some basis for predicting the structure of the parent acids. We note other, more complex species containing poly-antimony clusters have been reported by others [20, 34, 35].

For complete synthesis and analysis of these compounds refer to the publications in the Appendices.

5.1 $[K_2H_8(RSb)_{12}O_{30}]^{2-}$ (R = *p*-ClC_6H_4-)

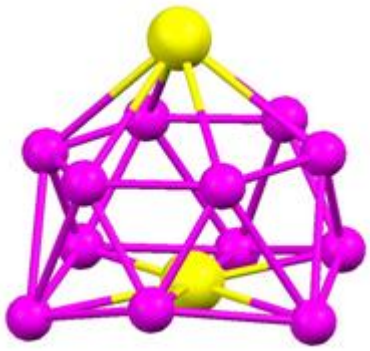

Figure 5.1: $[K_2H_8(RSb)_{12}O_{30}]^{2-}$
Purple = antimony, yellow = potassium.

The core of this anion consists of a hexagonal planar ring of six Sb atoms with another puckered ring of six Sb atoms directly below it, forming a hexagonal antiprism all linked together through oxygen bonding. This core structure has two cation binding sites, the first is encapsulated within the puckered Sb_6 hexagonal ring and is 10 coordinate, while the other is situated above the planar hexagonal Sb_6 face and is 6 coordinate. This same arrangement has been found for several $[Na_2H_8(RSb)_{12}O_{30}]^{2-}$ analogues.

5.2 $(ZnCl)_4[Zn(RSb)_{12}O_{28}]^{2-}$ (R = *p*-ClC_6H_4-)

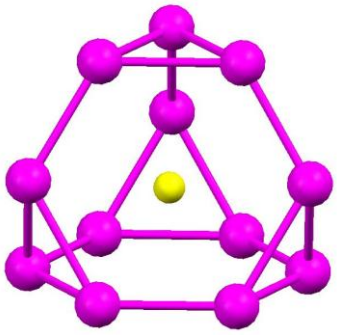

Figure 5.2: $(ZnCl)_4[Zn(RSb)_{12}O_{28}]^{2-}$
Purple = antimony, yellow = zinc.

The encapsulation of zinc in the arylstibonic acid structure has resulted in a structure with a core consisting of Sb_{12} but with a different truncated tetrahedral arrangement with the one Zn^{2+} occupying the centre. The other four zinc chlorides are tetrahedrally coordinated to the triangular faces.

5.3 $[LiH_3(RSb)_{12}O_{28}]^{4-}$ (R = *p*-MeC_6H_4-)

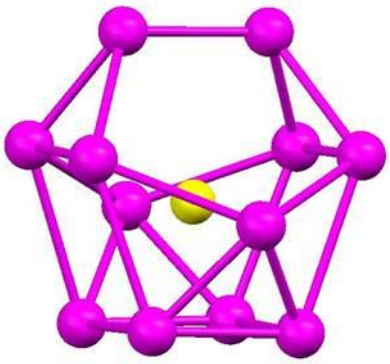

Figure 5.3: $[LiH_3(RSb)_{12}O_{28}]^{4-}$
Purple = antimony, yellow = lithium.

The X-ray analysis of this derivative showed that it again consisted of a Sb_{12} core but with a differing basket arrangement where lithium occupies the cation site situated in the centre, tetrahedral coordinated to four framework oxygen atoms.

5.4 $[BaH_{10}(RSb)_{14}O_{34}]$ (R = *p*-MeC_6H_4-)

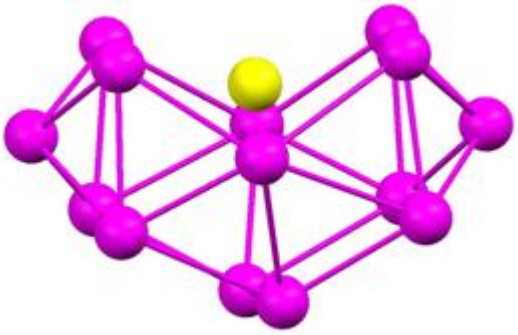

Figure 5.4: $[BaH_{10}(RSb)_{14}O_{34}]$
Purple = antimony, yellow = barium.

The inclusion of barium into the structure of an arylstibonic acid has had a dramatic effect on the structure. X-ray crystallographic analysis of this derivative showed that it consisted of a Sb_{14} core in a bowl arrangement with a cation site in the centre encapsulating barium. This is considerably different to the Sb_{12} aggregate cores that have been seen previously.

This structure is in complete agreement with the ESI-MS investigations described in section 4.1.2 concerning the addition of barium to arylstibonic acids. This showed that when barium was introduced to *p*-chlorophenylstibonic acid it resulted in the formation of clusters where the Sb_{16} aggregation was the dominant species, $[BaH_8(RSb)_{14}O_{34}]^{2-}$. The subsequent structural determination of the *p*-tolyl- analogue shows that this bowl-like geometry is adopted for at least two arylstibonic acids. It also indicates a possible structural assignment for the Tl^+ species $[TlH_9(RSb)_{14}O_{34}]^{2-}$ (see section 4.1.1).

5.5 Discussion

From the few examples it is clear that different geometries are available even for clusters with the same nuclearity. In terms of predicting the structure of the parent acids then the Li^+ derivative may reflect this, since this consists of a $Sb_{12}O_{28}$ core for which corresponds to the ESI-MS analysis of the acids (see section 3.3) more so than the $Sb_{12}O_{30}$ arrangement for the K^+ derivative. The Zn^{2+} derivative, although having a $Sb_{12}O_{28}$ core, is less likely to reflect the structure of that parent acid as the inclusion of the tetrahedrally coordinated $ZnCl_4$ may result in a structural reconfiguration.

The Zn^{2+} polyoxostibonate derivative consists of a similar geometry to those published by Baskar [20], whereas the Li^+ derivative is novel in its geometry.

6 Mixed-Metal Polyoxometalates

As a clearer picture and understanding of arylstibonic acids as polyoxometalates began to develop during the course of this thesis, intrigue at the possibility of synthesising mixed-metal polyoxometalates increased. A preliminary study to see if it was possible to replace a portion of the core antimony atoms with a different element and what differences this would bring about.

The similarities (although limited) between arylstibonic and arylarsonic acids made arsenic-based derivatives an obvious first choice. A wide range of arylarsonic acids was able to be procured from Lloyd as part of investigations previously carried out at Waikato [3].

Initially five arylarsonic acids were chosen to be trialled against one arylstibonic acid. These mixtures were prepared by dissolving *p*-chlorophenylstibonic acid in acetonitrile and adding an equivalent mole ratio of the arylarsonic acid (*p*-fluorophenyl-, *p*-nitrophenyl-, *m*-nitrophenyl-, *p*-methoxyphenyl- and phenyl-arsonic acid). The detailed experimental procedures for each are outlined in section 2.7.

6.1 ESI-MS

These mixed-metal polyoxometalate solutions were examined on a Bruker MicrOTOF under standard operating conditions in the same manner that the arylstibonic acids were processed, as outlined in section 3.3.

6.1.1 *p*-$ClC_6H_4SbO_3H_2$ + *p*-$FC_6H_4AsO_3H_2$

ESI-MS analysis of the solution just after preparation resulted in the following spectrum (Figure 6.1). The dominant peak can be attributed to an arylarsonic trimer, $[H_5(FC_6H_4As)_3O_9]^-$ m/z 658.853 (calc. m/z 658.848). The peak at m/z 1390.584 is that of a mixed As/Sb species $[H_5(FC_6H_4As)_4(ClC_6H_4Sb)_2O_{15}]^-$ (calc. m/z 1390.576) with an As_4Sb_2 core.

Upon leaving the solution to stand at room temperature for 24 h (Figure 6.2), the mixed As/Sb species ($[H_5(FC_6H_4As)_4(ClC_6H_4Sb)_2O_{15}]^-$) increased intensity to become the primary species present.

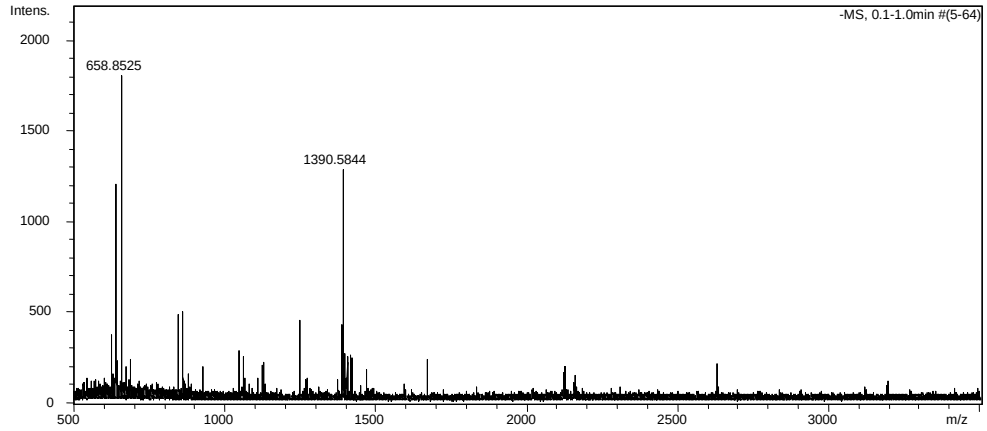

Figure 6.1: ESI-MS of p-$ClC_6H_4SbO_3H_2$ + p-$FC_6H_4AsO_3H_2$

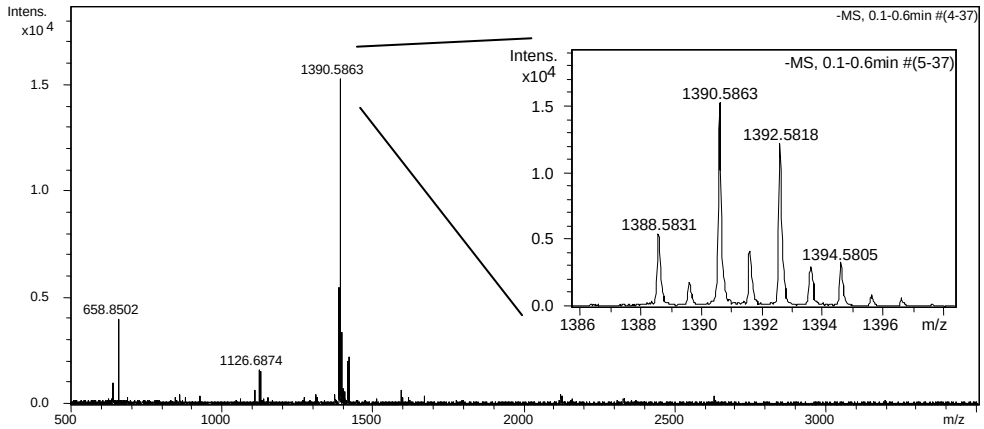

Figure 6.2: ESI-MS of p-$ClC_6H_4SbO_3H_2$ + p-$FC_6H_4AsO_3H_2$, 24 h

Peaks also become apparent, although relatively weak, that could be assigned to species with differing composition ratios, $[H_5(FC_6H_4As)_4(ClC_6H_4Sb)_1O_{13}]^-$ at m/z 1126.687 (calc. m/z 1126.683) and $[H_5(FC_6H_4As)_5(ClC_6H_4Sb)_2O_{17}]^-$ at m/z 1592.528 (calc. m/z 1592.517). These are As_4Sb and As_5Sb_2 species respectively.

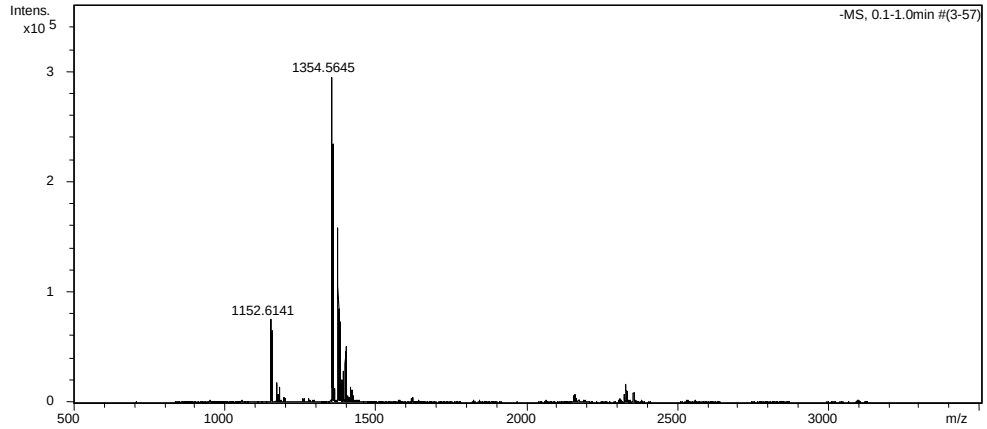

Figure 6.3: ESI-MS of recrystallised p-$ClC_6H_4SbO_3H_2$ + p-$FC_6H_4AsO_3H_2$

Another 1:1 mole ratio mixture was prepared but this time it was allowed to evaporate and the residue was then recrystallised from acetonitrile. This was done to determine if the 1:2 ratio species ($[H_5(FC_6H_4As)_4(ClC_6H_4Sb)_2O_{15}]^-$) was in fact the favoured aggregation and in an attempt to grow crystals. ESI-MS analysis of the resultant product showed that it was indeed the corresponding species, m/z 1354.565 = $[H(FC_6H_4As)_4(ClC_6H_4Sb)_2O_{13}]^-$ (calc. m/z 1354.555) (Figure 6.3) but with further condensation through loss of two water molecules. The peak at m/z 1152.614 is $[H(FC_6H_4As)_3(ClC_6H_4Sb)_2O_{11}]^-$ (calc. m/z 1152.614), is an As_3Sb_2 species.

6.1.2 *p*-$ClC_6H_4SbO_3H_2$ + *p*-$O_2NC_6H_4AsO_3H_2$

Initial ESI-MS analysis of the mixture solution resulted in the following spectrum (Figure 6.4).

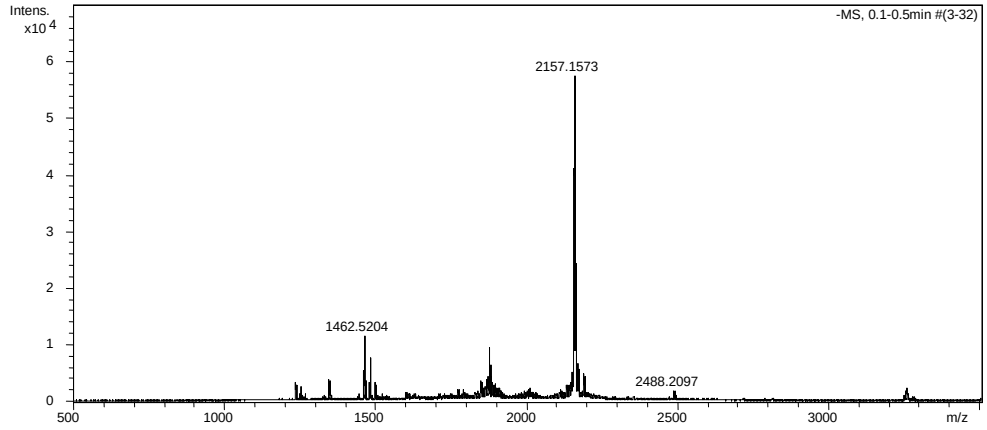

Figure 6.4: ESI-MS of p-$ClC_6H_4SbO_3H_2$ + p-$O_2NC_6H_4AsO_3H_2$

The primary species present was that of a Sb_{16} type cluster, $[H_6(ClC_6H_4Sb)_{16}O_{36}]^{2-}$ (m/z 2157.157, calc. m/z 2157.162). This species is only a minor component of the pure acid, so the arsenic acid is somehow promoting its formation, possibly as a result in a change of pH. There was also evidence supporting the formation of mixed As/Sb polyoxometalates. The peak at m/z 1462.520 is a mixed As/Sb species with the molecular formula of $[H(O_2NC_6H_4As)_4(ClC_6H_4Sb)_2O_{13}]^-$ (calc. m/z 1462.533). This is the direct analogue of the species found in section 6.1.1). Accompanying this are satellite species with varying degrees of hydration. These species all have the same composition ratio of 1:2 (arylstibonic to arylarsonic acid) as the *p*-fluorophenylarsonic acid derivative. The relatively weak signal at m/z 2488.210

represents a species of differing composition ratio, As_6Sb_4, $[H_5(O_2NC_6H_4As)_6(ClC_6H_4Sb)_4O_{23}]^-$ (calc. m/z 2488.213).

Leaving the mixture solution to sit for a further 24 h (Figure 6.5) resulted in an overall increase in intensity of the mixed As/Sb species respective to that of the individual homonuclear species.

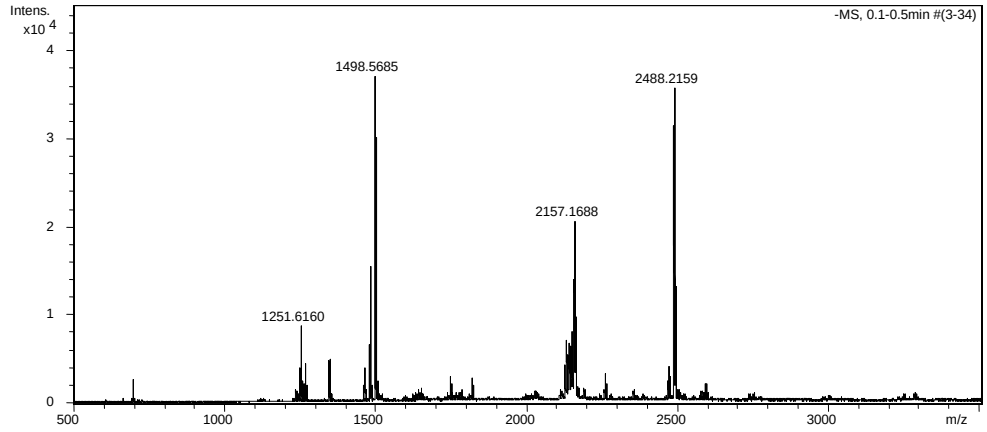

Figure 6.5: ESI-MS of p-$ClC_6H_4SbO_3H_2$ + p-$O_2NC_6H_4AsO_3H_2$, 24 h

The peak at m/z 1498.569 is directly related to the previously seen $[H(O_2NC_6H_4As)_4(ClC_6H_4Sb)_2O_{13}]^-$ species by an increase in the number of associated water molecules, $[H_5(O_2NC_6H_4As)_4(ClC_6H_4Sb)_2O_{15}]^-$ (calc. m/z 1498.554). This species is now the same as seen with the *p*-$ClC_6H_4SbO_3H_2$ + *p*-$FC_6H_4AsO_3H_2$ analogue. The signal at m/z 1251.616 can be attributed to another species with a differing composition ratio, As_3Sb_2, $[H(O_2NC_6H_4As)_3(ClC_6H_4Sb)_2O_{11}]^-$ (calc. m/z 1251.608).

6.1.3 *p*-$ClC_6H_4SbO_3H_2$ + *m*-$O_2NC_6H_4AsO_3H_2$

The mixture with the related *meta* substituted nitro arsenic derivative resulted in the subsequent spectrum as shown in Figure 6.6. This derivative initially behaved in a similar fashion to that of the *p*-nitrophenylarsonic acid, but with the $[H(O_2NC_6H_4As)_4(ClC_6H_4Sb)_2O_{13}]^-$ species present at a slightly elevated intensity, m/z 1462.526 (calc. m/z 1462.533).

The similarities ended when the solution was left for a further 24 h (Figure 6.7). The peaks associated with the mixed As/Sb species did not increase to the same extent that they did with the *para* derivative. The relative intensities of $[H_5(O_2NC_6H_4As)_4(ClC_6H_4Sb)_2O_{15}]^-$ (m/z 1498.562, calc. m/z 1498.554) species

decreased slightly and the peak attributed to the $[H_5(FC_6H_4As)_6(ClC_6H_4Sb)_4O_{23}]^-$ (m/z 2488.228, calc. m/z 2488.213) species increased somewhat.

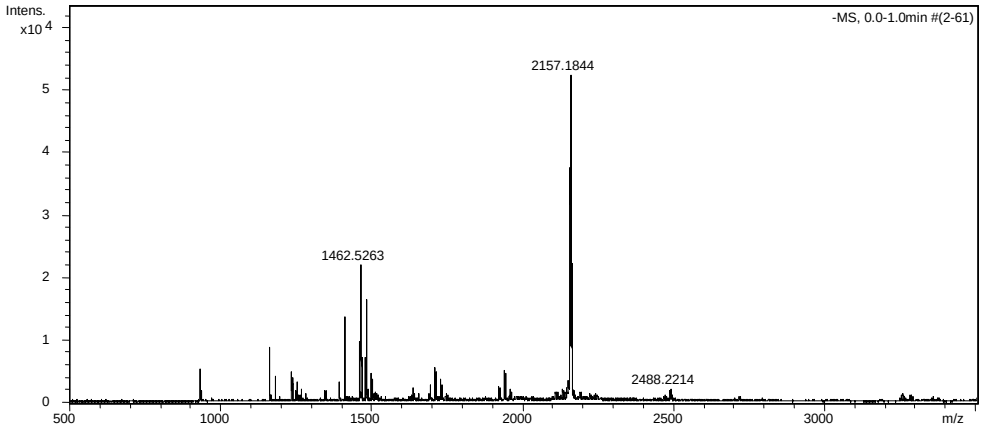

Figure 6.6: ESI-MS of p-$ClC_6H_4SbO_3H_2$ + m-$O_2NC_6H_4AsO_3H_2$

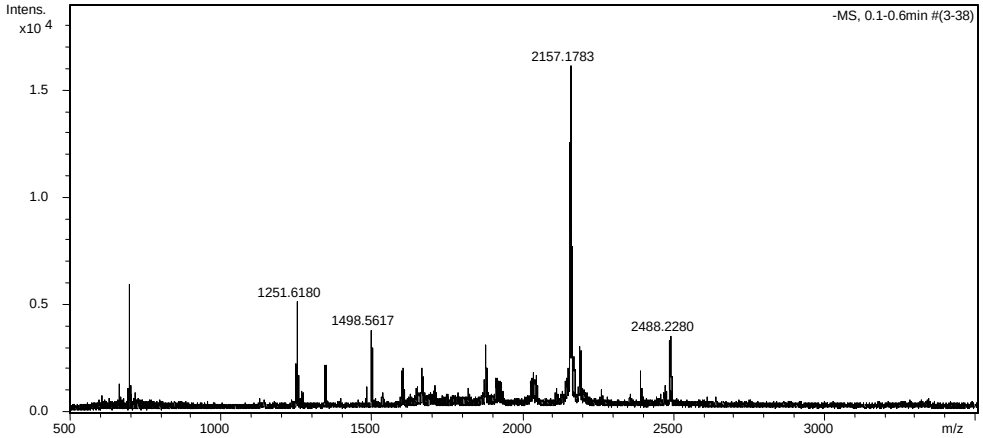

Figure 6.7: ESI-MS of p-$ClC_6H_4SbO_3H_2$ + m-$O_2NC_6H_4AsO_3H_2$, 24 h

6.1.4 *p*-$ClC_6H_4SbO_3H_2$ + $C_6H_5AsO_3H_2$

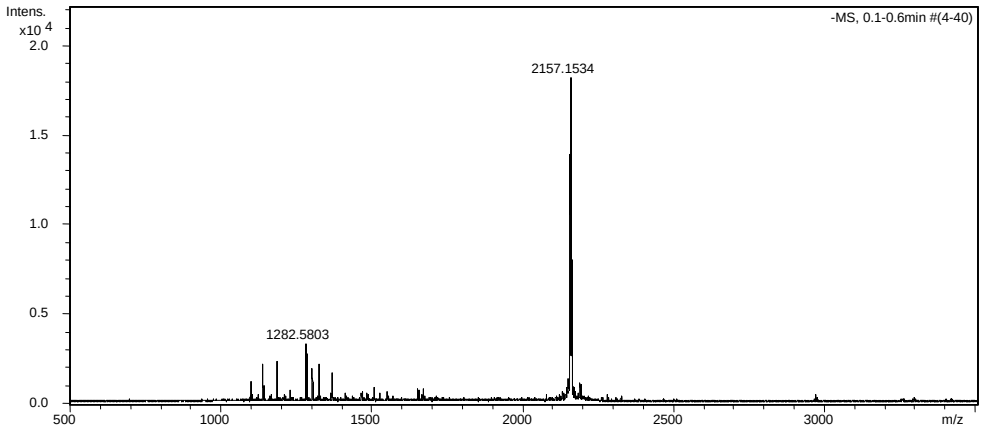

Figure 6.8: ESI-MS of p-$ClC_6H_4SbO_3H_2$ + $C_6H_5AsO_3H_2$

The non-substituted phenylarsonic acid when combined with *p*-chlorophenylstibonic acid appears to have formed a mixed-metal aggregation of the type $[H(C_6H_5As)_4(ClC_6H_4Sb)_2O_{13}]^-$, m/z 1282.580 (calc. m/z 1282.593). However, as with the nitro- derivatives the dominant species present is that of the Sb_{16} aggregate.

On standing for 24 h at room temperature the mixed As/Sb species decrease in relative intensity while the individual arylarsonic and arylstibonic substituents increased.

6.1.1 *p*-$ClC_6H_4SbO_3H_2$ + *p*-$MeOC_6H_4AsO_3H_2$

This permutation resulted in little of interest, even after allowing the mixture solution to stand for several days (analysed at 0, 24 and 48 h.). The *p*-methoxy-substituent appears to have halted the formation of any mixed As/Sb aggregates as the resultant spectra consisted of only the individual previously observed arylstibonic and arylarsonic acid constituents.

6.2 Discussion

This initial trial into mixed As/Sb polyoxometalates has shown that they are indeed possible to synthesise easily by combining the two compounds in acetonitrile.

When considering only the *p*-chlorophenylstibonic acid, the five arylarsonic acids investigated (apart from *p*-methoxyphenylarsonic acid) appear to favour the formation of mixed As/Sb aggregates consisting of four arylarsonic acid molecules and two arylstibonic acid molecules. These species in solution, when analysed via ESI-MS also unambiguously favour low levels of deprotonation resulting in only one associated charge. This is unlike the arylstibonic acids where they are quite stable with higher degrees of deprotonation. This may in part be due to the size of the aggregations formed, where the smaller mixed As/Sb polyoxometalates may only be capable of supporting a limited degree of deprotonation without further fragmentation.

The *p*-fluorophenylarsonic acid derivative appears to be particularly stable as the signals associated with the individual arylstibonic and arylarsonic acids were all but absent, replaced by the mixed As/Sb aggregations. This behaviour is dissimilar to that of the permutations where *p*-nitrophenyl-, *m*-nitrophenyl- and

phenyl-arsonic acid derivatives were used. The *p*-chlorophenylstibonic acid is still dominant as the Sb_{16} ($[H_6(ClC_6H_4Sb)_{16}O_{36}]^{2-}$) species. With additional time, the intensity of the Sb_{16} species appears to decrease proportional to an increase in intensity of the mixed As/Sb aggregates.

The differences in intensity between the *p*-nitrophenyl- and *m*-nitrophenyl-arsonic acid mixed-metal polyoxometalates may in part be due to the shift of the substituents around the phenyl ring and the physical and chemical properties that this imparts. The shift to the *meta* position may bring about a steric consideration as although few steric interactions are observed for the larger Sb_{12} type clusters, the decrease in cluster size may result in a more noticeable steric hindrance effect. The shift will also result in a change of the electronic effects of the phenyl ring system which may contribute to the observable differences.

This was only a brief exploration into the possibility and behaviour of mixed As/Sb polyoxometalates, with many permutations remaining to be explored. Unfortunately despite concentrated efforts none of the mixed species so far examined have provided single crystals suitable for X-ray structural determination.

Comparable work has been carried out into mixed-metal polyoxometalates using phosphonates in conjunction with arylstibonic acids [34, 35]. These investigations resulted in polyoxometalates consisting of various composition ratios. Although the phosphonate derivative $[Cu_3O_4(SbAr)_2(O_3P^tBu)_4(py)_3]$ published by Ali *et al.* has a similar ratio to the As_4Sb_2 clusters, the structural determination shows that copper is incorporated into the core. Thus it does not provide much insight into the structures of the aggregates observed here.

Recently a comprehensive review of hybrid organic-inorganic polyoxometalate compounds, including organoantimony derivatives has been published [36].

7 Conclusions

The investigations carried out within this thesis have made progress in answering the 100 year old problem as to the elucidation of the true structure and nature of arylstibonic acids.

ESI-MS, along with elemental and IR analysis have shown that arylstibonic acids predominantly exist in the solid state as high molecular weight dodecanuclear clusters, $[H_8(RSb)_{12}O_{28}]$.

The stability of these polyoxometalates has been probed with the use of ESI-MS to determine that while indefinitely stable in acetonitrile, in water they appear to hydrolyse to monomeric forms, particularly at higher pH.

ESI-MS investigations into arylstibonic acids and their affinity for metal ions have aided parallel work carried out by colleagues, resulting in the structural elucidation of a number of Sb-containing polyoxometalate derivatives.

Preliminary research into mixed-metal polyoxometalates using arylstibonic and arylarsonic acids has shown that there is a tendency to form As_4Sb_2 aggregates. This investigation has only just touched on the surface of the possibilities in this field.

8 References

1. Doak, G. O.; Freedman, L. D., *Organometallic compounds of arsenic, antimony, and bismuth*. Wiley: New York, (1970).

2. Riddel, W., Aryl antimony compounds. *Trans. Roy. Soc. Can.*, **23** (1929), 45.

3. Lloyd, N. C.; Morgan, H. W.; Nicholson, B. K.; Ronimus, R. S., Substituted phenylarsonic acids; structures and spectroscopy. *J. Organomet. Chem.*, **693** (2008), 2443.

4. Doak, G. O., The structure of arylstibonic acids. *J. Am. Chem. Soc.*, **68** (1946), 1991.

5. Macallum, A. D., o-Amino- and o-acetamidophenylstibonic acids. *J. Soc. Chem. Ind., London*, **42** (1923), 468T.

6. Morgan, G. T., *Organic compounds of arsenic & antimony*. Longmans, Green, and Co.: (1918).

7. Michaelis, A.; Reese, A., Ueber aromatische Antimonverbindungen und eine neue Bildungsweise aromatischer Arsenverbindungen. *Ber. Dtsch. Chem. Ges.*, **15** (1882), 2876.

8. Schmidt, H. Chemische Fabrik von Heyden. Ger. Pat. 254421, (Aug. 3, 1911).

9. Christiansen, W. G., *Organic derivatives of antimony*. Chem. Cat. Co.: New York, (1925).

10. Schmidt, H., Über aromatische Antimonverbindungen. *Justus Liebigs Ann. Chem.*, **421** (1920), 174.

11. Dunning, F.; Reid, E. E., Azo dyes containing antimony. II. *J. Am. Chem. Soc.*, **49** (1927), 2869.

12. Dunning, F.; Reid, E. E., Some azo dyes containing antimony. *J. Am. Chem. Soc.*, **48** (1926), 2959.

13. Doak, G. O., A modified Bart reaction. *J. Am. Chem. Soc.*, **62** (1940), 167.

14. Doak, G. O.; Steinman, H. G., The preparation of stibonic acids by the Scheller reaction. *J. Am. Chem. Soc.*, **68** (1946), 1987.

15. Wieber, M.; Waltz, J., Methanestibonic acid. *Z. Naturforsch., B: Chem. Sci.*, **45** (1990), 1615.

16. Schmidt, H., Über aromatische Antimonverbindungen, V. *Ber. Dtsch. Chem. Ges. B*, **55** (1922), 697.

17. Fargher, R. G.; Gray, W. H., The chemotherapy of antimony. Comparison of the antimonyl tartrates with the organic compounds of antimony. *J. Pharmacol. Exp. Therapeut.*, **18** (1921), 341.

18. Gray, W. H.; Lamb, I. D., Crystalline salts derived from p-aminophenylstibonic acid. *J. Chem. Soc.*, (1938), 401.

19. Bowen, L. H.; Long, G. G., Mössbauer study of stibonic and stibinic acids: structural implications from orbital population analysis. *Inorg. Chem.*, **17** (1978), 551.

20. Baskar, V.; Shanmugam, M.; Helliwell, M.; Teat, S. J.; Winpenny, R. E. P., Reverse-keggin ions: Polycondensation of antimonate ligands give inorganic cryptand. *J. Am. Chem. Soc*, **129** (2007), 3042.

21. Beckmann, J.; Finke, P.; Hesse, M.; Wettig, B., Well-defined stibonic and tellurinic acids. *Angew. Chem., Int. Ed.*, **47** (2008), 9982.

22. Blessing, R. H., An empirical correction for absorption anisotropy. *Acta Cryst*, **A51** (1995), 33.

23. Sheldrick, G. M., SHELX97: Programs for crystal structure analysis. *University of Göttingen, Germany*, (1997).

24. Farrugia, L. J., WinGX suite for small-molecule single-crystal crystallography. *Appl. Crystallogr.*, **32** (1999), 837.

25. Clark, C. J.; Nicholson, B. K.; Wright, C. E., Arylstibonic acids $[H_8(RSb)_{12}O_{28}]$; precursors to organometallic isopolyoxostibonates $[Na_2H_9(RSb)_{12}O_{30}]^-$, (R = aryl). *Chem. Comm.*, (2009), 923.

26. Zaitseva, E. G.; Medvedev, S. V.; Aslanov, L. A., Crystal and molecular structures of caesium phenylpentachloroantimonate $Cs[PhSbCl_5]$, potassium phenylpentabromoantimonate $K[PhSbBr_5]$, and caesium hexachloroantimonate $Cs[SbCl_6]$. *J. Struct. Chem.*, **31** (1990), 92.

27. Zaitseva, E. G.; Medvedev, S. V.; Aslanov, L. A., Crystal and molecular structures of ammonium and dimethylammonium phenylpentachloroantimonates $NH_4[PhSbCl_5]$ and $(CH_3)_2NH_2[PhSbCl_5]$ and ammonium phenylpentabromoantimonate $NH_4[PhSbBr_6]$. *J. Struct. Chem.*, **31** (1990), 97.

28. Zaitseva, E. G.; Medvedev, S. V.; Aslanov, L. A., Ligand interaction in anionic $Sb^{(V)}$ phenyl halide complexes. *J. Struct. Chem.*, **31** (1990), 261.

29. Miras, H. N.; Wilson, E. F.; Cronin, L., Unravelling the complexities of inorganic and supramolecular self-assembly in solution with electrospray and cryospray mass spectrometry. *Chem. Comm.*, (2009), 1297.

30. Rishi, V.; Oh, W. J.; Heyerdahl, S. L.; Zhao, J.; Scudiero, D.; Shoemaker, R. H.; Vinson, C., 12 Arylstibonic acids that inhibit the DNA binding of five B-ZIP dimers. *J. Struct. Biol.*, **170** (2010), 216.

31. Simmons, T. L.; McCloud, T. G., Analysis of stibonic acids by ion exchange chromatography with ESI-MS/photodiode array detection. *J. Liq. Chrom. Relat. Tech.*, **26** (2003), 2041.

32. Nakamoto, K., *Infrared and Raman spectra of inorganic and coordination compounds*. 3rd ed.; Wiley: New York, (1978).

33. Nicholson, B. K.; Clark, C. J.; Wright, C. E.; Groutso, T., Isopolyoxometalates of Antimony: Arylstibonic Acids $[H_8(RSb)_{12}O_{28}]$ and Derived Dodecanuclear Polyoxostibonates $[M_2H_{10-x}(RSb)_{12}O_{30}]^{x-}$, M = Na or K. *Organometallics*, (2010), DOI: 10.1021/om1008692.

34. Ali, S.; Muryn, C. A.; Tuna, F.; Winpenny, R. E. P., Synthesis and structural and magnetic characterisation of copper (ii) complexes of mixed phosphonate-antimonate ligands. *Dalton Trans.*, **39** (2009), 124.

35. Ali, S.; Baskar, V.; Muryn, C. A.; Winpenny, R. E. P., Mixed antimonate-phosphonate ligands as polydentate bridging oxygen donors. *Chem. Comm.*, **2008** (2008), 6375.

36. Dolbecq, A.; Dumas, E.; Mayer, C. R.; Mialane, P., Hybrid Organic-Inorganic Polyoxometalate Compounds: From Structural Diversity to Applications. *Chem. Rev.*, **110** (2010), 6009.

9 Appendices

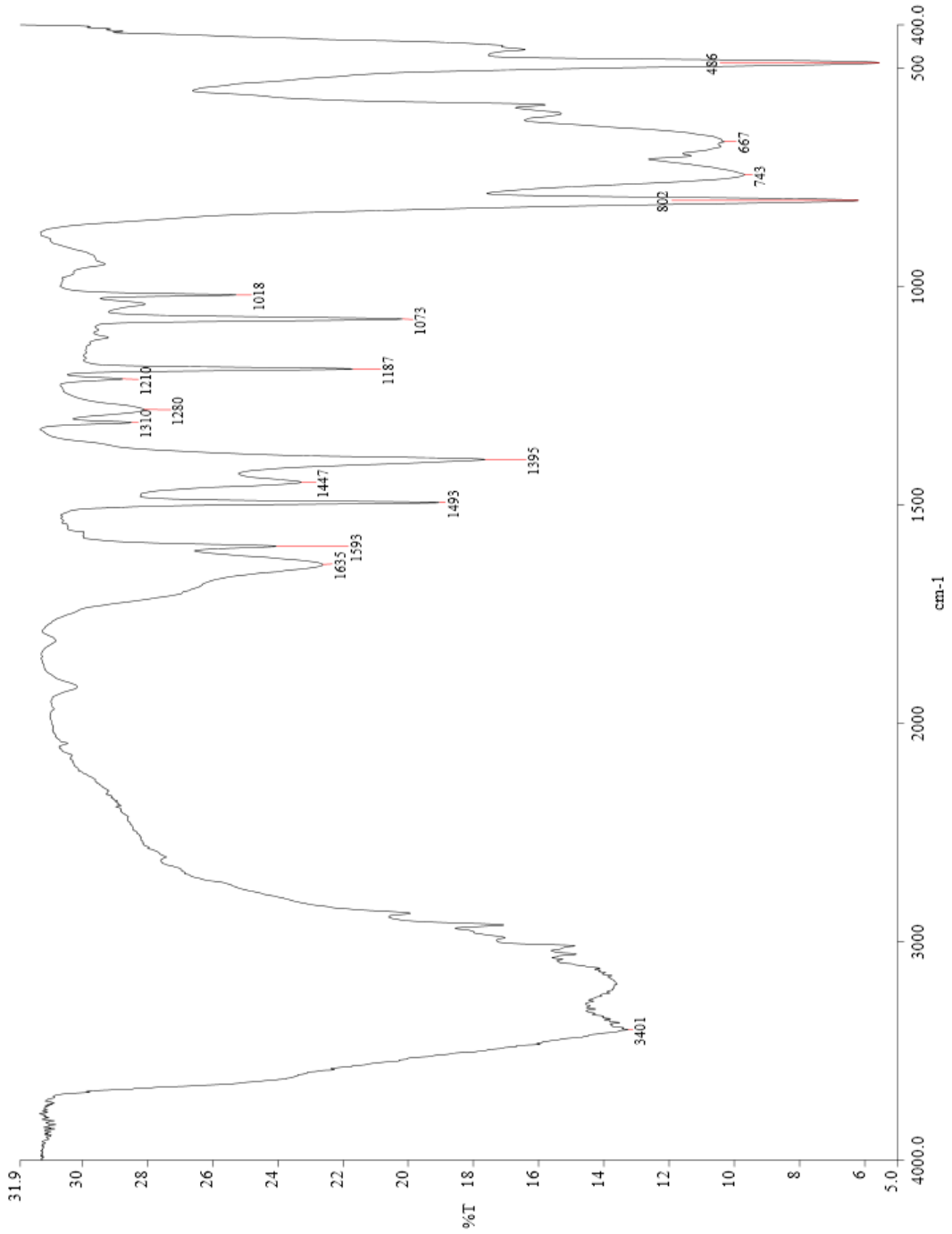

Figure 9.1: IR spectrum of p-tolylstibonic acid

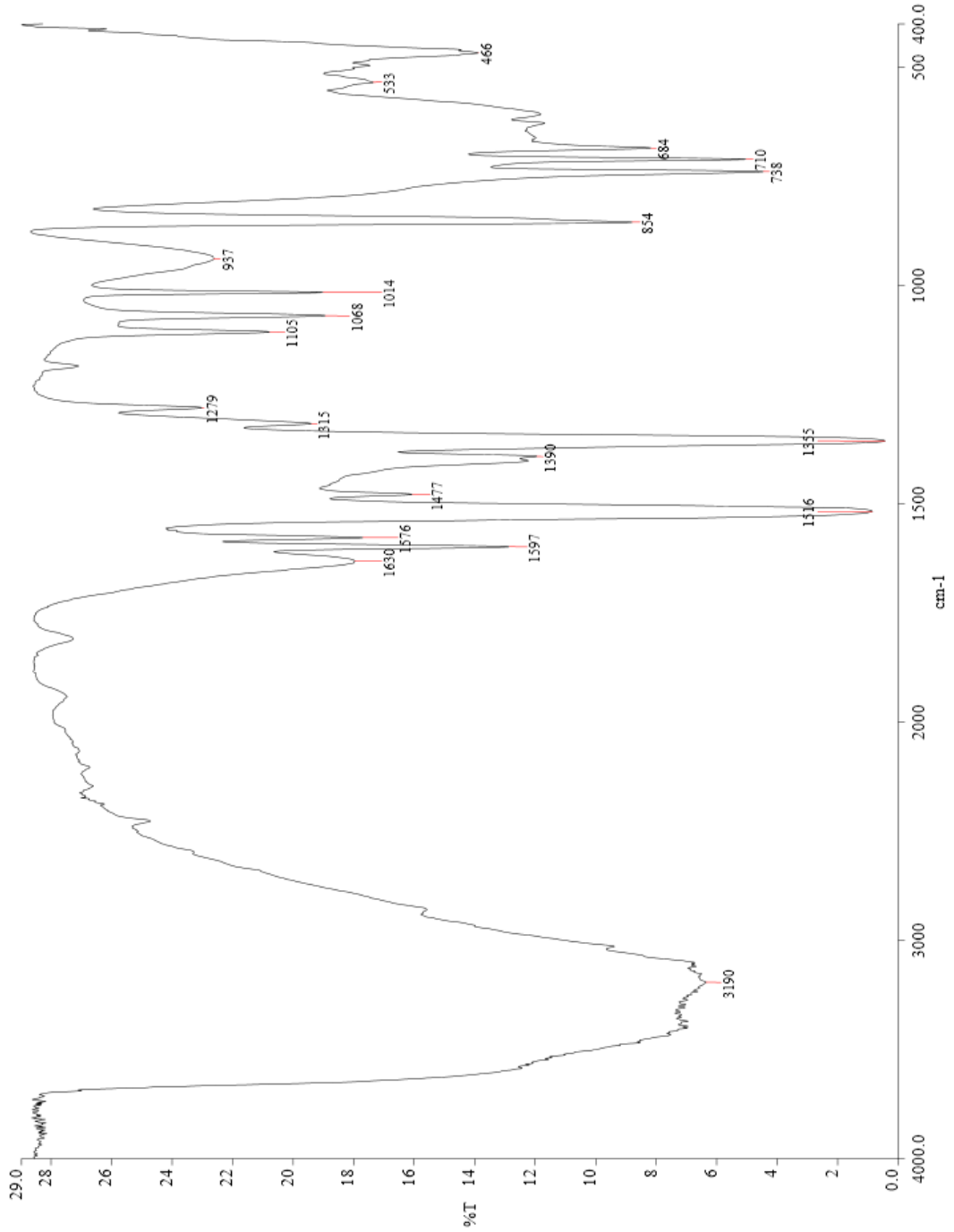

Figure 9.2: IR spectrum of p-nitrophenylstibonic acid

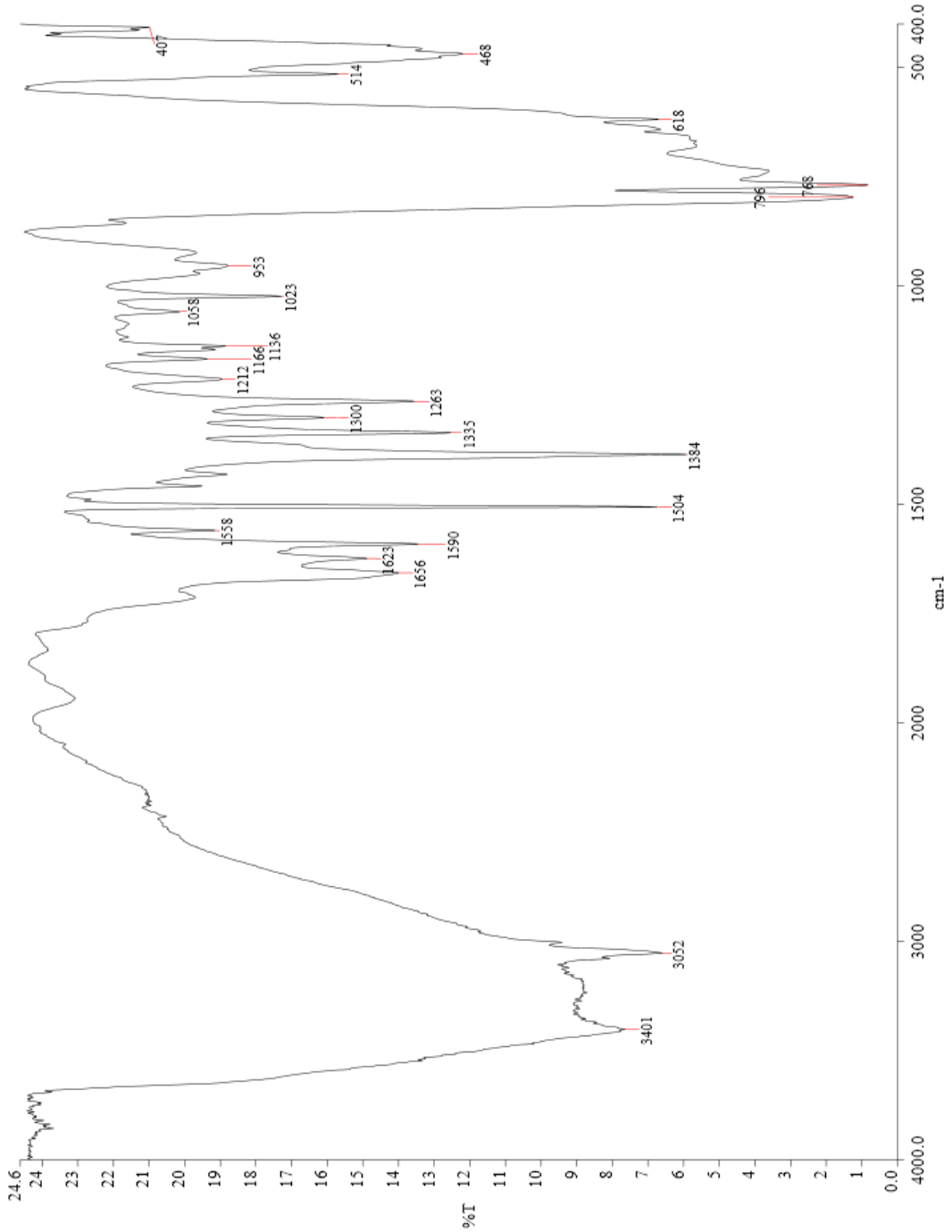

Figure 9.3: IR spectrum of α-naphthylstibonic acid

Two papers covering aspects of the work that this thesis entailed have been published concurrently [25, 33]. Reprints of these have been included here;

Arylstibonic acids $[H_8(RSb)_{12}O_{28}]$; precursors to organometallic isopolyoxostibonates $[Na_2H_9(RSb)_{12}O_{30}]^-$, (R = aryl)†

Christopher J. Clark,[a] Brian K. Nicholson*[b] and Cody E. Wright[b]

Received (in Cambridge, UK) 15th September 2008, Accepted 1st December 2008
First published as an Advance Article on the web 14th January 2009
DOI: 10.1039/b816113e

Electrospray ionisation mass spectrometry shows that arylstibonic acids, $RSbO_3H_2$, give rise to oxo-bridged clusters derived from $[H_8(RSb)_{12}O_{28}]$ which act as inorganic crown ligands towards Na^+ cations; structure determination of one derivative revealed a cage-like anion $[Na_2H_9(p\text{-}O_2NC_6H_4Sb)_{12}O_{30}\cdot 4H_2O]^-$.

In contrast to the arylarsonic acids, $ArAsO_3H_2$, which are well-defined molecular species with four-coordinate As,[1] arylstibonic acids have largely undetermined structures but are assumed to be oligomeric or polymeric in the solid state.[2] Mössbauer studies have been interpreted in terms of five-coordinate Sb.[3] Very recently, an example with a very bulky aryl group has been reported as an oxygen-bridged dimer, $(2,6\text{-}Mes_2C_6H_3Sb)_2O_2(OH)_4$.[4]

We now report ESI-MS data for some arylstibonic acids which indicate high-nuclearity aggregation and show that these are a source of a novel class of well-defined polyoxometallates. The very extensive field of polyoxometallates (POMs) has been largely restricted to the early transition metals, especially Mo or W, as exemplified by the Keggin and Dawson ion families.[5] Main group elements, including As and Sb, have been incorporated into the framework to give hetero-POMs.[6] However there are very few previous reports of iso-POMs from the p-block elements.[7]

A sample of $RSbO_3H_2$ (R = p-ClC_6H_4–)[8] was purified by dissolving it in aqueous ammonia and allowing slow vapour diffusion of acetic acid to precipitate it as an off-white powder.‡ This was soluble in MeCN and an ESI-MS of the resulting solution gave the spectrum shown in Fig. 1. The dominant peak can be unambiguously assigned to $[H_7(RSb)_{12}O_{28}]^-$ (m/z 3253.744 *cf.* calc. 3253.756). The characteristic observed and calculated isotope patterns arising mainly from the two isotopes of Sb (^{121}Sb 57%, ^{123}Sb 43%) and Cl (^{35}Cl 75%, ^{37}Cl 25%) match perfectly. There was also the corresponding doubly-charged peak for $[H_6(RSb)_{12}O_{28}]^{2-}$ (m/z 1626.379, calc. 1626.375). Each of these peaks had a satellite corresponding to the analogues with one H^+ replaced by a Na^+. There are some less intense peaks which arise from higher nuclearities, but clearly the Sb_{12} one is most favoured under these conditions.

If the stibonic acid is not carefully purified, or if a small amount of NaOH is added,§ or even if the solution of the purified sample is left standing in normal glassware, the parent acid peaks are completely replaced by those of the sodium adducts $[Na_3H_3(RSb)_{12}O_{28}]^{2-}$ (m/z 1659.343, calc. 1659.347), $[Na_2H_4(RSb)_{12}O_{28}]^{2-}$ (m/z 1648.354, calc. 1648.356), and $[NaH_5(RSb)_{12}O_{28}]^{2-}$ (m/z 1637.361, calc. 1637.365). The corresponding singly-charged ions $[Na_4H_3(RSb)_{12}O_{28}]^-$ and $[Na_3H_4(RSb)_{12}O_{28}]^-$ were represented in the region around m/z 3300.

Other stibonic acids $RSbO_3H_2$ for R′ = p-$CH_3C_6H_4$ and R″ = p-$O_2NC_6H_4$ under the same conditions behaved identically, giving the same series of sodium adduct ions.

We have not yet obtained single crystals of the parent acid suitable for structure determination, but when the solution formed by dissolving p-$O_2NC_6H_4SbO_3H_2$ in NaOH was treated with $[PhCH_2NMe_3]Br$, slow evaporation provided crystals¶ suitable for X-ray structure determination.†‖ This revealed the anion shown in Fig. 2, as part of an overall formula of $PhCH_2NMe_3[Na_2H_9(p\text{-}O_2NC_6H_4Sb)_{12}O_{30}\cdot 4H_2O]\cdot xH_2O$. The nine H atoms of the anion were not located directly, but are required for charge neutrality; six of them will probably be associated with the terminal O atoms (see below) as –OH groups, while the other three are presumably

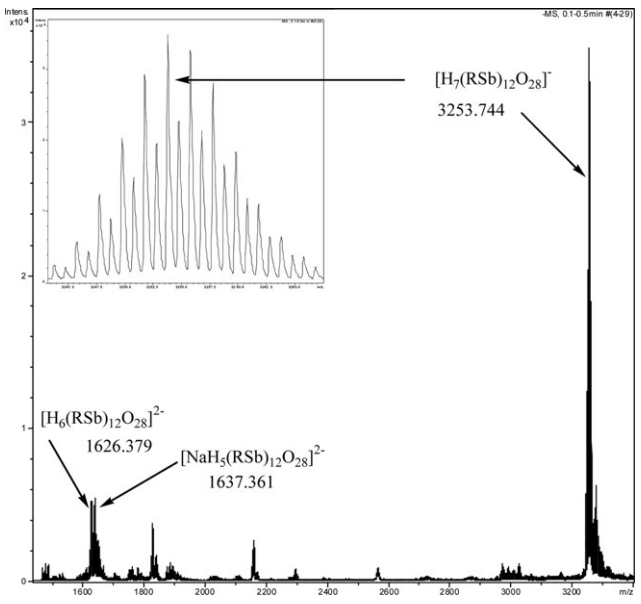

Fig. 1 The ESI-MS of '$RSbO_3H_2$' in MeCN showing ions derived from the cluster $[H_8(RSb)_{12}O_{28}]$ (R = p-ClC_6H_4–). The inset is an expansion of the m/z 3253 envelope showing the characteristic isotope pattern.

[a] *Biosensors and Biomeasurement, Plant and Food Research, Ruakura Research Centre, Private Bag 3123, Hamilton 3240, New Zealand*
[b] *Department of Chemistry, School of Science and Engineering, University of Waikato, Private Bag 3105, Hamilton 3240, New Zealand. E-mail: b.nicholson@waikato.ac.nz; Fax: +64 7 838 4219; Tel: +64 7 856 2889*

† Electronic supplementary information (ESI) available: Experimental procedures and X-ray crystal structure determination. CCDC 702086. For ESI and crystallographic data in CIF or other electronic format see DOI: 10.1039/b816113e

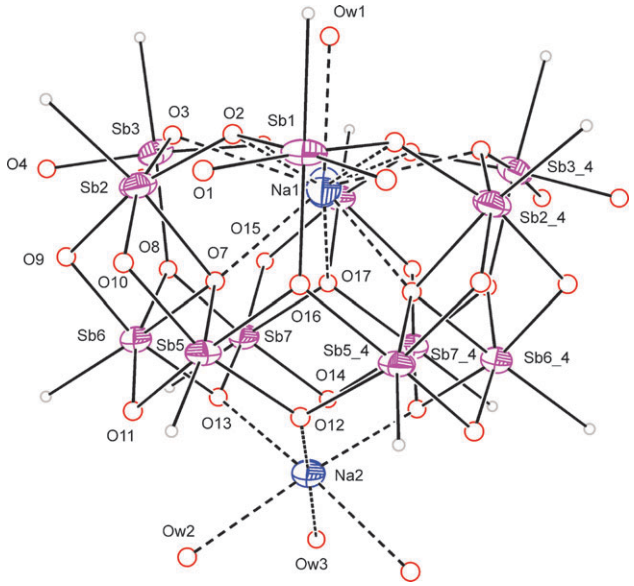

Fig. 2 The core structure of the anion revealed in the crystal structure determination of $(PhCH_2NMe_3)[Na_2H_9(R''Sb)_{12}O_{30}(H_2O)_4]\cdot xH_2O$ ($R'' = p\text{-}O_2NC_6H_4$–). The red circles are oxygen atoms, and the small grey circles represent the *ipso* carbon atoms of the $p\text{-}O_2NC_6H_4$– rings.

attached to the cage O atoms. In addition to the four H_2O molecules closely associated with the anion by coordination to Na^+, there are also many other water molecules in the lattice which are poorly defined, as is common in structures of this type.

The anion is a cage formed by twelve hexacoordinate R″Sb groups at the apices of a hexagonal antiprism, linked by O atoms. Six of the Sb atoms are arranged in a puckered hexagonal array (av. Sb···Sb 3.640 Å), with the other six in a planar hexagonal array (av. Sb···Sb 3.135 Å) parallel to it, and *ca.* 3 Å apart. The oxygen atoms can be divided into eighteen μ_2-O, six μ_3-O and six terminal ones (presumably –OHs). The average Sb–O distances are 1.980, 2.088 and 1.979 Å respectively for the μ_2, μ_3 and terminal examples.

The overall symmetry of the cage, ignoring the conformation of the aryl rings, is C_{3v}; with the rings included the anion has crystallographically-imposed mirror symmetry.

Held within the cage are two Na^+ ions. Na(1) has an unusual 10-coordination. Six of the coordination sites are occupied by a planar hexagonal array of the μ_2-O atoms from the puckered Sb layer (Na···O (av.) 2.777 Å). The Na^+ is displaced 0.76 Å out of the oxygen plane towards the interior of the cage. The remaining coordination is from three of the μ_3-O atoms that link the two Sb layers together (Na···O (av.) 2.570 Å), with a coordinated H_2O occupying the 10th site on the other side of the hexagon (Na···O 2.68(3) Å). This hexagonal-planar site is clearly analogous to those in ligands such as crown ethers while the truncated conical void within which the ion is embraced suggests a cavitand cage. A similarly-held cation site was described by Cronin *et al.*[9] for the inorganic crown POM $[H_{12}W_{36}O_{120}]^{12-}$, though for their example the O atoms were from terminal oxo ligands which formed a puckered ring in contrast to crown-ethers which have a planar array of bridging oxygens. Our example is a closer analogue with a planar array of μ-O atoms providing coordination, and with average cross-ring O···O distances of 5.34 Å compared with values of *ca.* 5.5 Å in 18-crown-6 ligands.[10]

Na(2) is six-coordinate with three sites occupied by μ_2-O atoms from the anion and the other three by coordinated water molecules. The mass spectrometry experiments indicate that the coordinated water molecules are readily lost, and one Na^+, presumably Na(2), can be extruded, but the remaining Na^+ is held tenaciously and no ions were observed in the ESI-MS where this had been removed, even under quite severe conditions.

There is a difference in the apparent degree of hydration of the core-cluster unit between the ESI-MS results in MeCN, which indicate a parent formula $[H_8(RSb)_{12}O_{28}]$, and the crystal structure result which is derived from $[H_{12}(RSb)_{12}O_{30}]$ after crystallisation from aqueous solutions, a difference of $2H_2O$. It is not yet clear whether this arises from the different solvent conditions or from very facile loss of two H_2O in the mass spectrum, possibly by condensation of four of the terminal –OH groups to give two more μ-O units. Previous reports suggest that ESI-MS results for POMs usually, but not always, provide a good correlation between species in solution, and those subsequently crystallised.[11]

The core structure of the $p\text{-}O_2NC_6H_4Sb$ POM has been reported before as part of a complex structure assigned the overall formula** $[Na_{21}(PhSb)_{48}O_{114}]\cdot 46H_2O\cdot 4MeCN$, isolated in small yields from a reaction mixture consisting of $PhSbO_3H_2$, Ni^{2+} and NaOMe in MeCN–H_2O.[12] The $[Na_2H_9(ArSb)_{12}O_{30}\cdot 4H_2O]$ cores of both structures are essentially superimposable, despite the different aryl groups and crystal packing arrangements. We also have preliminary crystal structures of the corresponding $Rb[Na_2H_9(p\text{-}MeC_6H_4Sb)_{12}O_{30}\cdot 4H_2O]$ and $Ph_4P[Na_2H_9(p\text{-}MeC_6H_4Sb)_{12}O_{30}\cdot 4H_2O]$ analogues and they also have the same core structure, so this appears to be a highly conserved arrangement.

The stability of this $(ArSb)_{12}$ unit is further shown by related structures formed with other cations. When $p\text{-}MeC_6H_4SbO_3H_2$ was dissolved using KOH in place of NaOH a solid was obtained for which the dominant signal in the ESI-MS was assigned to $[K_3H_7(p\text{-}MeC_6H_4Sb)_{12}O_{30}]^{2-}$ (m/z 1579.647, calc. 1579.651). Similarly with $Ca(OH)_2$ as base, the product gave ESI-MS peaks for $[Ca_2H_6(p\text{-}MeC_6H_4Sb)_{12}O_{30}]^{2-}$ (m/z 1560.679, calc. 1560.664). Conversely LiOH or CsOH gave a different range of polyoxostibonates which have yet to be characterised fully, suggesting Li^+ is too small, and Cs^+ too large, to be complexed within the same species.

The strong affinity for Na^+ was illustrated when $p\text{-}O_2NC_6H_4SbO_3H_2$ was dissolved using Et_3N as base; the main product was shown by ESI-MS to be the sodium adduct $[Na_2H_4(p\text{-}O_2NC_6H_4Sb)_{12}O_{28}]^{2-}$ presumably formed from adventitious Na^+ from the glassware, or carried over from synthesis of the acid. Similarly when the $[Na_2H_4(p\text{-}O_2NC_6H_4Sb)_{12}O_{28}]^{2-}$ complexes are mixed with an aqueous solution of Rb^+, there is little if any exchange of cations, as shown by ESI-MS.

In conclusion, we have shown that $RSbO_3H_2$ forms an aggregate $[H_8(RSb)_{12}O_{28}]$, at least when crystallised from NH_3(aq.)–HOAc. This serves as a parent for a novel range of isopolyoxostibonates, stable under alkaline conditions (it is noteworthy that transition-metal POMs form under *acidic* conditions). The cage behaves as an inorganic crown ligand,

with a strong affinity for Na^+ and other similarly-sized cations. The new species can be synthesised with a variety of different aryl groups which should allow some tuning of electronic and steric properties. There is ESI-MS evidence for other high-nuclearity POMs based on polyoxostibonates, as yet not fully characterised, which may be optimised with different cations or conditions. There is also clearly potential to use arylstibonic acids for a range of hetero-POMs.

We thank Dr Tania Groutso, University of Auckland, for collection of X-ray data and Anna Jagger and Daniel Hailstone for synthesis of stibonic acids.

Notes and references

‡ Preparation of $[H_8(RSb)_{12}O_{28}]$ (R = *p*-ClC_6H_4–). A sample of $RSbO_3H_2$ (R = *p*-ClC_6H_4–) was purified by suspending a small sample (*ca.* 0.5 g) in water, and adding NH_3(aq.) (2 mol l^{-1}) dropwise until dissolution was just effected. The open flask was placed in a desiccator containing conc. CH_3COOH, which was allowed to diffuse into the stibonic acid solution, and the product precipitated as an off-white powder. Found: C 26.93; H 2.46. Calc. for $C_{72}H_{56}Cl_{12}O_{28}Sb_{28}$ C 26.56; H 1.73%. ESI-MS (a fresh sample in MeCN): (*m*/*z* (calc.), assignment, relative intensity): 3275.719 (3275.738), $[NaH_6(RSb)_{12}O_{28}]^-$, 18%; 3253.744 (3253.756), $[H_7(RSb)_{12}O_{28}]^-$, 100%; 3025.866, 3007.859, 2989.844, 2969.837, (all 1^- ions, unassigned, appear to be Sb_{11} species), 2565.054 (3^- ion, unassigned, appears to be Sb_{28} species); 2157.189 (2157.162), $[H_6(RSb)_{16}O_{36}]^{2-}$, 9%; 1826.314 ($2^-$ ion, unassigned, appears to be Sb_{13} species); 1648.353 (1648.356), $[Na_2H_4(RSb)_{12}O_{28}]^{2-}$, 4%; 1637.361 (1637.365), $[NaH_5(RSb)_{12}O_{28}]^{2-}$, 18%; 1626.366 (1626.375), $[H_6(RSb)_{12}O_{28}]^{2-}$, 18%.

§ Preparation of sodium salt solutions from $[H_8(RSb)_{12}O_{28}]$ (R = *p*-ClC_6H_4–). $RSbO_3H_2$ (R = *p*-ClC_6H_4–) was suspended in water and an aqueous solution of NaOH (2 mol l^{-1}) was added dropwise until the solid had dissolved. This solution was allowed to evaporate until a white powder formed. This was filtered and dried. A small portion of the solid was dissolved in MeCN and examined by ESI-MS: (*m*/*z* (calc.), assignment): 3341.684 (3341.642) $[Na_4H_3(RSb)_{12}O_{28}]^-$; 3319.702 (3341.664) $[Na_3H_4(RSb)_{12}O_{28}]^-$; 1659.343 (1659.347) $[Na_3H_3(RSb)_{12}O_{28}]^{2-}$; 1648.354 (1648.356) $[Na_2H_4(RSb)_{12}O_{28}]^{2-}$. The same peaks were observed if a drop of NaOH solution was added to a MeCN solution of purified $[H_8(RSb)_{12}O_{28}]$.

¶ Isolation of crystals of $(PhCH_2NMe_3)[Na_2H_9(R''Sb)_{12}O_{30}(H_2O)_4]\cdot xH_2O$ (R″ = *p*-$O_2NC_6H_4$–). *p*-Nitrophenylstibonic acid (245 mg, 8.4 × 10^{-4} mol) was dissolved in water (50 ml) containing 0.6 ml 2 M NaOH (pH = 11.2). Ten ml of this solution (1.7 × 10^{-4} mol stibonic acid, 2.4 × 10^{-4} mol Na^+) was subsequently combined with benzyltrimethylammonium bromide (46 mg, 2 × 10^{-4} mol) dissolved in water (1 ml) forming a fine pale-yellow precipitate. The solution was left to evaporate to dryness. The dried precipitate crystallised from 2 : 1 (v/v) acetonitrile–water solution (6 ml) by slow evaporation, whereupon pale-yellow needles formed within 3 weeks.

‖ $C_{82}H_{81}N_{13}Na_2O_{58}Sb_{12}\cdot xH_2O$, M_r 3683.58, monoclinic, space group *C*2/*m*, *a* = 30.6262(6), *b* = 22.5295(4), *c* = 25.1789(8) Å, β = 122.569(1)°, *U* = 14641.2(6) Å^3, *Z* = 4, D_c = 1.671 g cm^{-3}, μ(Mo-Kα) = 2.26 mm^{-1}, *F*(000) = 7048, *T* = 90(2) K. Crystal size 0.31 × 0.17 × 0.14 mm^3. Total data 165 946, unique data 16 399 (R_{int} 0.083), observed ($I > 2\sigma(I)$) data 10 514, θ range 2–27°. Refinement (on F_o^2) converged with R_1 0.0620 ($I > 2\sigma(I)$), wR_2 0.1917 (all data), GoF 1.138, Δe = 2.3/−1.6 e Å^{-3}. Only the four H_2O molecules coordinated to the Na^+ cations have been included in the formula and M_r calculation; lattice H_2O molecules (approximately 15 of them) were poorly defined so were removed from the refinement using the SQUEEZE procedure of PLATON.[13]

** This formula does not appear complete from charge neutrality considerations; $[Na_{21}H_{15}(PhSb)_{48}O_{114}]$ is more probable.

1 N. C. Lloyd, H. W. Morgan, B. K. Nicholson and R. S. Ronimus, *J. Organomet. Chem.*, 2008, **693**, 2443.
2 G. O. Doak, *J. Am. Chem. Soc.*, 1946, **68**, 1991.
3 L. H. Bowen and G. G. Long, *Inorg. Chem.*, 1978, **17**, 551.
4 J. Beckmann, P. Finke, M. Hesse and B. Wettig, Abstract P845, XXIII International Conference on Organometallic Chemistry, Rennes, July, 2008; *cf.* J. Beckmann, T. Heek and M. Takahashi, *Organometallics*, 2007, **26**, 3633.
5 M. T. Pope, *Heteropoly and Isopoly Oxometallates*, Springer-Verlag, Berlin, 1983; M. T. Pope and A. Müller, *Angew. Chem., Int. Ed.*, 1999, **30**, 34; D. L. Long, E. Burkholder and L. Cronin, *Chem. Soc. Rev.*, 2007, **36**, 105.
6 P. Gouzerh and A. Proust, *Chem. Rev.*, 1998, **98**, 77; A. Proust, R. Thouvenot and P. Gouzerh, *Chem. Commun.*, 2008, 1837; Y. D. Chang and J. Zubieta, *Inorg. Chim. Acta*, 1996, **245**, 177.
7 P. C. Andrews, G. B. Deacon, C. M. Forsyth, P. C. Junk, I. Kumar and M. Maguire, *Angew. Chem., Int. Ed.*, 2006, **45**, 5638; E. V. Dikarev, H. Zhang and B. Li, *Angew. Chem., Int. Ed.*, 2006, **45**, 5448.
8 G. O. Doak and H. G. Steinman, *J. Am. Chem. Soc.*, 1946, **68**, 1987.
9 D. L. Long, H. Abbas, P. Kögerler and L. Cronin, *J. Am. Chem. Soc.*, 2004, **126**, 13880; D. L. Long, O. Brücher, C. Streb and L. Cronin, *Dalton Trans.*, 2006, 2852.
10 *e.g.* H. Noth and M. Warchhold, *Eur. J. Inorg. Chem.*, 2004, 1115.
11 E. C. Alyea, D. Craig, I. Dance, K. Fisher, G. Willett and M. Scudder, *CrystEngComm*, 2005, **7**, 491; D.-L. Long, C. Streub, Y.-F. Song, S. Mitchell and L. Cronin, *J. Am. Chem. Soc.*, 2008, **130**, 1830.
12 V. Baskar, M. Shanmugam, M. Helliwell, S. J. Teat and R. E. P. Winpenny, *J. Am. Chem. Soc.*, 2007, **129**, 3042.
13 P. Van der Sluis and A. L. Spek, *Acta Crystallogr., Sect. A: Found. Crystallogr.*, 1990, **46**, 194.

ORGANOMETALLICS
Article

Organometallics **XXXX,** *XXX,* 000–000 A
DOI: 10.1021/om1008692

Isopolyoxometalates of Antimony: Arylstibonic Acids $[H_8(RSb)_{12}O_{28}]$ and Derived Dodecanuclear Polyoxostibonates $[M_2H_{10-x}(RSb)_{12}O_{30}]^{x-}$, M = Na or K

Brian K. Nicholson,*[,†] Christopher J. Clark,[‡] Cody E. Wright,[†] and Tania Groutso[§]

[†]*Chemistry Department, University of Waikato, Private Bag 3105, Hamilton 3240, New Zealand,* [‡]*Bioengineering Technologies, Plant and Food Research, Ruakura Research Centre, Private Bag 3123, Hamilton 3240, New Zealand, and* [§]*Chemistry Department, University of Auckland, PO Box 92019, Auckland, New Zealand*

Received September 7, 2010

Electrospray ionization mass spectrometry shows arylstibonic acids, *p*-$XC_6H_4SbO_3H_2$ (X = methyl, nitro, or chloro), and 1-naphthylstibonic acid exist in MeCN as dodecanuclear aggregates $[H_8(RSb)_{12}O_{28}]$. With KOH or NaOH these form polyoxometalate ions $[M_2H_8(RSb)_{12}O_{30}]^{2-}$ (M = K or Na) with a hexagonal antiprismatic array of the Sb atoms, as shown by X-ray crystallographic structures for three new examples. There is one firmly encapsulated 10-coordinate M^+ ion within an inorganic 12-crown-6 moiety $\{Sb_6O_6\}$ in the hexagonal channel and one six-coordinate M^+.

Introduction

Arylstibonic acids, of nominal formula $RSbO_3H_2$, have been known for over 100 years.[1] However, in contrast to the simple molecular arylarsonic acids, their precise form is unknown since they invariably exist as amorphous powders with limited solubility in aqueous solution, except when it is alkaline. Their titration behavior is complicated and variable.[2] It is generally concluded that they are polymeric species involving five- or six-coordinate Sb with μ-O linkages,[3] with early Mossbauer studies favoring trigonal-bipyramidal geometry.[4] A recent crystal structure determination[5] of a sterically hindered compound, 2,6-$Mes_2C_6H_3SbO_3H_2$, showed a molecular dimer with a central Sb_2O_2 core and five-coordinate Sb, but the bulky R groups in this instance prevent higher aggregation; thus the result cannot be used as a specific basis for deducing the arrangement in stibonic acids with smaller aryl groups.

ESI-MS is a powerful method for determining species in solution,[6] so we decided to investigate the oligomerization of stibonic acids and now report that under appropriate conditions these acids form polyoxostibonate cages with intriguing structures. Herein we describe the mass spectrometric behavior of the acids $RSbO_3H_2$ [R = *p*-ClC_6H_4, *p*-MeC_6H_4, *p*-$O_2NC_6H_4$, and 1-naphthyl] and present the characterization and structural determinations of Na^+ or K^+ salts of high-nuclearity polyoxyanions formed by them.[7] Preliminary details of the present work have been communicated earlier.[8]

Related examples of organopolyoxostibonates, or mixed oxometalates incorporating organo-antimony, have been reported only recently, prepared under different conditions from those used and described herein.[9,10]

Experimental Section

Preparation of the arylstibonic acids was carried out essentially using the procedure established by Doak and Steinman.[11] For convenience a typical synthesis is included below. No melting point data are given, as these substances do not have well-defined melting or decomposition temperatures.[11] For the preparation of the derivatives of the acids the crude yield (contaminated with other salts) will be essentially quantitative. However the crystalline material from the slow evaporation of

*To whom correspondence should be addressed. E-mail: b.nicholson@waikato.ac.nz.

(1) (a) Doak, G. O.; Freedman, L. D. *Organometallic Compounds of Arsenic, Antimony and Bismuth*; Wiley: New York, 1970. (b) Dunning, F.; Reid, E. E. *J. Am. Chem. Soc.* **1926**, *48*, 2959. (c) Riddell, W.; Basterfield, S. *Trans. R. Soc. Can., Ser. 3* **1929**, *23*, 45.

(2) (a) Schmidt, H. *Justus Liebigs Ann. Chem.* **1920**, *421*, 174. (b) Schmidt, H. *Ber.* **1922**, *55B*, 697.

(3) Doak, G. O. *J. Am. Chem. Soc.* **1946**, *68*, 1991.

(4) Bowen, L. H.; Long, G. G. *Inorg. Chem.* **1978**, *17*, 551.

(5) Beckman, J.; Finke, P.; Hesse, M.; Wettig, B. *Angew. Chem., Int. Ed.* **2008**, *47*, 9982.

(6) (a) Henderson, W.; McIndoe, J. S. *Mass Spectrometry of Inorganic, Coordination and Organometallic Compounds*; J. Wiley and Sons: New York, 2005. (b) Henderson, W.; Nicholson, B. K.; McCaffrey, L. J. *Polyhedron* **1998**, *17*, 4291. (c) Long, D.-L.; Streb, C.; Song, Y.-F.; Mitchell, S.; Cronin, L. *J. Am. Chem. Soc.* **2008**, *130*, 1830. (d) Alyea, E. C.; Craig, D.; Dance, I.; Fisher, K.; Willett, G.; Scudder, M. *CrystEngComm* **2005**, *7*, 491. (e) Miras, H. N.; Wilson, E. F.; Cronin, L. *Chem. Commun.* **2009**, 1297.

(7) Early attempts at characterizing salts of aryl stibonic acids are described in: Fargher, R. G.; Gray, W. H. *J. Pharmacol.* **1921**, *18*, 341. See also: Gray, W. H.; Lamb, I. D. *J. Chem. Soc.* **1938**, 401.

(8) Clark, C. J.; Nicholson, B. K.; Wright, C. E. *Chem. Commun.* **2009**, 923.

(9) (a) Gouzerh, P.; Proust, A. *Chem. Rev.* **1998**, *98*, 77. (b) Beckmann, J.; Heek, T.; Takahashi, M. *Organometallics* **2007**, *26*, 3633. (c) Beckmann, J.; Hesse, M. *Organometallics* **2009**, *28*, 2345. (d) Chandrasekhar, V.; Thirumoorthi, R. *Organometallics* **2009**, *28*, 2637. (e) Ali, S.; Baskar, V.; Muryn, C. A.; Winpenny, R. E. P. *Chem. Commun.* **2008**, 6375.

(10) (a) Jami, A. K.; Prabhu, S. R.; Baskar, V. *Organometallics* **2010**, *29*, 1137. (b) Prabhu, M. S. R.; Jami, A. K.; Baskar, V. *Organometallics* **2009**, *28*, 3953. (c) Piedra-Garza, L. F.; Dickman, M. H.; Moldovan, O.; Breunig, H. J. *Inorg. Chem.* **2009**, *48*, 411.

(11) Doak, G. O.; Steinman, H. G. *J. Am. Chem. Soc.* **1946**, *68*, 1987.

MeCN is variable, depending on how long the solution is left to concentrate, how much noncrystalline compound precipitates out, etc. Crystals are initially highly solvated with lattice water, some of which at least is lost as soon as the crystals are collected. This makes a formal yield somewhat difficult to define. ESI-MS was carried out on a Bruker MicrOTOF instrument, operating under standard conditions in negative ion mode, with samples made up in MeCN immediately before infusion. Assignment of ions was aided by matching the characteristic patterns generated by the ^{121}Sb (57%) and ^{123}Sb (42%) isotopes. Peaks are reported as the m/z with the greatest intensity in the isotopic envelope.

Preparation and Characterization of p-$ClC_6H_4SbO_3H_2$. 4-Chloroaniline (6.38 g, 0.05 mol) was dissolved in ethanol (125 mL) in a 500 mL wide-mouth conical flask, surrounded by an ice-bath, with an efficient stirrer. Concentrated sulfuric acid (2.7 mL, 5 g) and $SbCl_3$ (11.4 g, 0.05 mol) were added. Once the latter had completely dissolved, a solution of sodium nitrite (3.5 g in 5 mL of water) was added to initiate diazotization. This thick mixture was stirred for 30 min. Cuprous bromide (1 g) was added and the ice-bath removed. As the mixture warmed, nitrogen evolved spontaneously. Stirring was continued for 24 h to ensure complete nitrogen evolution. Steam distillation was used to remove the alcohol. The residue of crude stibonic acid was collected on a Buchner funnel, washed with water, and air-dried.

The crude acid was dissolved in concentrated hydrochloric acid (ca. 1 L) and filtered, and a solution of pyridine (5 mL) in concentrated HCl (20 mL) added. The precipitated pyridinium salt, $[pyH][ClC_6H_4SbCl_5]$, was collected on a sintered glass filter, washed several times with concentrated hydrochloric acid, and left to dry. It was dissolved in the minimum volume of dilute sodium carbonate solution (ca. 2 L of a 1% (w/v) solution) and filtered. The free acid was obtained by the dropwise addition of dilute hydrochloric acid while stirring rapidly. The precipitate was collected by filtration and washed thoroughly with water acidified with a few drops of dilute hydrochloric acid. After air drying the yield was 12.3 g, 87%, assuming a formula of p-$ClC_6H_4SbO_3H_2$.

The product was further purified by dissolving a sample (2 g) in a mixture of water and concentrated NH_3(aq) (2:1, ca. 300 mL) in a plastic beaker. The open beaker was placed in a closed desiccator containing glacial acetic acid. The acid diffused into the solution over several days, precipitating the stibonic acid as an off-white powder, which was collected by gravity filtration. Recovery was 80−90%. Anal. Found: C 26.93; H 2.46. Calcd for $C_6H_6ClO_3Sb$: C 25.44; H 2.14; Calcd for $C_{72}H_{56}Cl_{12}O_{28}Sb_{12}$: C 26.56; H 1.73. ESI-MS (m/z, assignment, (calc), intensity, R = p-ClC_6H_4): 3275.719, $[NaH_6(RSb)_{12}O_{28}]^-$, (3275.738), 18%; 3253.744, $[H_7(RSb)_{12}O_{28}]^-$, (3253.756), 100%; 2157.189 $[H_6(RSb)_{16}O_{36}]^{2-}$, (2157.162), 9%; 1648.353, $[Na_2H_4(RSb)_{12}O_{28}]^{2-}$, (1648.356), 4%; 1637.361, $[NaH_5(RSb)_{12}O_{28}]^{2-}$, (1637.365), 18%; 1626.366 $[H_6(RSb)_{12}O_{28}]^{2-}$, (1626.375), 18%. IR (KBr disk, cm^{-1}): 3400 (s, br), 3190 (s), 1634 (m), 1573 (m), 1477 (s), 1383 (s), 1182 (w), 1090 (s), 1067 (s), 1013 (s), 947 (w), 814 (s), 728 (s), 663 (s), 602 (w), 489 (s).

Preparation and Characterization of p-$MeC_6H_4SbO_3H_2$. Similarly, from p-toluidine a white powder was obtained in 79% initial yield. Anal. Found: C 33.35; H 3.49. Calcd for $C_7H_9O_3Sb$: C 31.98; H 3.45; Calcd for $C_{84}H_{92}O_{28}Sb_{12}$: C 33.51; H 3.08. ESI-MS (m/z, assignment, (calc), intensity, R = p-MeC_6H_4): 3008.434, $[H_7(RSb)_{12}O_{28}]^-$, (3008.419), 100%; 1993.619 $[H_6(RSb)_{16}O_{36}]^{2-}$ (1993.604), 3%; 1503.719 $[H_6(RSb)_{12}O_{28}]^{2-}$, (1503.706), 18%. IR (KBr disk, cm^{-1}): 3401 (s, br), 3200 (s), 1635 (m), 1593 (m), 1493 (m), 1447 (w), 1395 (s), 1310 (w), 1280 (w), 1210 (w), 1187 (m), 1073 (m), 1018 (w), 802 (s), 743 (s), 667 (s), 600 (w), 486 (s), 460 (w).

Preparation and Characterization of p-$O_2NC_6H_4SbO_3H_2$. This was prepared from p-nitroaniline using the same method, except that the crude acid was dissolved in a 1:1 mixture of MeOH and concentrated HCl to form the pyridinium salt. The product was an off-white powder, crude yield 92% calculated as p-$O_2NC_6H_4SbO_3H_2$. ESI-MS showed that Na^+ was strongly incorporated even after two diffusion purifications. Anal. Found: C 26.11; H 2.76; N 4.76. Calcd for $C_6H_6NO_5Sb$: C 24.52; H 2.06; N 4.76; Calcd for $C_{72}H_{56}N_{12}O_{52}Sb_{12}$: C 25.56; H 1.67; N 4.96; Calcd for $NaC_{72}H_{55}N_{12}O_{52}Sb_{12}$: C 25.4; H 1.63; N 4.94. ESI-MS (m/z, assignment, (calc), intensity, R = p-$O_2NC_6H_4$): 1700.535 $[NaH_5(RSb)_{12}O_{28}]^{2-}$, (1700.514), 100%; 1146.688, $[Na_2H_5(RSb)_{12}O_{29}]^{3-}$, (1146.671), 100%; 1139.359, $[NaH_6(RSb)_{12}O_{29}]^{3-}$, (1139.344), 80%. IR (KBr disk, cm^{-1}): 3400 (s, br), 3190 (s, br), 1630 (m), 1597 (m), 1576 (m), 1516 (s), 1477 (w), 1390 (m), 1355 (s), 1315 (w) 1279 (w), 1105 (m), 1068 (m), 1014 (m), 937 (w), 854 (s), 738 (s), 710 (s), 684 (s), 600 (w), 533 (w), 466 (m).

Preparation and Characterization of (1-naphthyl)SbO_3H_2. This was prepared following the same procedure from α-naphthylamine (7.16 g, 0.05 mol) in ethanol (200 mL). The crude acid was dissolved in 1:1 MeOH/conc HCl (1.5 L) to form the pentachlorostibonate salt. The precipitation after dissolving in Na_2CO_3 solution was with dilute nitric acid. The product, (1-naphthyl)SbO_3H_2, was obtained as an off-white solid (20%), which ESI-MS showed contained very little Na^+, so it was not purified further. Anal. Found: C 38.8; H 2.55. Calcd for $C_{10}H_9O_3Sb$: C 40.2; H 3.03%; Calcd for $C_{120}H_{92}Sb_{12}O_{28}$: C 41.9; H 2.7%. ESI-MS (m/z, assignment, (calc), intensity, R = naphthyl): 3442.413, $[H_7(RSb)_{12}O_{28}]^-$, (3442.422), 100%. IR (KBr disk, cm^{-1}): 3401 (s, br), 3052 (s), 1656 (m), 1623 (w), 1590 (m), 1558 (w), 1504 (s), 1384 (s), 1335 (m), 1300 (w), 1263 (m), 1212 (w), 1166 (w), 1136 (w), 1058 (w), 1023 (m), 953 (w), 796 (s), 768 (s), 745 (m), 680 (m), 618 (w), 514 (w), 468 (m), 407 (w).

Preparation of Crystals of $K_4[H_8(p\text{-}ClC_6H_4Sb)_{12}O_{30}]\cdot 58H_2O$. p-Chlorophenylstibonic acid (244 mg, 0.86 mmol) was dissolved in water (50 mL) containing KOH (0.6 mL of 2 mol L^{-1}, pH = 12.0). Potassium nitrate (50 mg, 0.5 mmol) was dissolved in 25 mL of the alkaline stibonate solution (giving overall 0.43 mmol of Sb, 1.1 mmol K^+), and the clear solution was left to evaporate to dryness. The white residue crystallized from a MeCN (10 mL)/H_2O (0.2 mL) solution by slow evaporation, forming colorless block crystals. IR (KBr disk, cm^{-1}): 3370 (s, br), 1631 (s, br), 1572 (m), 1477 (s), 1384 (s), 1183 (w), 1090 (s), 1066 (s), 1013 (s), 821 (s), 726 (s), 654 (s), 603 (s), 491 (s), 457 (w).

Preparation of Crystals of $Rb_{0.67}Na_{2.33}[H_9(p\text{-}MeC_6H_4Sb)_{12}O_{30}]\cdot 20H_2O$. p-Tolylstibonic acid (221 mg, 0.84 mmol) was dissolved in water containing NaOH (0.6 mL of 2 mol L^{-1}, pH 11.2). A 10 mL aliquot of this solution was combined with RbI (43 mg, 0.2 mmol) in water (1 mL) (ratio of Sb:Na:Rb 17:24:20), and the clear solution was left to evaporate to dryness. The resulting white solid was crystallized from MeCN/H_2O solution (4:1 v/v, 5 mL) by slow evaporation to give clear, truncated square-pyramidal crystals after three weeks. IR (KBr disk, cm^{-1}): 3414 (s, br), 3015 (w), 2920 (w), 1638 (m), 1593 (m), 1492 (s), 1472(w), 1455 (m), 1392 (m), 1308 (w), 1210 (w), 1186 (m), 1074 (s), 1018 (w), 974 (w), 891 (w), 803 (s), 726 (m), 658 (s), 605 (m), 581 (m), 488 (s), 450 (m).

Preparation of Crystals of $[Ph_4P][Na_2H_9(p\text{-}MeC_6H_4Sb)_{12}O_{30}]\cdot xH_2O$. p-Tolylstibonic acid (221 mg, 0.84 mmol) was dissolved in water (50 mL) containing NaOH (0.6 mL of 2 mol L^{-1}, pH 11.2). A 10 mL aliquot of this solution was combined with a solution of $[Ph_4P]Br$ (84 mg, 0.2 mmol) in water (5 mL), giving a fine white suspension, which was left to evaporate to dryness. The resulting powder was crystallized from MeCN (4 mL)/H_2O (0.2 mL) by slow evaporation to give colorless crystals within four weeks.

ESI-MS of the crystals redissolved in MeCN: m/z 1525.689, calc for $[H_4Na_2(p\text{-}MeC_6H_4Sb)_{12}O_{28}]^{2-}$ 1525.688; m/z 3390.494, calc for $[H_4Na_2\ (p\text{-}MeC_6H_4Sb)_{12}O_{28}+Ph_4P]^-$ 3390.507.

X-ray Crystal Structure Determinations. Crystals were rapidly transferred from the mother liquor onto the diffractometer and cooled immediately to ca. 90 K, since they invariably lost crystallinity on exposure to air, presumably due to loss of lattice solvent (water and/or MeCN). Data were collected on a Bruker Apex II CCD diffractometer and processed routinely, including

absorption corrections using a multiscan method (SADABS).[12] Because of the relatively poor diffraction, the size of the molecules, and the presence of extensive lattice water molecules, the refinements were not routine. Each was treated differently, as presented below. Structures were solved using the SHELXS97 program[13] and refinement on F_o^2 was with SHELXL97[13] operating under the WinGx interface.[14]

Solution and Refinement for $K_4[H_8(p\text{-}ClC_6H_4Sb)_{12}O_{30}]\cdot 58H_2O$. The structure was solved by direct methods to reveal the 24 Sb atoms in the asymmetric unit. Subsequent difference maps revealed the remainder of the complex anions and the K^+ cations. Further analysis gave the positions of 77 O atoms from the lattice water molecules, and these refined cleanly with isotropic temperature factors. Another 39 O atoms were located in sensible positions, but were less well defined; thus these were refined with a common, isotropic temperature factor. All the included water molecules formed a reasonable H-bonded network with sensible O···O distances. There are probably only a few extra water molecules unaccounted for because of the relatively small (ca. 600 Å^3, 4%) remaining void volume in the cell. The aryl-ring H atoms were included in calculated positions, but the H atoms of the water molecules and the eight that must be associated with each of the anions for charge neutrality were not included.

Crystal and refinement data: $C_{72}H_{144}Cl_{12}K_4O_{88}Sb_{12}$, M_r 4446.6, triclinic, space group $P\bar{1}$, a = 20.3732(6) Å, b = 23.0650(7) Å, c = 34.213(1) Å, α = 87.386(2)°, β = 86.265(2)°, γ = 83.649(2)°; U = 15932.5(8) Å^3, Z = 4, D_c = 1.854 g cm^{-3}, μ(Mo K$_\alpha$) = 2.4 mm^{-1}, F(000) = 8632. T = 89(2) K. Crystal size: 0.44 × 0.28 × 0.20 mm^3. Total data 359 194, unique data 72 182 (R_{int} 0.070), θ range 1−27.5°. Refinement converged with R_1 = 0.0918 ($I > 2\sigma(I)$), wR_2 = 0.2430 (all data), GoF = 1.085, Δe = 3.1/−4.9 e Å^{-3}.

Solution and Refinement for $Rb_{0.67}Na_{2.33}[H_9(p\text{-}MeC_6H_4Sb)_{12}O_{30}]\cdot 20H_2O$. The crystals diffracted weakly, giving data with an average $I/\sigma(I)$ of only 3.6. The structure was solved by direct methods to give the positions of the 12 Sb atoms. A subsequent difference map showed all the anion O atoms and the three cations. These were refined as mixed Na^+/Rb^+ with tied occupancy factors summing to 1.0 and with temperature factors constrained to be the same. Ultimate refinement showed only Na^+/Rb^+(3) had significant (50%) contribution from Rb^+, the other two cation sites being solely Na^+. With further cycles the tolyl rings were located, but some were clearly disordered. The aryl rings were constrained as rigid hexagons using AFIX 66, with temperature factors constrained by the SIMU and DELU options of SHELXL97.[13]

Four H_2O molecules coordinated to Na^+ cations were well-defined. In addition there were another 16 lattice water molecules included in the refinement, some reasonably well-defined, others clearly having partial occupancy or loosely held positions. Although some of them refined with unrealistic temperature factors, this appeared to model the included solvent reasonably well since PLATON[15] indicated only small voids left in the unit cell. All non-H atoms were treated anisotropically, but H atoms were not included given the poor quality of the data.

Scheme 1. Preparation of Aryl Stibonic Acids by the Method of Doak and Steinman[11]

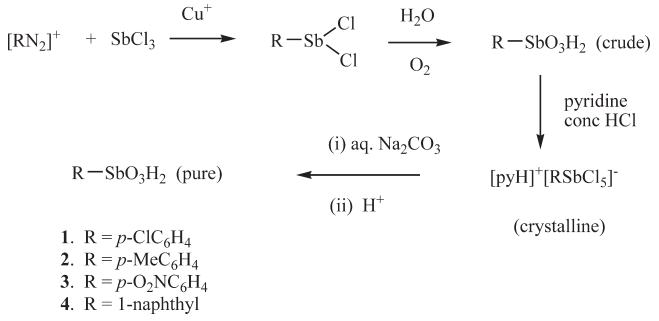

1. R = *p*-ClC$_6$H$_4$
2. R = *p*-MeC$_6$H$_4$
3. R = *p*-O$_2$NC$_6$H$_4$
4. R = 1-naphthyl

Crystal and refinement data: $C_{84}H_{124}Na_{2.66}O_{50}Rb_{0.67}Sb_{12}$, M_r 3498, monoclinic, space group $P2_1/n$, a = 17.7337(5) Å, b = 24.9225(8) Å, c = 27.4111(9) Å, β = 98.190(2)°, U = 11991.3(6) Å^3, Z = 4, D_c = 1.938 g cm^{-3}, μ(Mo Kα) = 2.95 mm^{-1}, F(000) = 6756. T = 89(2) K. Crystal size 0.22 × 0.12 × 0.12 mm^3. Total data 125 562, unique data 21 102 (R_{int} 0.098), observed ($I > 2\sigma(I)$) data 11 852, θ range = 2−25°. Refinement converged with R_1 = 0.0970 ($I > 2\sigma(I)$), wR_2 = 0.2878 (all data), GoF = 1.082, Δe = 3.4/−2.1 e Å^{-3}.

Solution and Refinement for $[Ph_4P][Na_2H_9(p\text{-}MeC_6H_4Sb)_{12}O_{30}]\cdot xH_2O$. Unfortunately the crystals diffracted weakly, giving data with an average $I/\sigma(I)$ of only 2.2. The structure was solved by direct methods (SHELXS97) to give the positions of the 12 Sb atoms. A subsequent difference map showed all the anion O atoms and the two Na^+ cations. With further cycles the tolyl rings and the Ph_4P^+ cation were located, but were not well defined. The phenyl carbon atoms of the cation were constrained as rigid hexagons using the AFIX 66 option of SHELXL97, while the tolyl rings were constrained using the SAME, SIMU, and DELU options.

The four H_2O molecules coordinated to Na^+ cations were well defined, as was one lattice water that links two anions through H bonding. However the rest of the lattice solvent (presumably H_2O though it may also include MeCN) was very diffuse and could not be modeled sensibly.

Without the solvent included the refinement converged with R_1 = 0.166, wR_2 = 0.435. To remove the diffuse solvent contribution, the SQUEEZE[16] routine of PLATON was invoked. This allowed refinement to give R_1 = 0.125 and wR_2 = 0.346.

While the results were sufficient to demonstrate that the anion has the same structure as that found for the $PhCH_2NMe_3^+$ example in our earlier report,[8] and the Rb^+ example above, the quality of the determination precludes any detailed analysis of bond parameters.

Crystal and refinement data: $C_{108}H_{123}Na_2O_{35}PSb_{12}$, M_r = 3519.01, orthorhombic, space group *Pcab*, a = 28.5319(7) Å, b = 29.5235(7) Å, c = 38.2815(10) Å, U = 32246.9(14) Å^3, Z = 8, D_c = 1.450 g cm^{-3}, μ(Mo Kα) = 2.05 mm^{-1}, F(000) = 13 600. T = 90(2) K. Crystal size 0.44 × 0.29 × 0.13 mm^3. Total data 27 4394, unique data 25 318 (R_{int} 0.133), observed ($I > 2\sigma(I)$) data 14 781, θ range = 2−24°. (Data are calculated from the refinement against the SQUEEZED data, so ignore contributions from the diffuse lattice solvent.) Refinement converged with R_1 = 0.125 ($I > 2\sigma(I)$), wR_2 = 0.346 (all data), GoF = 1.101, Δe = 3.4/−1.8 e Å^{-3}.

Results and Discussion

Preparation of Arylstibonic Acids 1−4. Arylstibonic acids are traditionally prepared using the Scheller reaction, as modified by Doak and Steinman (Scheme 1).[11] The key to the procedure is the conversion of the initial crude acid (which contains Sb_2O_3 as an impurity, among others) to a well-defined pyridinium salt [pyH][$RSbCl_5$], which can be purified by recrystallization.

Hydrolysis of this salt under mildly alkaline conditions precipitates the acid as an amorphous powder, which can be collected and dried. The purity of the arylstibonic acids thus formed was assessed by Doak and Steinman only by elemental analysis for Sb, varying amounts of water of crystallization being assigned to achieve matching data. Given the

(12) Blessing, R. H. *Acta Crystallogr.* **1995**, *A51*, 33.
(13) Sheldrick, G. M. *SHELX97, Programs for Crystal Structure Analysis*; University of Gottingen: Germany, 1997.
(14) Farrugia, L. J. *J. Appl. Crystallogr.* **1999**, *32*, 837.
(15) Spek, A. L. *Acta Crystallogr.* **1990**, *A41*, C34.
(16) Van der Sluis, P.; Spek, A. L. *Acta Crystallogr.* **1990**, *A46*, 194.

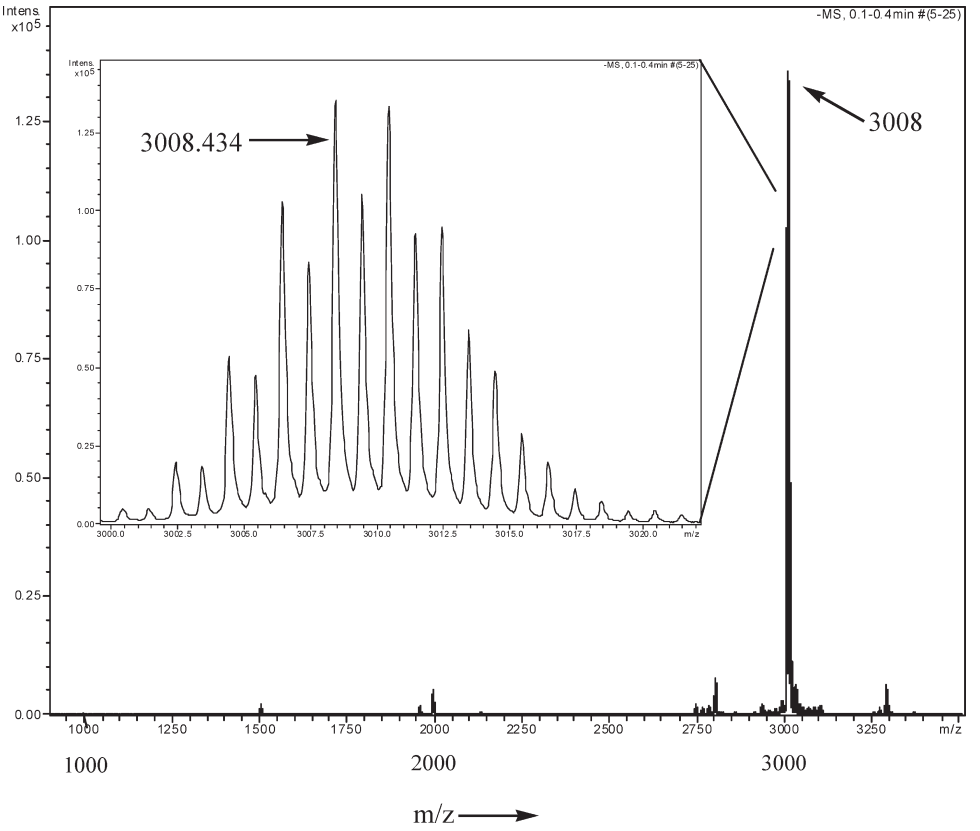

Figure 1. Negative ion ESI mass spectrum of *p*-tolylstibonic acid in MeCN, showing the dominant peak assigned to $[H_7(MeC_6H_4Sb)_{12}O_{28}]^-$ (calcd *m*/*z* 3008.419). The inset shows the characteristic isotope envelope for the parent ion arising mainly from the two isotopes of Sb.

strong affinity that the acids appear to have for cations (see below), it seems likely that material prepared by the published method would have contained some Na^+ from the hydrolysis step. To avoid this, we have added an extra purification step that involves dissolving the acid in the minimum amount of aqueous NH_3 and allowing CH_3COOH to slowly diffuse in to precipitate the acid. This works successfully with *p*-ClC_6H_4 and *p*-MeC_6H_4, examples 1 and 2, but the *p*-$O_2NC_6H_4$ example 3 still contained significant amounts of Na^+ even after two such purification cycles. Modification of the preparation by using a sequence of NH_3(aq) in place of the Na_2CO_3, followed by HCl for the hydrolysis of the pyridinium (*p*-nitrophenyl)pentachlorostibonate, gave material that was free of Na^+ adducts in the ESI-MS, but the overall purity of the sample was compromised. Further attempts to purify it led to incorporation of adventitious sodium, showing a particularly strong affinity for complexation with this example. In contrast, (1-naphthyl)SbO_3H_2 (**4**) showed a much lower affinity for Na^+ and did not need the extra purification step to provide ESI-MS spectra with little contribution from adducts. Compounds **1**−**3** are well known, but the 1-naphthyl compound **4** has not been characterized previously.

Elemental analysis cannot reliably distinguish between the nominal mononuclear formula $RSbO_3H_2$ and the polynuclear form $[H_8(RSb)_{12}O_{28}]$ that is indicated from the mass spectra (see below), though there is a better match for the latter in each case.

ESI-MS of Arylstibonic Acids. Samples of each of the arylstibonic acids were dissolved in MeCN and examined using ESI-MS. In every case, the dominant peaks could be assigned from mass measurements and from the distinctive isotope patterns to the anions derived from a parent acid of formula $[H_8(RSb)_{12}O_{28}]$. These were mainly $[H_7(RSb)_{12}O_{28}]^-$ and/or the corresponding doubly charged species $[H_6(RSb)_{12}O_{28}]^{2-}$. Figure 1 shows a typical spectrum.

Interestingly, the *p*-Me and 1-naphthyl examples gave mainly the 1^- ions, while the *p*-Cl compound gave both 1^- and 2^- ions in a ratio of ca 2:1. In contrast, the *p*-NO_2 species gave mainly 2^- and 3^- ions, which incorporated Na^+ ions, such as $[NaH_5(RSb)_{12}O_{28}]^{2-}$, showing the difficulty of complete purification for this compound. The specificity for the dodecanuclear aggregation for all these derivatives was remarkable. Other minor peaks appeared to arise from Sb_{11}, Sb_{13}, Sb_{16}, and Sb_{28} species, but these were barely significant. The main peaks were usually accompanied by satellites corresponding to species where one or more H^+ had been replaced by Na^+ to give, for example, $[NaH_6(RSb)_{12}O_{28}]^-$. For very fresh samples these were relatively minor and presumably arose either from traces of Na^+ carried over from the preparation or from adventitious Na^+ from the mass spectrometer source. However if the samples were left in standard glassware for any length of time, the Na^+ species increased as cations were leached from the glassware, indicating a strong affinity for complexation by the acid cluster. As noted above, the *p*-NO_2 example had an especially high affinity for cations. There is clearly some dependence on the relative electron-withdrawing nature of the R groups controlling the charge on the ions, and for all examples the sodium salts showed a greater tendency to form the 2− or 3− ions than did the parent acids, which appeared mainly as 1− ions under the same conditions.

The $[Na_xH_y(RSb)_{12}O_{28}]^{z-}$ aggregates appeared indefinitely stable in MeCN solution, with ESI-MS unchanged

Table 1. Negative Ion ESI-MS Data for Arylstibonic Acids in MeCN Obtained from the NCI Chemotherapeutics Repository[a]

NCI code	formula	*m/z*	assignment
NSC13735	4-Cl-3-$O_2NC_6H_4SbO_3H_2$	3793.64	$[H_7(RSb)_{12}O_{28}]^-$
		2051.72	$[H_6(RSb)_{13}O_{30}]^{2-}$
		1896.28	$[H_6(RSb)_{12}O_{28}]^{2-}$
NSC13742	2-$O_2NC_6H_4SbO_3H_2$	3402.04	$[NaH_6(RSb)_{12}O_{28}]^-$
NSC13743	3-$O_2NC_6H_4SbO_3H_2$	3380.07	$[H_7(RSb)_{12}O_{28}]^-$
		1827.98	$[H_6(RSb)_{13}O_{30}]^{2-}$
		1818.98	$[H_8(RSb)_{12}O_{29}]^{2-}$
		1689.52	$[H_6(RSb)_{12}O_{28}]^{2-}$
NSC13746	Na[4-$HO_3SC_6H_4SbO_3H$]	no significant high-mass peaks in MeCN[b]	
NSC13748	4-$(H_2N)O_2SC_6H_4SbO_3H_2$	1683.18 (in MeCN)	$[NaH_4(RSb)_{16}O_{36}]^{3-}$
		1675.87 (in H_2O)	$[H_5(RSb)_{16}O_{36}]^{3-}$
NSC13776	4-[$(HOC_2H_4)NH$]$O_2SC_6H_4SbO_3H_2$	no significant high mass peaks in MeCN[b]	
NSC13778	3-$(HO_2CCHCH)C_6H_4SbO_3H_2$	no significant peaks in MeCN or H_2O	
NSC13782	4-$(HOC_2H_4NH)C(O)C_6H_4SbO_3H_2$	no significant peaks in MeCN or H_2O	

[a] The provenance of the archived samples is largely unknown, and the samples may not be pure (R. H. Shoemaker, personal communication). [b] $[RSbO_3H.nH_2O]^-$ signals in low-mass region in H_2O.

after 24 h in MeCN in the absence of a source of cations. Furthermore, a mixture of MeCN solutions of the *p*-Cl- and *p*-Me-phenylstibonic acids showed peaks corresponding to the individual dodeca-clusters with no scrambling to give mixed species even after a week at room temperature.

MeCN was the solvent of choice for running ESI-MS. MeOH could also be used and gave the same species initially, but slow development of peaks arising from esterification gave ions such as $[H_5(RSb)_{12}O_{27}(OMe)]^{2-}$. 1,2-Dichloroethane or MeCN/H_2O (1:1) gave the same species as in MeCN, but overall ionization efficiency was lower, while tetrahydrofuran caused breakdown of the cluster units.

These results initially seemed to conflict with reports that arylstibonic acids could be analyzed by HPLC/ESI-MS, giving peaks assignable to monomeric Sb species.[17] However these chromatographic analyses were carried out by dissolving the solid acids in 0.05 M NaOH at 45 °C for 30 min before eluting with aqueous NH_4OAc at pH 9. These conditions apparently served to hydrolyze the Sb_{12} aggregates to monomeric species. To confirm this supposition, a sample of *p*-chlorophenylstibonic acid was dissolved in 0.05 M NaOH under the reported conditions. This solution then gave peaks in the low mass region assignable to $[RSbO_3H \cdot nH_2O]^-$ (*m/z* 282.899, 300.911, and 318.923, respectively, for $n = 0-2$) and related dimers and trimers.

During the course of the present study, Rishi et al. described the inhibition of DNA binding to B-ZIP dimers, using 12 arylstibonic acids that were sourced from the National Cancer Institute archives.[18] To extend our ESI-MS investigation, we requested some of the same samples and analyzed these in MeCN. Results are summarized in Table 1 and generally indicate that these examples also aggregate. The 2-nitro-, 3-nitro-, and 3-nitro-4-chlorophenylstibonic acids all showed clean ions from the equivalent Sb_{12} species discussed above, although interestingly, reasonably abundant signals from Sb_{13} clusters were also present for the latter two examples.

The other compounds listed in Table 1 gave no equivalent peaks in MeCN, possibly because of low solubility. In H_2O or MeCN, the *p*-sulfamoylphenylstibonic acid uniquely gave signals assigned to an Sb_{16} cluster derived from $[H_8(RSb)_{16}O_{36}]$, with only traces of Sb_{12} species. The other examples in H_2O gave only low mass ions associated with mainly monomers $[RSbO_3H]^-$ and related dimers.

In summary, it appears that, rather than variable polymeric species, solid arylstibonic acids are well-defined aggregates of formula $[H_8(RSb)_{12}O_{28}]$ and that these dissolve intact in MeCN solutions. Other nuclearities, especially Sb_{13} and Sb_{16} species, are often present but are only minor contributors, except for the one example described above. In water, these clusters are initially intact but hydrolyze to give monomeric $RSbO_3H^-$, and this breakdown is enhanced at higher pH.

Unfortunately we have been unable as yet to grow single crystals of any of these acids for full structural characterization, but the possible structures can perhaps be deduced from the structures of salts derived from the acids, as described below. We note that formally the species $[H_8(RSb)_{12}O_{28}]$ is the equivalent of the well-known isopolytungstate $[H_2W_{12}O_{40}]^{6-}$ [with the R group on Sb(V) a surrogate for the O on W(VI)],[19] providing a possible analogy for structural prediction. There is also comparison with the Keggin ion structural isomers such as $[PMo_{12}O_{40}]^{3-}$, which would also indicate a cuboctahedron, dodecahedral core for the Sb atoms in arylstibonic acid clusters if the α-isomer was to be formed. However analogies between polyoxometalates with main group (Sb) and transition metals (Mo or W) may be complicated by the recent theoretical findings that imply that the stability order of $[PW_{12}O_{40}]^{3-}$ Keggin species ($\alpha > \beta > \gamma > \delta > \varepsilon$) is completely reversed for $[Mn(MeSb)_{12}O_{28}]^{6-}$ aggregates.[20]

Structure of $K_2[K_2H_8(p\text{-}ClC_6H_4Sb)_{12}O_{30}] \cdot 58H_2O$. Crystals of a potassium salt of *p*-chlorophenylstibonic acid suitable for X-ray structural analysis were grown from MeCN/H_2O solution. These were found to correspond to the tetrapotassium salt $K_4[H_8(p\text{-}ClC_6H_4Sb)_{12}O_{30}]$.

(17) (a) Simmons, T. L.; McCloud, T. G. *J. Liq. Chromatogr. Relat. Technol.* **2003**, *26*, 2041. (b) Akee, R., unpublished data, **2010**.

(18) Rishi, V.; Oh, W. J.; Heyerdahl, S. L.; Zhao, J. F.; Scudiero, D.; Shoemaker, R. H.; Vinson, C. *J. Struct. Biol.* **2010**, *170*, 216.

(19) (a) Long, D.-L.; Abbas, H.; Kögerler, P.; Cronin, L. *J. Am. Chem. Soc.* **2004**, *126*, 13880. (b) Wang, J.; Ren, Q.; Zhao, J. *J. Coord. Chem.* **2008**, *61*, 192. (c) Zavalij, P.; Guo, J.; Whittingham, M. S.; Jacobson, R. A.; Pecharsky, V.; Bucher, C. K.; Hwu, S. J. *J. Solid State Chem.* **1996**, *123*, 83.

(20) Zhang, F. Q.; Guan, W.; Zhang, Y. T.; Xu, M. T.; Li, J.; Su, Z. M. *Inorg. Chem.* **2010**, *49*, 5472.

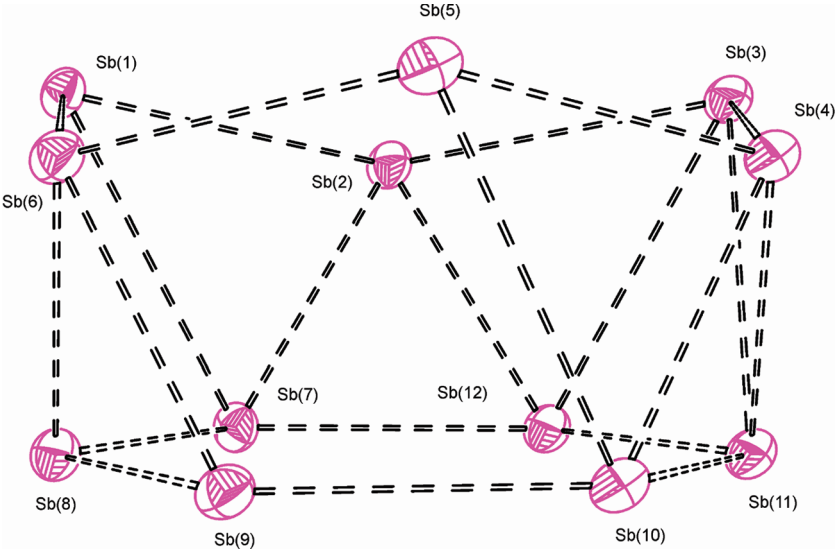

Figure 2. Hexagonal antiprismatic arrangement of the 12 Sb atoms in the $[K_2H_8(p\text{-}ClC_6H_4Sb)_{12}O_{30}]^{2-}$ anion. The same arrangement is found for the two sodium-containing anions.

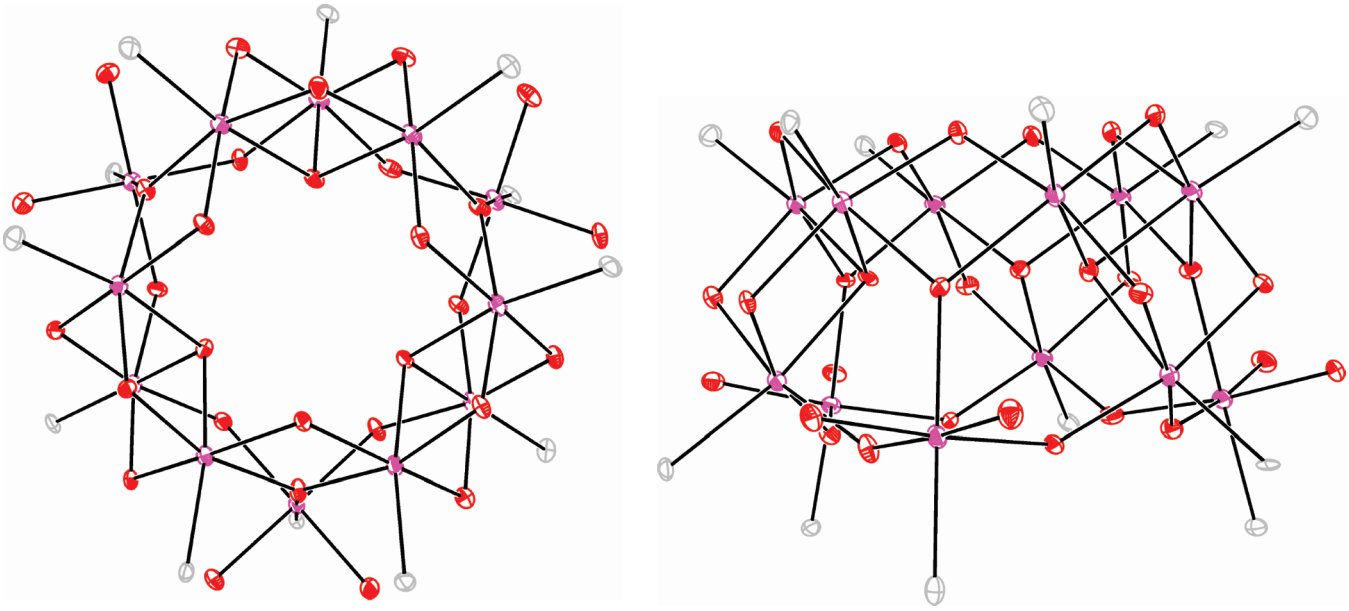

Figure 3. Two views of the $[K_2H_8(p\text{-}ClC_6H_4Sb)_{12}O_{30}]^{2-}$ anion, with the K^+ ions omitted and only the *ipso* carbon atoms of the aryl rings included. Purple = Sb, red = O, gray = C.

The lattice contains two independent anions in the asymmetric unit, but these have very similar structures; hence the following discussion is based on average parameters. Figures 2–4 show views of the anion. The core unit consists of 12 six-coordinate Sb atoms, each with one p-ClC_6H_4 group attached and five O atoms. The basic arrangement of the Sb_{12} unit is an irregular hexagonal antiprism (Figure 2).

The lower Sb_6 array is planar, while the upper Sb_6 array is a puckered chair arrangement. The Sb atoms are linked by 30 O atoms, divided into 18 double-bridging, six triple-bridging, and six terminal ones (presumably Sb–OH). The overall symmetry of the oxostibonate framework (stripped of the attached aryl rings and cations) is C_{3v} (Figure 3a). There must be an extra two H^+ associated with the cluster from charge considerations, but their positioning is undefined.

The aryl rings are of two types. Those attached to Sb atoms in the planar array form three pairs arranged face-to-face, while those from the puckered array of Sb atoms are splayed out to form a bowl-shaped cavity (Figure 4), which may function as a cavitand.

There are four distinct sites for the potassium cations. Each of the anions has a firmly encapsulated K^+. This sits within the puckered hexameric face, coordinated in a planar hexagonal array by six of the μ-O atoms from the anion (average O···K^+ 2.79 Å). There are further interactions with three of the interlayer μ_3-O atoms (O···K^+ 2.72 Å), and the coordination of this cation is completed by a loosely held H_2O molecule sitting above the face (O...K^+ 3.47 Å). This generates a 10-coordinate K^+ in total. For this site the anion is behaving as an inorganic crown ligand, as illustrated in Figure 5, with cross ring O...O distances of 5.46 Å, compared with *ca* 5.55 Å in 18-crown-6 K^+ complexes.[21]

For each anion there is a second K^+ sitting below the other face of the hexagonal antiprism, coordinated to three μ-O

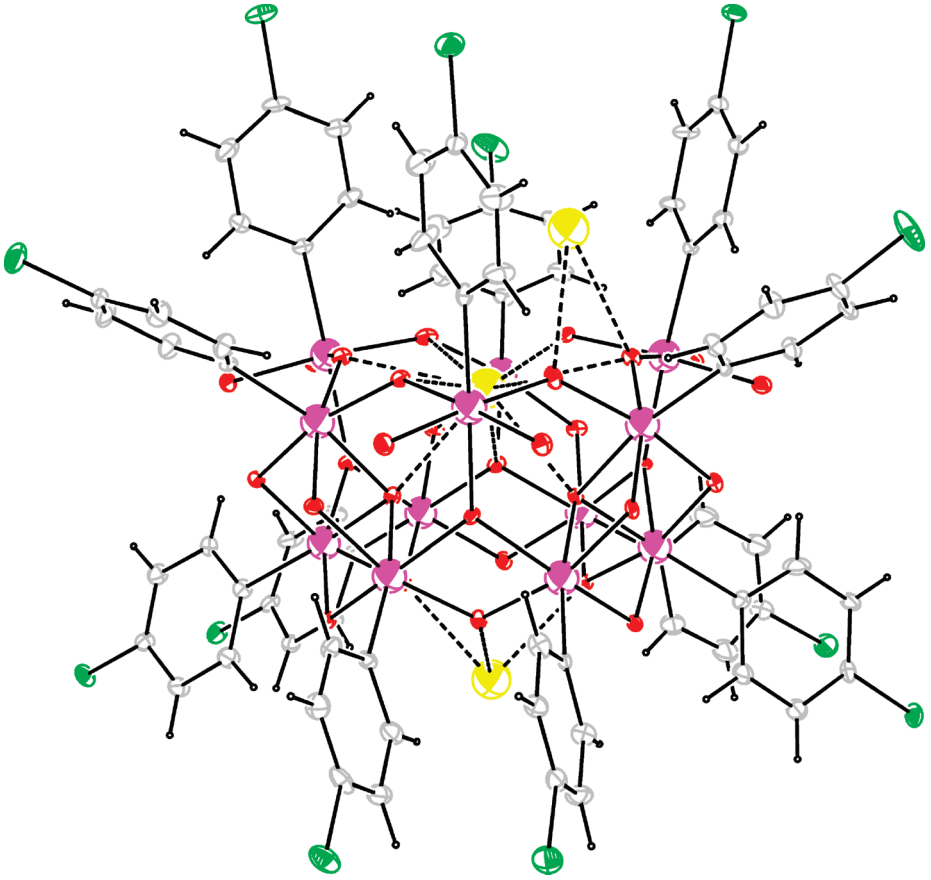

Figure 4. Full structure of the $[K_2H_8(p\text{-}ClC_6H_4Sb)_{12}O_{30}]^{2-}$ anion, showing the coordination of three different K^+ ions (the fourth K^+ is not closely associated with the anion). Purple = Sb, green = Cl red = O, yellow = K, light gray = C.

atoms (average O···K^+ 2.62 Å) from the anion, with three water molecules (average O···K^+ 2.48 Å) making up octahedral coordination.

The third K^+ in each case is within the bowl-shaped cavity generated by the protruding aryl rings above the puckered six-membered face. There are small differences in this case between the two independent anions in the asymmetric unit. There are two interactions with μ-O from the anion and three coordinated H_2O molecules (one or two of which are also weakly bridging to the K^+ ion in site 1). In addition there is a weak interaction with a Cl atom from a p-ClC_6H_4 group from the adjacent anion (Cl···K^+ 3.49/3.64 Å), and the K^+ is positioned so that it lies above the face of one of the p-ClC_6H_4 rings, (K^+···ring plane 3.32/3.37 Å). This interaction places the K^+ to one side of the cavity, breaking the C_{3v} symmetry of the rest of the anion.

The fourth K^+ in each case is in a general lattice position, each coordinated by five H_2O (average K^+···OH_2 distances 2.78 Å), and each is positioned symmetrically above one of the aryl rings of an anion (K^+···ring-plane distances 3.75 and 3.25 Å for K(4) to the ring attached to Sb(6) and K(8) to the ring attached to Sb(16), respectively).

The remainder of the structure consists of solvent within the lattice. A total of 116 H_2O molecules in the asymmetric unit were located and refined, and these gave sensible O···O distances for an H-bonded array, linking the anions and cations together. Analysis gives ca. 4% remaining void volume, so there are probably a few extra molecules not accounted for, but overall the solvent molecules are unusually well behaved.

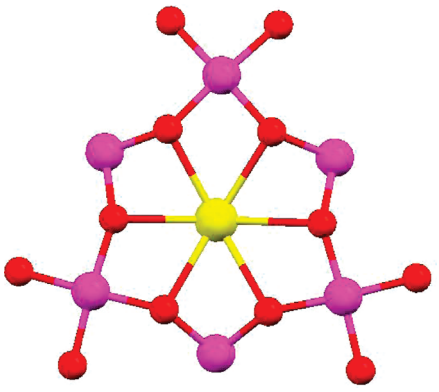

Figure 5. Cross-section of the 10-coordinate K^+ site in the $[K_2H_8(p\text{-}ClC_6H_4Sb)_{12}O_{30}]^{2-}$ anion, showing the 12-crown-6 $\{Sb_6O_6\}$ feature. The O···O cross-ring distance is 5.46 Å. The same arrangement is found for the Na^+ derivatives, with O···O distances of ca. 5.31 Å. Purple = Sb, red = O, yellow = K (or Na).

Structure of $Rb_{0.67}Na_{0.33}[Na_2H_9(p\text{-}MeC_6H_4Sb)_{12}O_{30}]\cdot 20H_2O$. The structure of a mixed Rb^+/Na^+ salt was determined and was found to be closely related to the K^+ salt discussed above. The same core hexagonal antiprism was found, with three cation sites similar to those already described. Despite the crystals growing from a solution where the Rb^+:Na^+ ratio was ca. 1:1, refinement showed that the two sites most

(21) (a) Cambridge Crystallographic Data Base, **2010**. (b) Ariga, K.; Kumitake, T. *Supramolecular Chemistry—Fundamentals and Applications*; Springer-Verlag: Heidelberg, 2006.

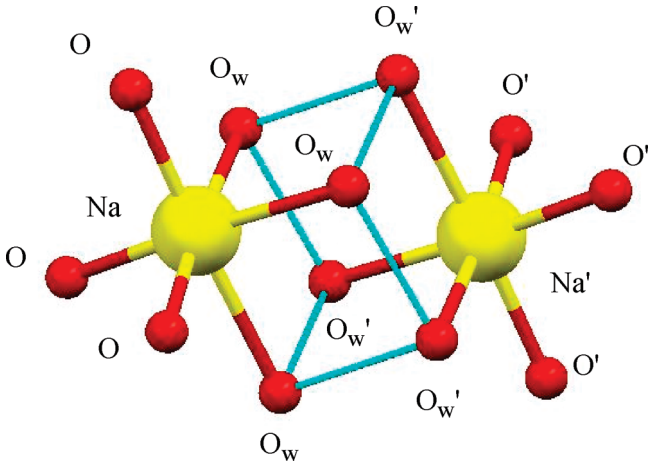

Figure 6. Cubane-like H-bonding moiety that links two anions via the six-coordinate Na^+ ions in all of the known sodium derivatives of arylstibonic acids. O_w and O_w' are coordinated water molecules, O and O′ are μ-oxygen atoms from the anion framework.

closely associated with the anion were occupied only by Na^+ cations, with the third site having $^2/_3$:$^1/_3$ mixed Rb^+:Na^+ occupancy.

Once again there is one cation, Na(1), that is firmly encapsulated in the crown face of the anion. In this case the O···O is 5.31 Å (cf. 5.46 Å for the larger K^+ example), and the Na^+ is displaced by 0.83 Å from the O_6 plane toward the interior of the anion (0.61 Å in the K^+ example). There are three links to μ_3-O atoms from the middle of the anion, and there is a single H_2O attached on the upper site. The second Na^+ occupies the lower Sb_6 face, again coordinated to three μ-O from the anion framework, with a further three H_2O molecules completing six-coordination. This unit is involved in an aesthetically pleasing link to the equivalent site on an adjacent anion via the H-bonded cubic arrangement illustrated in Figure 6, with Na^+−O−H···O−Na^+ bridges. We are unaware of a precedent for this type of linking of Na^+, which would more usually be joined by μ-OH_2 bridges, an arrangement that may be precluded here by the bulk of the anion.

The third cation site is in the pocket formed by the aryl rings and contains mixed Rb^+/Na^+ (2:1). It is linked to Na(1) by a bridging H_2O ligand and is coordinated to two μ-O from the anion. The remaining sites around the cation are occupied by three of the *p*-tolyl rings which sandwich the cation with distances of 3.30, 3.49, and 3.55 Å from the cation to the least-squares planes of the rings, indicating weak π-bonding. This type of π-interaction between aryl rings and group 1 cations is now well-established for other systems.[22]

The lattice water in this structure was less well-defined. Twenty H_2O were located, and these refined reasonably well to give a H-bonding network holding the main units together. However there still remained significant electron density that could not be modeled sensibly.

Structure of $(Ph_4P)[Na_2H_9(p\text{-}MeC_6H_4Sb)_{12}O_{30}](H_2O)_4\cdot xH_2O$. This crystal structure was of poor quality, with lattice water that could not be modeled successfully. It is less reliable than the others, but the overall features are clear. It consists of separated Ph_4P^+ cations and the same $[(RSb)_{12}O_{30}]$ anion as found for the other two examples. In this case there are only two Na^+ cations, one occupying the 10-coordinate inorganic crown site and one on the opposite face with six-coordination made up from three μ-O atoms and three H_2O. This latter Na^+ is again involved in linking two anions together through the same cubic arrangement found for the Rb^+ compound (cf. Figure 6). The third cation site found for the K^+ and Rb^+ compounds is now vacant, which allows for overall C_{3v} symmetry to be retained for the anions.

The bond parameters are very similar to those of the Rb compound, with O···O cross-ring distances of 5.28 Å, and again the Na^+ is displaced by 0.83 Å from the least-squares plane of the six crown-type oxygen atoms.

Discussion

When the acids $[H_8(RSb)_{12}O_{28}]$ are dissolved in alkaline solution, salts are formed. If KOH is used, crystals containing a tetra-anion are formed, namely, $[K_4H_8(RSb)_{12}O_{30}]$. If NaOH is used and other cations are added, then salts of a trianion are formed, including so far $[PhCH_2NMe_3][Na_2H_9(RSb)_{12}O_{30}]$,[8] $[Ph_4P][Na_2H_9(RSb)_{12}O_{30}]$, and $Rb_{0.67}Na_{0.33}[Na_2H_9(RSb)_{12}O_{30}]$. As an interesting historical note, as early as 1921 Fargher and Gray isolated solids from the reaction of arylstibonic acids with NaOH and found Na:Sb ratios of up to 1:3, consistent with our present results, though they were unable to provide an explanation.[7]

The anions found in the crystal structures correspond to a parent acid of formula $[H_{12}(RSb)_{12}O_{30}]$, which contrasts with the formula for the precursor acids indicated from the ESI-MS study of $[H_8(RSb)_{12}O_{28}]$. Possibly formation of the salts has concomitantly added two H_2O to the core unit, presumably via opening of two Sb−O−Sb bridges to generate sites for coordination of the tightly held cations. Alternatively, two H_2O may be readily lost in the mass spectrometer from an acid of formula $[H_{12}(RSb)_{12}O_{30}]$, since the major peaks in the mass spectra of the salts correspond to two H_2O fewer than found by X-ray crystal structure; for example, for $[Ph_4P][Na_2H_9(RSb)_{12}O_{30}]$ the most intense peak corresponded to $[Na_2H_4(RSb)_{12}O_{28}]^{2-}$, though $[Na_2H_8(RSb)_{12}O_{30}]^{2-}$ was also present.

Despite differing aryl groups and different crystal packing, the structures of all of these derivatives (five independent Na^+ species, two independent K^+ ones) show a remarkably conserved anion configuration. Interestingly, this geometry was first reported by Baskar et al. as one subunit of a very complex compound assigned the formula $[Na_{21}(PhSb)_{48}O_{114}]\cdot 46H_2O\cdot 4MeCN$, which made it unclear as to the overall charge state, though there were three Na^+ cations associated with the Sb_{12} subunit.[23] For all of the known examples the basic unit is a hexagonal antiprism with one puckered and one planar array of μ-O linked Sb atoms, with overall C_{3v} symmetry. The distance between the least-squares planes through the two Sb_6 arrays is 3.0 Å, and the Sb···Sb distances in the planar array are shorter (ca. 3.15 Å) than those in the puckered array (ca. 3.64 Å for Na^+ salts, 3.67 Å for K^+ ones).

The Sb−O (terminal) bond lengths average around 1.99 Å in all examples, consistent with being single bonds and hence Sb−OH groups. The doubly bridging O atoms have similar

(22) (a) Ma, J. C.; Dougherty, D. A. *Chem. Rev.* **1997**, *97*, 1303. (b) Dougherty, D. A. In *Encyclopaedia of Supramolecular Chemistry*; Atwood, J. L.; Steed, J. W., Eds.; Marcel Decker: New York, 2004; p 214. (c) Pink, M; Sieler, J. *Inorg. Chim. Acta* **2007**, *360*, 1221. (d) Shukla, R.; Lindeman, S. V.; Rathore, R. *Chem. Commun.* **2009**, 5600.

(23) Baskar, V.; Shanmugan, M.; Helliwell, M.; Teat, S. J.; Winpenny, R. E. P. *J. Am. Chem. Soc.* **2007**, *129*, 3042.

Sb−O distances (1.97−2.00 Å), while the triply bridging ones are longer, as expected (ca. 2.1 Å).

Two cation sites are intimately associated with the anion. With the first, one hexagonal face acts as a $\{Sb_6O_6\}$ crown ligand, providing six in-plane O atoms for bonding with a further three framework oxygens attaching below the cation and a water molecule making up the tenth site above the cation, the polyoxometalate framework effectively acting as a corand.[24] For the K^+ example the cation is slightly less displaced from the hexagonal plane than in the Na^+ case, and the cross-ring O···O distances have expanded a little to accommodate the larger cation. The presence of a crown ligand moiety contained within the structure of a discrete polyoxometallate molecule appears unusually rare, but the $\{Sb_6O_6\}$ entity is closely similar, albeit slightly smaller, to those found in niobates $\{Nb_6O_6\}$ and the pores of large cluster molecules $\{Fe_3W_3O_6\}$, $\{Mo_6O_6\}$, $\{Mo_3V_3O_6\}$, and $\{Mo_4VKO_6\}$.[25] All contain a ring of six oxygen atoms that are essentially coplanar to within 0.013−0.083 Å, as in our case, and cross-ring O···O distances that range from 5.502 to 5.639 Å. Cations (K^+ or NH_4^+) ensnared by these ligands may be as little as 0.271 or as far as 1.523 Å from the plane of the oxygen atoms.

In contrast, the other hexagonal face is attached to the cation by only three framework oxygen atoms, with a further three terminal H_2O molecules completing the coordination. Whereas either Na^+ or K^+ can occupy these sites, there was no exchange with Rb^+ when crystallization was carried out in the presence of the larger cation.

When the remaining cations are large organic ones ($PhCH_2NMe_3^+$, Ph_4P^+), these are separate from the anions, occupying general lattice sites. However if there is a third small cation available, this is found in a pocket formed by the aryl groups above the puckered hexagonal face. This is attached to two μ-O from the framework and is bridged by a H_2O molecule to the high-coordinate cation in site 1. Remaining interactions are with the faces of the aryl rings in weak π-type bonding.[22] These interactions displace the cation from the C_{3v} axis toward one side of the pocket. In the case of the K^+ example, the fourth cation is only loosely associated with the outside of the anion through a weak π-interaction with an aryl ring.

For all the Na^+-containing examples the anions are linked through the cubic $\{O_3Na(H_2O)_6NaO_3\}$ H-bonded units (Figure 6), despite different crystal packing interactions. However this is not conserved for the K^+ compound, where the $O_3K(H_2O)_3$ moiety links indirectly to the adjacent anion via a network of H-bonded water molecules.

We have obtained crystals prepared from $Ca(OH)_2$, though the quality was such that only the basic core geometry could be determined. The same hexagonal-antiprism structure as found for the K^+ or Na^+ species was indicated, with Ca^{2+} ions in the two usual sites. This arrangement is obviously favored for these medium-sized cations.

The compounds reported herein represent new polyoxometalates that have a number of novel features: (i) they are formed from alkaline solutions, whereas the polyoxometalates formed by Mo, W, V, etc., are formed under acid conditions;[26] (ii) the anions form with an open structure, which generates a hexagonal channel; (iii) there is a very strong affinity for cations, particularly in the 10-coordinate site, which acts as an inorganic crown moiety; (iv) the same structure is adopted for Ph, *p*-ClC_6H_4, *p*-MeC_6H_4, and *p*-$O_2NC_6H_4$ derivatives, with either K^+ and Na^+ counterions, and probably also with Ca^{2+}; (v) the structural integrity of the anionic clusters is maintained in solution since ESI mass spectra indicate Sb_{12} species dominate.

We note that Baskar et al. have very recently characterized a Sb_{16} polyoxostibonate from *p*-chlorophenylstibonic acid in the presence of dimethylpyrazole, under thermal conditions in nonaqueous solvents,[10] so the aggregation processes of organostibonic acids can apparently be controlled using different templating cations and bases and different conditions. In future papers we will report results of our studies with other metal ions.

Acknowledgment. We thank Dr. Robert H. Shoemaker and the Drug Synthesis and Chemistry Branch, Developmental Therapeutics Program, Division of Cancer Treatment and Diagnosis, National Cancer Institute, Bethesda, MD, for generously supplying samples of arylstibonic acids from their archives.

Supporting Information Available: Full details of the crystal structure determinations, cif files, and extra structure diagrams are available free of charge via the Internet at http://pubs.acs.org.

(24) Steed, J. W.; Atwood, J. L. *Supramolecular Chemistry*; Wiley: New York, 2000.

(25) (a) Müller, A.; Botar, B.; Bögge, H.; Kögerler, P.; Berkle, A. *Chem. Commun.* **2002**, 2944. (b) Müller, A.; Sousa, F. L.; Merca, A.; Bögge, H.; Miro, P.; Fernandez, J. A.; Poblet, J. M.; Bo, C. *Angew. Chem., Int. Ed.* **2009**, *48*, 5934. (c) Todea, A. M.; Merca, A.; Bögge, H.; Glaser, T.; Pigga, J. M.; Langston, M. L. K.; Liu, T.; Prozorov, R.; Luban, M.; Schröder, C.; Casey, W. H.; Müller, A. *Angew. Chem., Int. Ed.* **2010**, *49*, 514. (d) Tsunashima, R.; Long, D.-L.; Miras, H. N.; Gabb, D.; Pradeep, C. P.; Cronin, L. *Angew. Chem., Int. Ed.* **2010**, *49*, 113.

(26) (a) Pope, M. T. *Heteropoly and Isopoly Oxometalates*; Springer-Verlag: Berlin, 1983. (b) Pope, M. T.; Müller, A. *Angew. Chem., Int. Ed.* **1999**, *30*, 34. (c) Long, D.-L.; Burkholder, E.; Cronin, L. *Chem. Soc. Rev.* **2007**, *36*, 105. (d) Long, D.-L.; Tsunashima, R.; Cronin, L. *Angew. Chem., Int. Ed.* **2010**, *49*, 1736.